Chemical separation and analysis of bioactive herbal compounds in licorice using capillary electrophoresis

by

Jia Cai

B.Sc., Tianjin Medical University, 1990

A THESIS

SUBMITTED IN PARTIAL FULFILLMENT OF

THE REQUIREMENTS FOR THE DEGREE OF

MASTER OF SCIENCE

In the Department Of Chemistry

SIMON FRASER UNIVERSITY

September 2003

Approval

Name: **Jia Cai**
Degree: M.Sc. Chemistry
Title of Thesis: **Chemical separation and analysis of bioactive herbal compounds in licorice using capillary electrophoresis**

Examining Committee:

Chair: **Dr. Neil Branda**
Associate Professor

Dr. Paul Li
Assistant Professor of Chemistry
Senior Supervisor

Dr. George Agnes
Associate Professor of Chemistry
Committee Member

Dr. Lynne Quarmby
Associate Professor of Biological Sciences
Committee Member

Dr. Hogan Yu
Assistant Professor of Chemistry
Internal Examiner

Date Approved: Sep 11, 2003

PARTIAL COPYRIGHT LICENCE

I hereby grant to Simon Fraser University the right to lend my thesis, project or extended essay (the title of which is shown below) to users of the Simon Fraser University Library, and to make partial or single copies only for such users or in response to a request from the library of any other university, or other educational institution, on its own behalf or for one of its users. I further agree that permission for multiple copying of this work for scholarly purposes may be granted by me or the Dean of Graduate Studies. It is understood that copying or publication of this work for financial gain shall not be allowed without my written permission.

Title of Thesis/Project/Extended Essay:

Chemical Separation and Analysis of Bioactive Herbal Compounds in Licorice using Capillary Electrophoresis.

Author:

(signature)

Jia Cai

(name)

Sept. 11, 2003

(date)

Abstract

Capillary electrophoresis (CE), which is a relatively new chemical separation technique, has been shown to be very effective for the analysis of a diverse array of charged and uncharged compounds, especially in complex mixtures and racemates. In this work, four bioactive components derived from licorice root, i.e. glycyrrhizin (GL), 18α-glycyrrhetinic acid (18α-GA), 18β-glycyrrhetinic acid (18β-GA) and isoliquiritigenin (IQ) were separated by CE. Since 18α-GA and 18β-GA are diastereoisomers having different pharmacological effects, their chemical separation and subsequent analysis in licorice is important. For the first time, separation of these diastereoisomers by CE using a chiral additive has been achieved. Subsequently, simultaneous separation of above four pharmacological active components in one run by CE was reported. Different modes of CE, such as capillary zone electrophoresis (CZE), micellar electrokinetic capillary chromatography (MECC), cyclodextrin-MECC (CD-MECC), were employed to optimize the chemical separation. Preliminary experiments started with CZE using a 50 mM sodium tetraborate buffer within a capillary tube of inner diameter 50 μm and length of 60.2 cm. A CE separation voltage of 17kV or 10kV was used. Detection was achieved at a distance of 50 cm or 10.2 cm from the capillary inlet using a diode array UV absorbance detector over the wavelength range from 190 to 300 nm. Two kinds of micelle systems in which surfactant molecules are present above their critical micelle concentrations (CMC) have been investigated. Using sodium dodecyl sulphate (SDS), chemical separation was achieved by 50 mM sodium tetraborate-20 mM β-CD-25 mM SDS-15% methanol-MECC system at pH 8.5. The addition of a chiral selector, β-CD,

improved the separation of 18α-GA and 18β-GA. Separation was also performed on another micelle system: sodium cholate (SC). A complete separation has been obtained by using 10 mM sodium tetraborate-20 mM β-CD-25 mM SC buffer system. The effects of various experimental parameters, including pH, surfactant concentration, temperature, organic modifier, on effective separation were investigated. The conditions of pH 8.5 and temperature at 25°C have resulted in more effective separations. Finally, the raw and roasted licorice roots have also been investigated for differences in the chemical composition in this study. Both samples were extracted with methanol, water and ethanol and these extracts were analyzed under the optimum CE conditions.

Acknowledgements

I would like to express my sincere thanks to my supervisor Dr. Paul Li. Without his continuous guidance and help, without his constant encouragement and patience, especially without his many hours reading drafts of this ever lengthening thesis, the thesis could have never been done.

I wish to thank my examination committee members, Dr. George Agnes, Dr. Lynne Quarmby and Dr. Hogan Yu. I am so grateful for their evaluation and suggestions of my thesis. In addition, I would like to thank my labmates and friends in SFU, especially to Laurent de Camprieu for his kindly teaching me how to culture cells; to James Li for printing out my thesis during my absence; to Micheal Sung for reading through the whole draft of my thesis and provides me precious suggestions.

Finally, I would like to express my endless gratitude to my parents. With high age and illness, they have taken care of my son for more than three years in order to make me complete my graduate study without any burden. From them, I learn the greatness of parents' love, which I can never pay back during my life. Sincere thanks to my family. Family has always been and will be the support for my life forever.

Table of Contents

List of Tables

List of Charts

List of Figures

Key Abbreviations

CE = capillary electrophoresis

GL = glycyrrhizin

18α - GA = 18α - glycyrrhetinic acid

18β - GA = 18β - glycyrrhetinic acid

IQ = isoliquiritigenin

TCM = traditional Chinese medicine

DMBA = 7, 12 - dimethylbenz[α]-anthracene

AST = aspartate transaminase

ALT = alanine aminotransferase

LDL = low-density lipoprotein

TPA = 12-*o*-tetradecanoylphorbol-13-acetate

HPLC= high performance liquid chromatography

TLC = thin-layer chromatography

GC = gas chromatography

GC-MS= gas chromatography-mass spectrometry

CZE = capillary zone electrophoresis

MECC = micellar electrokinetic capillary chromatography

EOF = electroosmotic flow

EPF = electrophoretic flow

CMC = critical micelle concentration

SDS = sodium dodecyl sulfate

SC = sodium cholate

CD = cyclodextrin

PDA = photodiode array

RSD = relative standard deviation

μTAS = micro total analysis system

ER = endoplasmic reticulum

AM = acetoxymethyl

F_E = applied electric force

q = charge of the ion

E = electric field strength

V = applied electric voltage

L_t = total capillary length

F_F = frictional force

η = viscosity of the buffer

ν_{ep} = electrophoretic velocity of molecule

γ = radius of the hydrated ion

μ = electrical mobility

ν = velocity

ε = dielectric constant

δ = electrical double-layer thickness or Debye radius

ξ = zeta potential

R = resolution

Chapter 1: Overview of Licorice

1.1 Introduction

Licorice, or liquorice, whose Latin name is *Glycyrrhiza glabra L.*, is a perennial herb which possesses sweet taste.[1] It abounds over an extensive area of the warm portions of Europe and Asia, such as Turkey and China.

Licorice has extensive pharmacological effects for the human being. The most common medical use for licorice is for treating upper respiratory ailments including coughs, hoarseness, sore throat and bronchitis.[2,3] The anti-ulcerative activity has been demonstrated extensively, and in China and Japan, licorice is applied clinically for the treatment of stomach ulcers.[4,5] Recent reports indicate that licorice has chemopreventive functions and it has been tested in mice. [6]

1.2 Bioactive chemical components in licorice

Many chemical compounds have been identified in licorice. Glycyrrhizin (α-D-glucopyranosiduronic acid, (3β,20β)-20-carboxy-11-oxo-30-norolean-12-en-3-yl 2-O-β-D-glucopyranuronosyl-(9Cl) (GL, Fig. 1a) which is a saponin, is the main ingredient. GL occurs naturally as its potassium or calcium salt. [7] Generally, the content of GL in licorice root is 6-14% (w/w). [8] This saponin comprises the disaccharide, β-D-glucurono-pyranosyl(1,2)-β-D-glucuronopyranose, linked to a triterpenoid aglycone, glycyrrhetinic

acid. Glycyrrhetinic acid has two diastereoisomers in the α-form (Olean-12-en-29-oic acid, 3-hydroxy-11-oxo, (3β,18α,20β)-(9Cl) (18α-GA)) and β-form (18β-GA) (Olean-12-en-29-oic acid, 3-hydroxy-11-oxo, (3β, 20β)-(9Cl)) (Fig. 1b and c).[9] The contents of 18α-GA and 18β-GA, which are diastereoisomers, are 0.13-0.71% (w/w) and 3.98-16.80% (w/w), respectively.[10] Under alkaline conditions, the β isomer of GA can be isomerized to its α isomer.[11] Another constituent of licorice is isoliquiritigenin (IQ) (2-propen-1-one, 1-(2,4-dihydroxyphenyl)-3-(4-hydroxyphenyl)-, (2E)-(9Cl)) whose structure is shown in Fig. 1d. IQ belongs to flavonoids and the content of IQ in licorice root is around 0.016-0.136% (w/w).[12] In addition, there are other constituents in licorice root, such as, neoliquiritin, liquiritin, licoflavone B, glabrene, isoliquiritin, licochalcone A, and so on.[13]

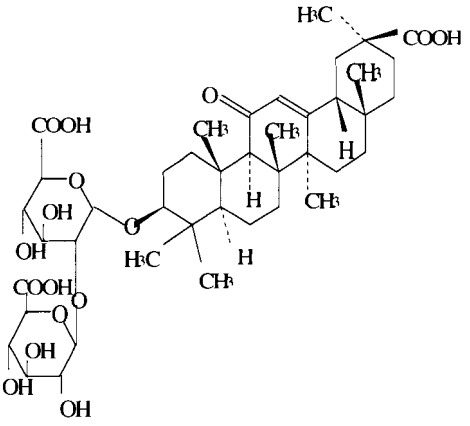

(a)

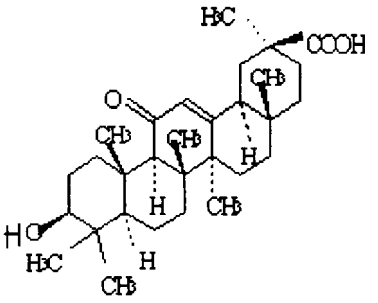

(b)

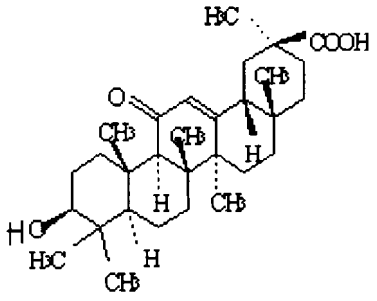

(c)

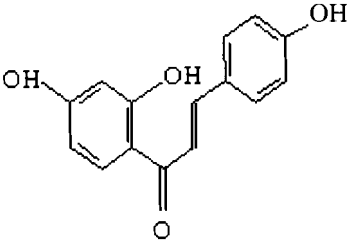

(d)

Fig. 1 Structures of (a) GL (b) 18α-GA (c) 18β-GA (d) IQ.

GL has been shown to possess important pharmacological activities, such as anti-viral, anti-inflammatory and anti-oxidative activities.[12] There have been some reports that GL has chemopreventive functions.[1,13] Clinical studies have shown GL to be effective against gastric ulcers, viral disorders and chronic hepatitis.[14] The molecular mechanism of antihepatotoxic effect of GL has been shown by its blocking the process of NF-κ*B* activation induced by hepatotoxins or oxygen free radicals.[15] That process is thought to be crucial in the fibrogenic process directly and in liver regeneration. In a recent study[16], feeding female Sencar mice with 0.05% (w/v) GL in the drinking water resulted in 36-41% inhibition against skin tumor initiation induced by 7,12-dimethylbenz[α]-anthracene (DMBA). This shows that GL has the potential as an anti-tumor agent. GL is one of the most commonly used ingredients in herbal extracts in traditional Chinese prescriptions.

The two diastereoisomers of GA, namely 18α-GA and 18β-GA possess different biological activities and physicochemical properties. Both exhibit strong anti-inflammatory effect which is similar to that of glucolocorticoid.[17] However, 18α-GA has a significantly greater effect than that of 18β-GA in several experimental models.[4] As reported by Amagaya *et al.*, the anti-inflammatory activity of 18α-GA was found to be greater than 18β-GA against edema (accumulation of an excessive amount of watery fluid in cells, tissues, induced by carrageenan) in mice.[10] Comparative studies of the two stereoisomers in the course of carcinogenesis show that, for anti-tumor-initiating activity, 18β-GA was more potent than 18α-GA; whereas, in the case of anti-tumor-promoting activity, the effects were approximately equal for both.[18] It is noteworthy that 18α-GA has been tested clinically in China against hepatitis (inflammation of the liver, usually

from a viral infection, sometimes from toxic agents), showing stronger effects in reducing the production of aspartate transaminase (AST) and alanine aminotransferase (ALT) than 18β-GA. [5]

IQ is another important compound recently found for clinical use. Traditionally, in Japan, licorice roots have long been used for the treatment of diabetic neuropathy.[19] IQ is considered to be effective in preventing diabetic complications because IQ has been identified to possess the most potent aldose-reductase-inhibiting activity, which was demonstrated by the inhibition of IQ on sorbitol accumulation in human red blood cells *in vitro*.[11] Moreover, oxidative damage to various tissues by free radicals has been implicated as the cause of diverse diseases. IQ is a very potent antioxidant toward low-density lipoprotein (LDL) oxidation. As LDL oxidation is a key event in the formation of early atherosclerotic lesion, the use of these natural antioxidants may be beneficial to prevent atherosclerosis. Furthermore, IQ inhibited inflammation caused by a topical application of 12-*o*-tetradecanoylphorbol-13-acetate (TPA) in mice, and IQ also inhibited DMBA-initiated and TPA-promoted skin papilloma formation.[21]

1.3 Raw and roasted licorice

In traditional Chinese medicine (TCM), some physicians often ask why a preparation made in light of the apparently correct Chinese formulation does not yield the expected clinical results. One of the possible reasons is that the herbal ingredients are not properly processed according to traditional indications.

Processing herbs to alter their properties was an ancient method used in TCM. This method can alter or enhance one or a number of specific bioactive chemical constituents.[22,23] Unprocessed or raw licorice is sweet and detoxifying and it is better for the treatment of fever, inflammation and cough.[10] Roasting raw licorice with the addition of honey makes the herb become a tonic to the spleen.[22] Samples of raw and roasted licorice root are shown in Fig. 2. But so far, it is not clear that which component in licorice root samples related to the corresponding pharmacological activity has been changed. Therefore, the study of the composition files of herbal samples in order to find out the chemical basis for the difference in pharmacological effects possesses significance.

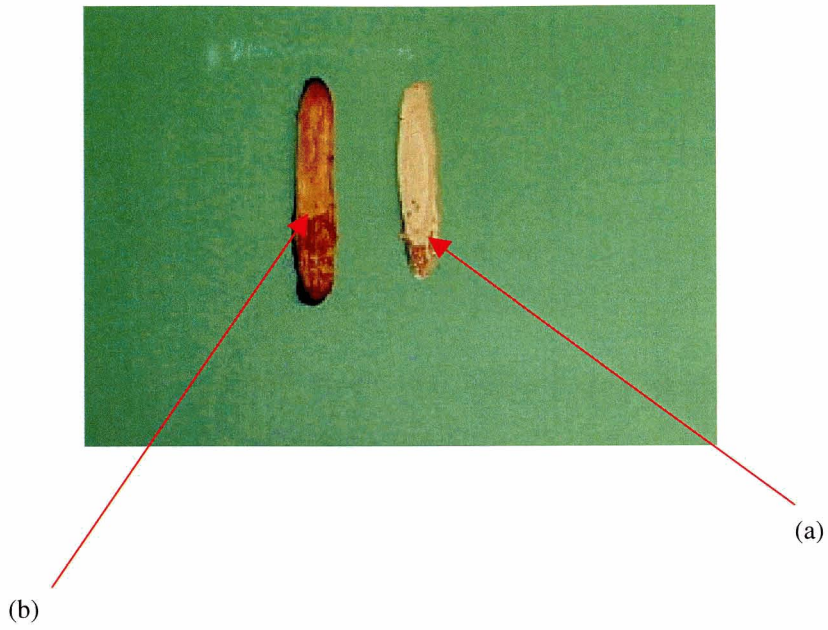

Fig. 2. Raw and roasted licorice root samples.
(a) raw licorice; (b) roasted licorice

Chapter 2 Separation of Bioactive Components in Licorice Root using Capillary Electrophoresis

2.1 Introduction

Owing to some proven pharmacological effects of GL, 18α-GA and 18β-GA and IQ, we are interested in analyzing these four compounds.

Several analytical techniques have been employed for the analysis of major bioactive components in licorice root. These methods include high performance liquid chromatography (HPLC)[24-31], thin-layer chromatography (TLC) [32,33], gas chromatography (GC) [34], gas chromatography-mass spectrometry (GC-MS) [8,35]. For 18α- and 18β- GA, since the biological activities of the two stereoisomers are quite different [36], an accurate and efficient method to assess their relative amount in GA samples is desirable. So far, only GC [10], HPTLC [36] and HPLC [4] methods have been used for the analysis of the two stereoisomers. GC methods are laborious and time-consuming because of the need of silyl or methyl derivatization to increase the volatility of the compounds. HPTLC is not so accurate because of the quantitation method by densitometry. Although good separation of the diastereoisomers could be achieved by HPLC, expensive chiral columns and large amounts of organic solvents should be used.

Recently, capillary electrophoresis (CE) has been shown to be very effective for the analysis of many compounds, especially for the materials with complex matrices.[37, 38] CE

has several advantages, such as high separation efficiency, simplicity of operation, low consumption of samples and solvents, over other chemical separation methods. Currently, several CE modes have been used to analyze licorice. [39-46] Capillary zone electrophoresis (CZE) was employed for the separation and determination of GL in licorice root and its preparations. Iwagami *et al.* analyzed glycyrrhizin in glycyrrhizae Radix and commercial oriental pharmaceutical preparations by using a high-performance capillary electrophoresis.[41] Zhang *et al.* developed a capillary zone electrophoresis method to separate and determined glycyrrhizin in Chinese medicinal preparations.[45] Li *et al.* had reported a micellar electrokinetic capillary chromatography (MECC) method for the separation and determination of five licorice components, including GL, GA and IQ.[39] Determination of Glycyrrhizic acid and 18-β-glycyrrhetinic acid in biological fluids by MECC has been reported.[44] Determination of glycyrrhizin and glycyrrhetinic acid in yinqiaojiedupian has been reported by capillary electrophoresis.[46] However, to date, separation of GL, 18α-GA, 18β-GA and IQ in a single run simultaneously by CE has not been published. Especially for the chiral separation of 18α-GA and 18β-GA by CE, no literature has been reported so far.

2.2 Capillary electrophoresis

Electrophoresis is a separation method.[47] By applying electric field a diverse array of charged compounds are separated based on the differential rate of migration times in a buffer solution. This separation technique was first developed by Tiselius in 1937 for the separation of serum proteins. In the 1960s, polyacrylamide gels were optimized with

stacking and resolving buffer systems for high resolution separations of native and sodium dodecyl sulfate (SDS)-complexed proteins. In the late 1970s, capillary electrophoresis (CE) was shown to be viable by Mikkers et al. Several years later, micellar electrokinetic chromatography (MEKC), capillary coating technique, etc. have been developed. CE has been demonstrated the potential for producing high-resolution separations of charged and uncharged compound, especially for complex mixtures and racemates.

The instrumental configuration for CE is shown in Fig. 3. The system consists of a high-voltage power supply, a capillary tube, two buffer reservoirs and a detector. The two ends of a capillary tube (with an internal diameter of 50 or 75 μm), which is filled with the buffer solution, are placed into two separate buffer reservoirs (inlet and outlet). The capillary tube, which is externally coated with polyimide, is quite flexible. The high-voltage direct-current power supply, which delivers up to 30kV, is connected to two electrodes (platinum) immersed in the buffer reservoirs. A sample is introduced into the capillary as a solution plug by either hydrodynamic flow or electromigration. In this work, hydrodynamic flow is employed. An on-column detector is located near the outlet end of the capillary. The ionic species in the sample plug migrate with different electrophoretic mobilities as determined by their charge-to-size ratio. These species eventually pass the detector where information is collected and stored by a data acquisition/analysis system. [48] A UV absorbance detector is commonly used for detection.

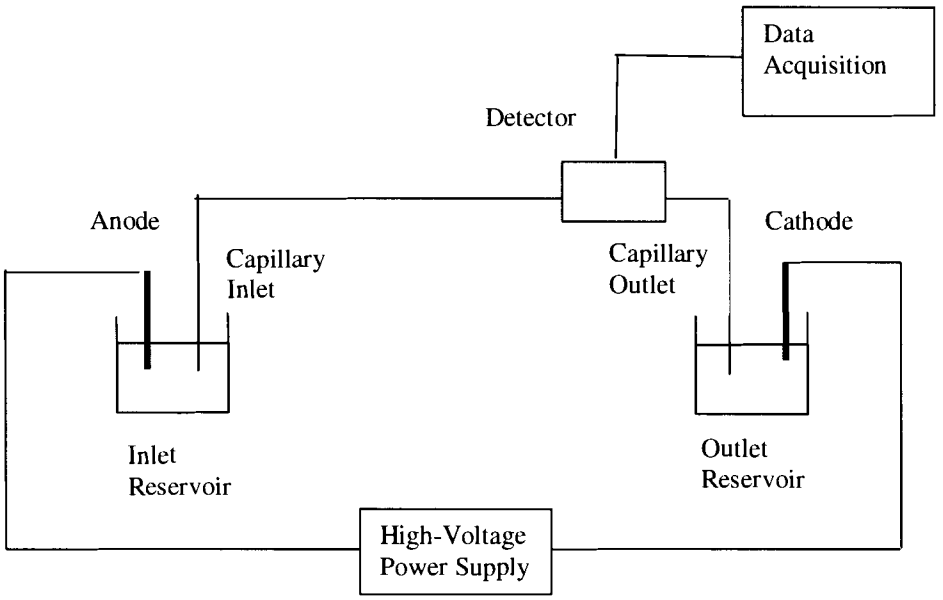

Fig. 3 Instrumental setup of CE.

The mechanism of separation in capillary zone electrophoresis (CZE) is based on the migration of charged molecules in an applied field. [49] There are two factors that affect the movement of ions, one is the applied electric force (F_E), given as follows:

$$F_E = qE \qquad (1)$$

where F_E is the electric force, q is the charge of the ion and E is the electric field strength, which is defined as follows:

$$E = \frac{V}{L_t} \qquad (2)$$

Where V is the applied electric voltage and L_t is the total capillary length.

The other factor is the frictional force, which depends on a number of parameters, shown in equation (3):

$$F_F = 6\pi\eta v_{ep}\gamma \qquad (3)$$

where F_F is the frictional force, η is the viscosity of the buffer, v_{ep} is the electrophoretic velocity of molecule and γ is the radius of the hydrated ion.

At equilibrium, these two forces are balanced, i.e. $F_E = F_F$. Combining equation (1) and (3), the velocity of electrophoretic flow (EPF) is shown in equation (4):

$$v_{ep} = \frac{qE}{6\pi\eta\gamma} \qquad (4)$$

More commonly, the electrical mobility (μ) instead of velocity (v) is employed. μ is defined as follows:[47]

$$\mu = \frac{v}{E} \qquad (5)$$

where v is the velocity, E is the electric field strength.

Therefore, from (4) and (5), electrophoretic mobility (μ_{ep}) of an ion can be expressed as:

$$\mu_{ep} = \frac{q}{6\pi\eta r} \qquad (6)$$

where q is the net charge of the ion, η is the viscosity of buffer, γ is the radius of the solvated ion.

Electroosmotic flow (EOF) is another distinguished feature in CE. A flow occurs because of the presence of a surface charge on the inner wall of an uncoated fused silica capillary.

At pH above 3, the surface silanol groups become ionized and an anionic charge on the capillary surface results in the formation of an electrical double layer. The resulting ionic distribution is shown in Fig. 4. [51]

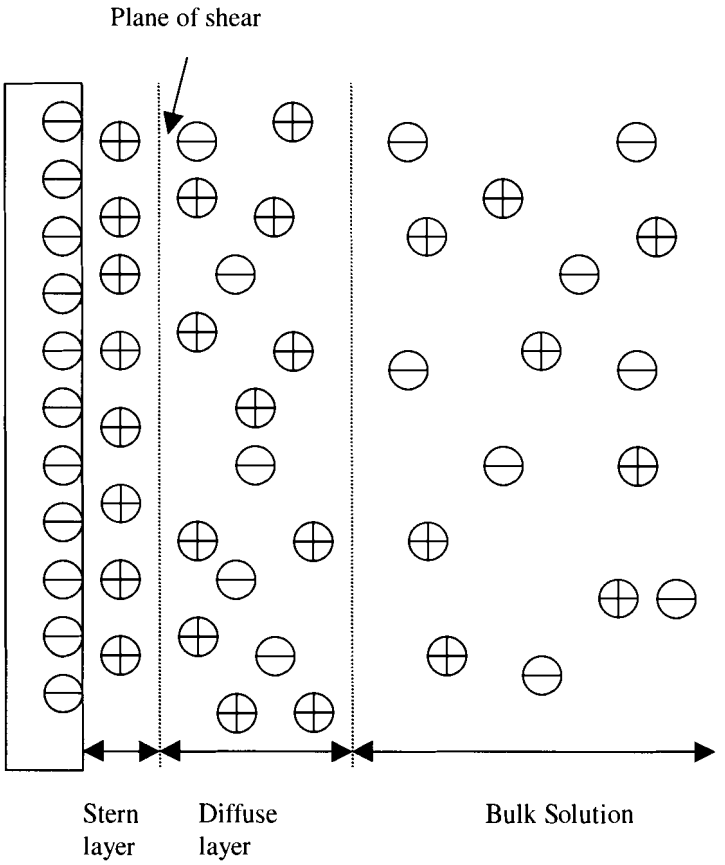

Fig. 4 Electrical double layer at the inner wall of capillary.

Positive ions of the added electrolyte accumulate in the electrical double layer at the capillary wall surface. The solvated positive ions move towards the negative electrode and drag the liquid mobile phase with them and this constitutes the EOF. This effect acts as a pumping mechanism to propel all molecules (cationic, neutral, and anionic) toward

the detector with separation ultimately determined by differences in the electrophoretic migration of the individual analytes.

The mobility of electroosmotic flow (EOF), μ_{eo} is defined by, [51]

$$\mu_{eo} = \frac{\xi\varepsilon}{4\pi\eta} \qquad (7a)$$

Where ε is the dielectric constant, η is the viscosity of the buffer, and ξ is the zeta potential measured at the plane of shear close to the liquid-solid interface. ξ depends on various factors including the concentration of the run buffer, [52]

$$\xi = \frac{4\pi\delta e}{\varepsilon} \qquad (7b)$$

where ε is the buffer's dielectric constant, e is the total excess charge in solution per unit area, δ is the electrical double-layer thickness or Debye radius given by

$$\delta = \frac{1}{3\times10^{7}\,|z|\,c^{1/2}} \qquad (7c)$$

where z is the number of valence electors and C is the buffer concentration.

The movement of an ion is governed by velocity (v_n) or net sum of EPF and EOF. [52] The net velocity (v_n) and net electrical mobility (μ_n), are given as follows:

$$v_n = v_{ep} + v_{eo} \qquad (8a)$$

$$\mu = \mu_{ep} + \mu_{eo} \qquad (8b)$$

where v_{ep} is the electrophoretic velocity,v_{eo} is the electroosmotic velocity, μ_{ep} is the electrophoretic mobility, μ_{eo} is the electroosmotic mobility.

Experimentally, v_{eo} and v_{ep} are determined as follows:

$$v_{eo} = \frac{L_d}{t_{eo}} \qquad (9)$$

$$v_{ep} = \frac{L_d}{t_m} \qquad (10)$$

where L_d is the distance of the capillary inlet to the detector, t_m is the migration time of analyte, t_{eo} is the migration time of the EOF marker, which is a neutral compound migrating at the EOF.

Combining equations (2), (5), (6), (7), (9), (10), we can express μ_{ep} in terms of t_m and t_{eo}:

$$\mu_{ep} = \mu_n - \mu_{eo} = \frac{L_t L_d}{V}\left(\frac{1}{t_m} - \frac{1}{t_{eo}}\right) \qquad (11)$$

Where μ_{ep} is the electrophoretic mobility of the test solute, μ_n is the net mobility, μ_{eo} is the electroosmotic mobility, t_m is the migration time for the test solute measured directly from the electropherogram, t_{eo} is the migration time for an uncharged solute, L_t is the total length of capillary, L_d is the length of capillary between injection and detection, and V is the applied voltage.

A successful separation process is indicated by a high value in resolution, R, between two separated species which is given by the expression: [53]

$$R = \frac{2(t_2 - t_1)}{(w_1 + w_2)} \qquad (12)$$

where t_1 is the migration time of the faster moving component, t_2 is the migration time of the slower moving component, and w_1 is the width of the peak at the baseline of the faster moving component, and w_2 is the width of the peak at the baseline of the slower moving component.

2.3 UV-detector

The schematic of UV-detector employed in CE is shown in Fig. 5.[54] It consists of several parts, such as lamp, lens, slit, grating and photodiode array. The mechanism is based on

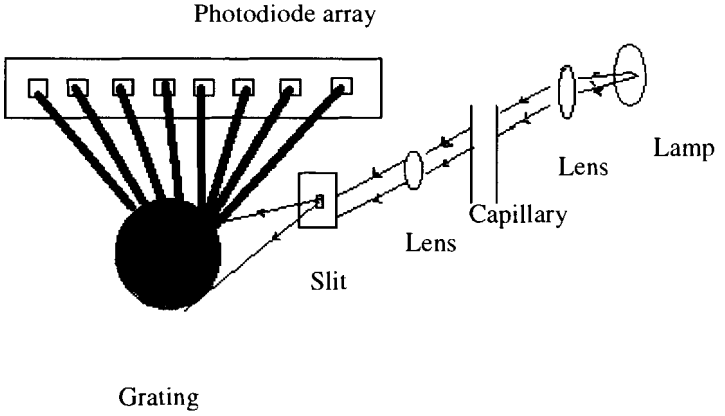

Fig. 5 A schematic of UV-detector.

the measurement of the absorbance (A) of solutions through the capillary having a path length of b cm. Ordinarily, the concentration of an absorbing analyte is linearly related to

absorbance. This is so called Beer's Law. It can be represented as the equation shown as follows:

$$A = \varepsilon bc \qquad (13)$$

where A is absorbacnce;

ε is extinction coefficient;

c is the concentration of analyte.

Deviations from the linear relationship between the measured absorbance and concentration when b is constant may occur. There are several factors may affect the result. 1. Real limitations to Beer's law. Beer's law is useful for the measurement of absorbance of low analyte concentrations. When analyte concentration is more than 0.01 M, the distance between molecules diminished and every molecule can affect the charge distributions of other molecules around it, which can affect the ability of the molecules to absorb a given wavelength of radiation and resulted in the deviation from the linear relationship between absorbance and concentration. Another limitation to Beer's law is that ε changes base on the refractive index of the medium caused by concentration changes. 2. Apparent chemical deviations. When analyte dissociates, associated, or reacts with a solvent, apparent deviation may occur. 3. Apparent instrumental deviations with polychromatic radiation. Beer's law is only applied to the monochromatic radiation. But practically, more than one wavelength radiation may produce, which resulted in the deviations. 4. Instrumental deviations in the presence of stray radiation.

2.4 Micellar electrokinetic capillary chromatography (MECC)

Several modes other than CZE have been used in CE, and one of which is micellar electrokinetic capillary chromatography (MECC). In MECC, surfactants at concentrations above their critical micelle concentrations are added in the run buffer solutions to form micelles. This extends the enormous separation power of CE to uncharged solutes. In CZE, micelles are not used, so uncharged solutes can not be separated.

A surfactant, which is an amphiphilic molecule, consists of a hydrophobic tail and a polar or ionic head group. Above a certain concentration, known as critical micelle concentration (CMC), surfactants begin to form roughly spherical aggregates, which are called micelles. At room temperature, sodium dodecyl sulphate (SDS), which is a synthetic surfactant, will form micelles above the CMC of 8 mM, the aggregation number is 63. [55] The chemical and micellar structures of SDS are shown in Fig.6.

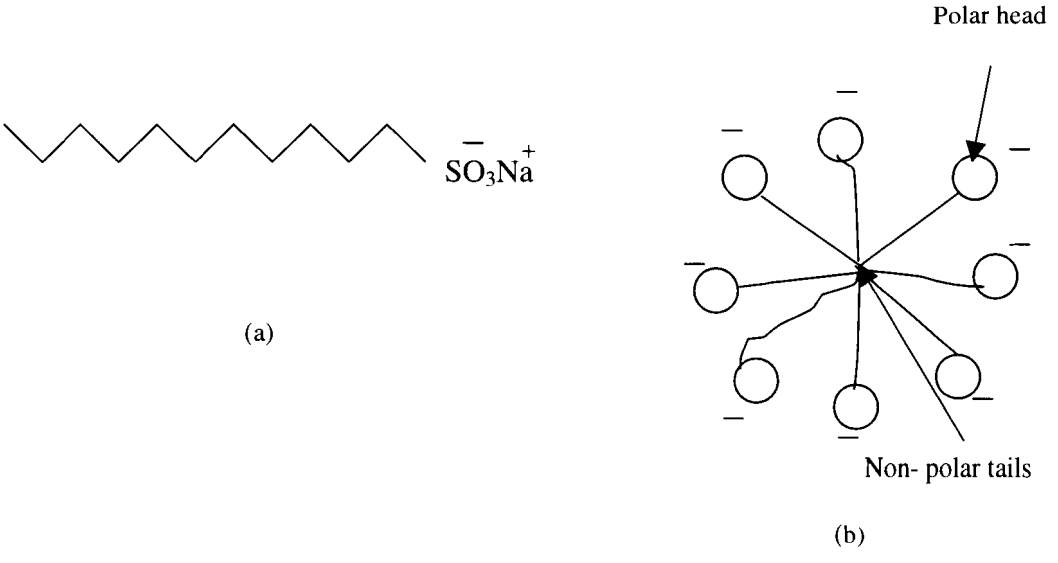

Fig. 6. Chemical and micellar structures of SDS.

Sodium cholate (SC) is another type of surfactant, see Fig.7a and 7b. Since SC exists naturally in bile, it is also called bile salt. The micellar structure of SC is quite different from that of SDS. SC possesses hydrophilic and hydrophobic faces as opposed to polar head groups and nonpolar tails. Consequently, SC exhibits a different type of aggregation behavior.[56] Each unit is held together by hydrophobic interactions between the nonpolar faces, the aggregation number is 2-4.

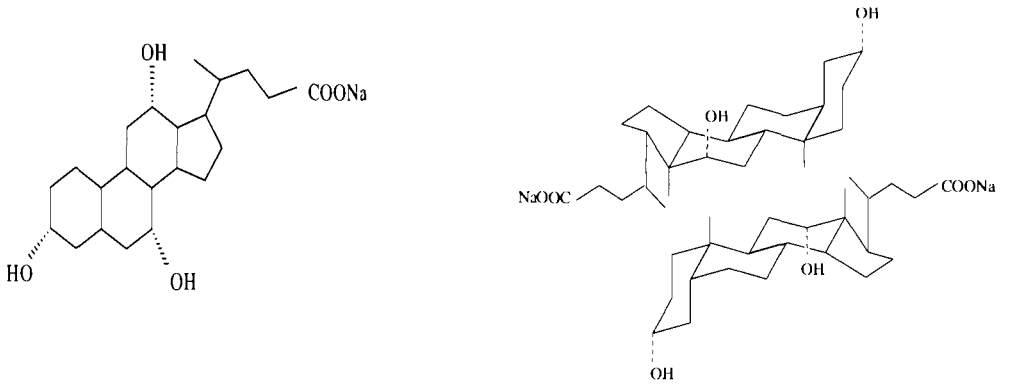

(a) (b)

Fig. 7. Chemical and micellar structures of SC.

Fig.8 illustrates the typical migration behavior of a neutral solute in MECC using an anionic surfactant in the running buffer. When an anionic surfactant such as SDS is employed, some neutral analytes that are incorporated into the micelle migrate at the velocity of the micelle, while other neutral analytes that remain free from the micelle migrate at the electroosmotic velocity. The negatively-charged micelle would migrate toward the positive electrode under the effect of electrophoresis. But, EOF, which is

usually of a higher magnitude than the electrophoretic migration of the micelle (under neutral or alkaline conditions), transports the bulk solution toward the negative electrode. So the anionic micelle also travels toward the negative electrode, but at a retarded velocity.[57] Thus, depending on different partition coefficients of the analytes into the micelles, separation of different analytes can be obtained. The analyte must migrate at a velocity between the electroosmotic velocity (fastest) and the velocity of the micelle (slowest). Highly polar neutral solutes which do not interact with the micelles migrate at the velocity of the EOF. Therefore, these solutes such as MeOH, acetone or mesityl-oxide, are often used as EOF marker.

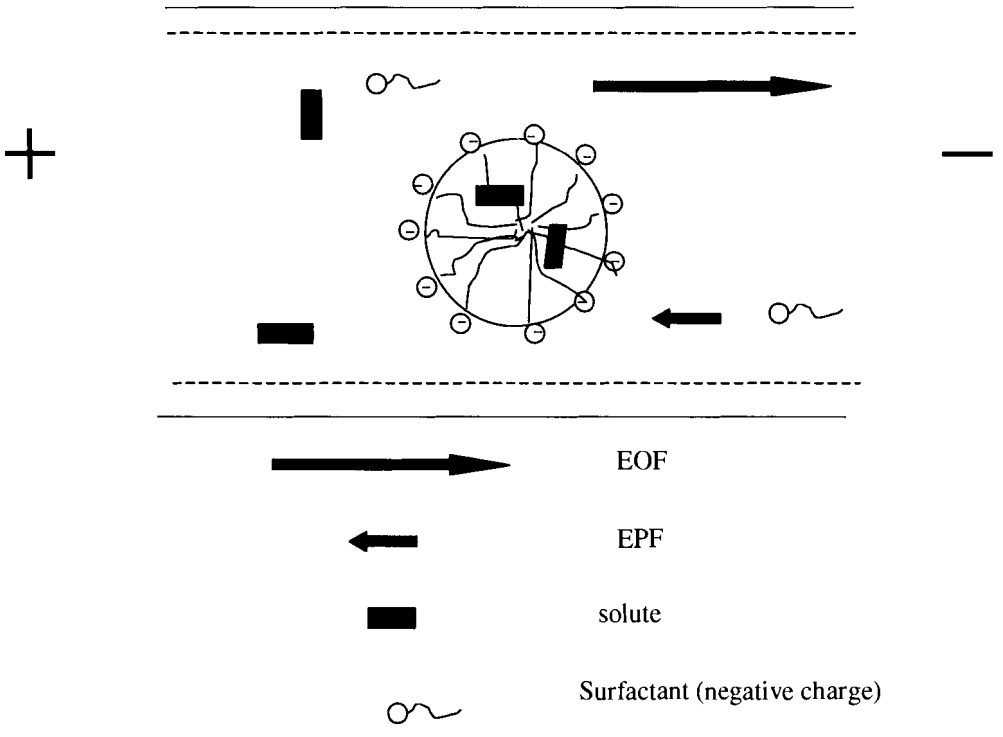

Fig. 8 Schematic diagram of the separation principle of MECC.

Neutral molecules can only be separated by their differential partition into micelles. Separation of charged species can also be enhanced by their differential partition into micelles in addition to their different electrophoretic mobility.

2.5 Cyclodextrin-modified micellar electrokinetic capillary chromatography (CD-MECC)

It has been well known that chiral substances may possess different pharmacological effects in biological systems, so thorough separations of chiral compounds are becoming increasingly important. Cyclodextrin (CD) is a buffer additive commonly used in order to improve the separation of geometrical, structural and optical isomers.[58] The basic structures of CD comprise of six, seven, or eight glucopyranose units attached by α–1,4 linkages and are referred to as α-, β-, γ- CD, respectively. The interior of the CD is quite hydrophobic and is chiral. Fig.9 shows the structure and shape of β-CD.

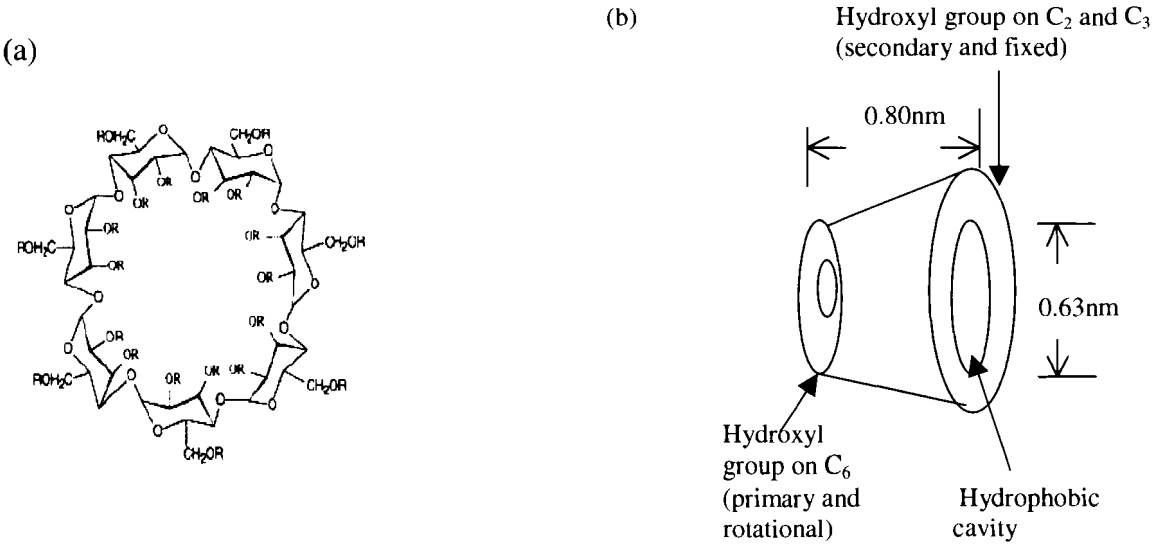

Fig. 9 Structure and shape of β-CD.
(a) chemical structure of β-CD (R=H) (b) shape of β-CD

When the solutes have identical mobilities, CDs can be employed in order to obtain separation. The principle of separation should be attributed to the different equilibrium constants for the formation of the inclusion complexes of different solutes interaction with the hydrophobic cavity of CD. Since β-CD is neutral, it migrates at the EOF. If the migration time of solutes is smaller and separation can not be achieved, micelles will be needed to elongate the analysis time. Fig. 10 shows the separation mechanism for CD-MECC.

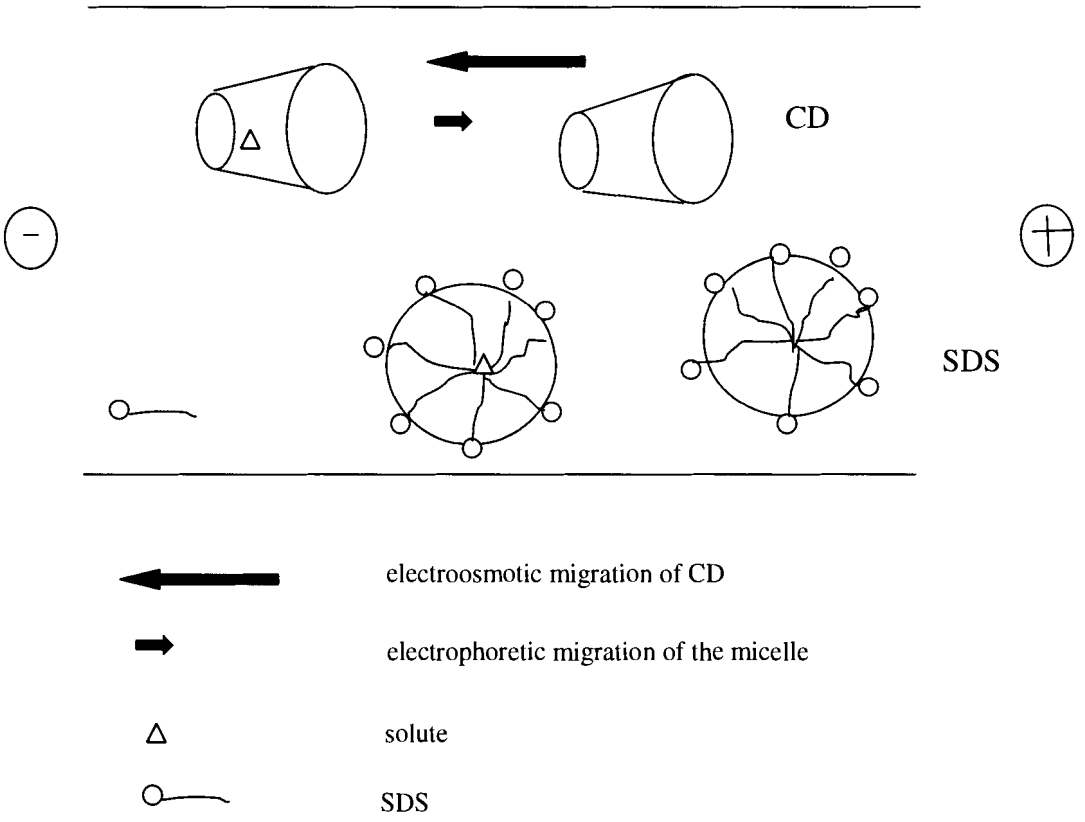

Fig. 10 Schematic illustration of the separation principle of CD-MECC.

Micelles and CDs have no interaction between each other when they coexist in aqueous solution. An uncharged cyclodextrin migrates to the negative electrode at the EOF velocity. The hydrophobic interior of CDs provides an alternative site for hydrophobic compounds which usually interact with micelles. Therefore, the separation mechanism is based on the differences in solutes' partition coefficient between the micelle and the CD. Hydrophobic compounds are then distributed between micelles and CDs.

2.6 Research Objectives

Analytical separation and quantitation of bioactive compounds in licorice is essential to developing a scientific basis for understanding of the many medical effects that have been observed clinically.

In this research, first, different modes of CE, such as CZE, MECC, CD-MECC, were employed to optimize the separation of four major bioactive components from licorice root extracts. Since 18α-GA and 18β-GA are diastereoisomers, their separation is more difficult. Common buffer additives, which included sodium dodecyl sulfate (SDS) and bile salts like sodium cholate (SC), were added to the buffer. Chiral-selective reagent such as β-cyclodextrin (β-CD) was employed for the separation of the two diastereoisomeric components. Parameters, such as buffer pH, capillary temperature, amount of organic modifier, were varied for the optimization of the separation of the licorice components. Second, several raw and roasted licorice root samples were analyzed by the optimized and other separation methods to examine any differences in composition profile.

Chapter 3. Experimental Section

3.1 Reagents

Glycyrrhizin (GL, CAS# 53956-04-0, 75%), isoliquiritigenin (IQ, CAS# 961-29-5, 99%) and 18α-glycyrrhetinic acid (18α-GA, 1449-05-4, 98%) were obtained from Sigma Chemical Co. (St. Louis, MO, USA), 18β-glycyrrhetinic acid (18β-GA, 471-53-4, 97%) was obtained from Aldrich Chemical Company (Milwaukee, WI, USA). Sodium dodecyl sulphate (SDS), sodium cholate (SC), β-cyclodextrin (β-CD) and sodium tetraborate were obtained from Sigma Chemical Co. Sodium hydroxide and hydrochloric acid were obtained from BDH Co. (Toronto, ON). Water that was purified to have resistance of 18 MΩ, Barnstead water purification system model (VWR Canlab, Mississauga, ON), was used. Methanol, in HPLC grade, was supplied by BDH. All chemicals are of analytical grade unless otherwise specified.

(1) Raw licorice root (S1) was obtained from Wing Shing Medical Co. (Vancouver, BC).

(2) Raw licorice root (S2) and roasted licorice root (S3) were obtained from Bo Ai Medicine Co. Ltd (Vancouver, BC.).

(3) Raw licorice root (S4a) and roasted licorice root (S4b) were from the same source as in (2). The raw licorice root (S4a) was heated with honey to obtain roasted licorice (S4b).

3.2 Instrument

3.2.1 CE

All experiments were carried out on a commercial CE system (MDQ, Beckman-Coulter, Fullerton, CA). CE separations were performed with the cathode at the detector end of the capillary. Uncoated fused-silica capillary columns (id, 50 μm or 75 μm), with a total length of 60.2 cm, were used. The temperature of the capillary was kept at 25°C, unless stated otherwise, using a liquid coolant flowing through the capillary cartridge. The temperature for sample storage was set at 4°C so that the samples were prevented from evaporation before experiments. The running voltage was 17kV unless stated otherwise. The photodiode array (PDA) detector was used to collect electropherogram from 190-400 nm, data rate is 4.0 data points per second. Electrophoregrams were reported at 254 nm, unless otherwise stated. Injections were performed in the hydrodynamic mode, and the injection time was set at 1s or 5s and injection pressure is 0.5 psi.

3.2.2 pH meter

3.2.2.1 Operation procedure

1. Rinse the electrode with deionized water and wipe the sides and tip carefully with a Kimwipe before measurement.
2. Immerse the electrode into a standard solution or sample solution within a beaker.

3. Press the button on the pH measurement mode, and wait for a while, read the value.
4. Press the button to standby mode, rinse the electrode with deionized water, put the electrode back in its KCl/AgCl storage solution.

3.2.2.2 Calibration

1. Press CAL. Press the CLEAR key once to remove the existing calibration.
2. Stir the electrode in the rinsing buffer of pH 4. Wipe with a Kimwipe. Stir the electrode in the clean buffer of same pH and press the READ key. When the Auto-Eye stops flashing, calibration at that pH 4 is complete.
3. Rinse the electrode with clean water, wipe, and repeat step 2 to calibrate at pH 7.
4. Press EXIT to finish the calibration.

3.3 Procedure

3.3.1 Preparation of buffers

For CZE mode, the running buffer was prepared by dissolving appropriate amount of borax (sodium tetraborate) in water to form 10 and 50 mM solutions, adjusted to the desired pH by 6M HCl. In MECC mode, the buffer was made by adding appropriate amount of SDS or SC to the sodium tetraborate buffer. For CD-MECC mode, a chiral additive, β-CD was added to the buffer solutions. The amounts of SDS, SC, and β-CD are expressed in final concentrations. All the run buffers employed in various experiments are coded and summarized in Table 1.

Buffer Name	composition
Buffer A	50 mM sodium tetraborate pH8.5
Buffer B	50 mM sodium tetraborate + 25 mM SDS pH8.5
Buffer C	50 mM sodium tetraborate + 25 mM SDS + 20 mM β-CD pH8.5
Buffer D	50 mM sodium tetraborate + 25 mM SDS + 20 mM β-CD + 10% MeOH pH8.5
Buffer E	50 mM sodium tetraborate + 25 mM SDS + 20 mM β-CD + 15% MeOH pH8.5
Buffer F	50 mM sodium tetraborate + 25 mM SDS + 20 mM β-CD + 20% MeOH pH8.5
Buffer G	50 mM sodium tetraborate + 25 mM SDS + 20 mM β-CD + 30% MeOH pH8.5
Buffer H	10 mM sodium tetraborate + 25 mM SC pH8.5
Buffer I	10 mM sodium tetraborate + 25 mM SC + 20 mM β-CD pH 8.5
Buffer J	10 mM sodium tetraborate + 25 mM SC + 20 mM β-CD pH 9.0
Buffer K	10 mM sodium tetraborate + 25 mM SC + 20 mM β-CD pH 9.5
Buffer L	10 mM sodium tetraborate + 25 mM SC + 20 mM β-CD pH 10.0
Buffer M	10 mM sodium tetraborate + 25 mM SC + 20 mM β-CD + 10% MeOH pH 8.5
Buffer N	10 mM sodium tetraborate + 25 mM SC + 20 mM β-CD + 15% MeOH pH 8.5
Buffer P	10 mM sodium tetraborate + 25 mM SC + 20 mM β-CD + 20% MeOH pH 8.5
Buffer Q	50 mM sodium tetraborate+ 35 mM SDS pH8.5
Buffer R	10 mM sodium tetraborate pH8.5
Buffer S	50 mM sodium tetraborate+ 25 mM SDS + 20 mM CD + 10 mM SC + 30% MeOH pH 8.5
Buffer T	10 mM sodium tetraborate + 25 mM SDS pH8.5
Buffer U	20 mM sodium tetraborate pH8.5
Buffer V	50 mM sodium tetraborate + 25 mM SDS + 20 mM CD + 10 mM SC + 25% MeOH pH8.5
Buffer W	50 mM sodium tetraborate + 50 mM SDS + 20 mM SC pH8.5

Table 1. compositions of all CE run buffers

3.3.2 Preparation of standard solutions

Appropriate amount of GL, IQ and 18β-GA were dissolved in methanol to form 1mg/ml stock solutions. Since 18α-GA was less soluble, its concentration for stock solution is 0.5 mg/ml. In earlier work the ratio of 18α-GA and 18β-GA was 1:1, in latter work, the ratio was 1:2. The standard mixture was made by adding 200μl of each standard, then diluting to 2 ml with 10 mM sodium tetraborate running buffer.

3.3.3 Preparation of licorice samples

Two methods have been used, namely reflux and sonication. (1) 7g of raw licorice root (S1 and S2) was refluxed with 80 ml of methanol (HPLC grade) at 80°C for 60 min. (2) A few pieces of raw licorice root (S2 and S4a) and roasted licorice root (S3, S4b) were ground with the mortar and pestle to fine powder. 0.5g of ground materials was weighed. The samples were mixed with 20ml of methanol (HPLC grade), ethanol (95%) or water, then sonicated and extracted for 30 min. The yellowish extract solutions were filtered and the residues were discarded. The liquid extract was stored at 4°C in the refrigerator before CE experiments.

3.3.4 Preparation of capillary cartridge

A length of 65 cm (see Fig.11) of fused silica capillary was cut according to the instrument manual.

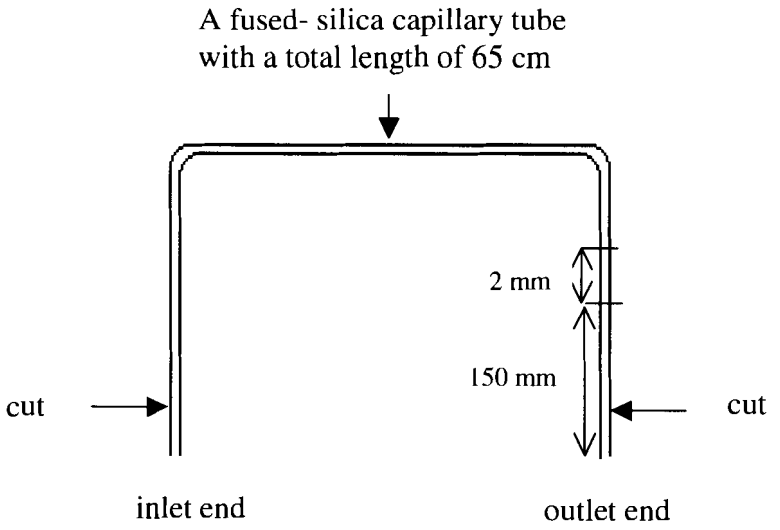

Fig.11 capillary preparation.

At a calculated length (150 mm from the outlet end) of capillary, a short section (2 mm width) of polyimide coating was burnt and wiped clean with acetone to create a detection window. The window allows UV light to pass through the fused silica capillary wall for detection. A plastic tube for liquid coolant circulation was set between the two ends of cartridge. The capillary was inserted into the plastic tube. The excessive length of capillary at both ends was cut out based on a template so that the total capillary length was 60.2 cm, and the distance from the inlet end to the detection window was 50 cm, and the distance from the outlet end to the detection window was 10.2 cm. An aperture block of 800μm slit width was inserted. Finally, an O-ring was put to create a cushion between the capillary window and the optical fiber end of the UV source. This step should be

performed at last. If the O-ring was inserted before insertion of the aperture block, the capillary would be broken.

3.3.5 Capillary conditioning

To condition the inner capillary surface, 1 mol/L HCl, water, 0.1 mol/L NaOH, water, running buffer were used in sequence according to the instrument manual. The rinse time were 5 min, 2 min, 10 min, 2 min, 2 min, respectively. The procedure was performed at the beginning of each day.

3.3.6 CE experiment

Between runs, the capillary was washed with water, methanol, and water for 1 min each. Filling the capillary with the running buffer was employed. The use of methanol in rinsing between runs helped to clean out capillary blockage, if any.

The sample was injected into the capillary by hydrodynamic flow. The amount of sample injected could be calculated by the injection time (1 or 5 s) and pressure (0.5 psi). The temperature of capillary was kept constant by means of the coolant. The coolant was occasionally filled into the storage tank by a 50 ml syringe if the liquid coolant level was low. Usually, 10 ml of coolant was added each time. If frequent addition of coolant was required, there would likely be a coolant leakage problem, and the capillary cartridge should be inspected and adjusted.

All the solutions were filtered through syringe filters containing a nylon membrane with a pore diameter of 0.45 μm. For a CE experiment, a method file (j3.met) was created, which was given in Appendix 1A. In the method sequence, several rinsing steps were required to clean and re-condition the capillary. Then the capillary was filled with the run buffer solutions before the injection of a sample was performed. Finally, an electric voltage was applied to initiate separation. Different CE modes (ie CZE, MECC, CD-MECC) were operated conveniently in the same instrument only using different run buffers. Important information about the method should be included in the method file so that subsequent data interpretation can be made easier with exact experimental conditions.

The CE instrument, which contained an autosampler, was highly automated to carry out various CE runs using different samples or different buffers. A batch file (e.g. 114.seq) was created, which was given in Appendix 1B. In each run, a method file (j3.met) was called. The same method file would be used for different samples as long as all the experimental conditions were identical. If a different run buffer (with different additives, pH) or different capillary temperature was used, a different method file was called. The method file, which was usually saved with data files for subsequent data processing, should never be altered. Current loss has been a common problem. This was caused by (1) capillary breakage. (2) precipitation of sample in the capillary. (3) gas bubble formation. These problems could be distinguished by noting if the current resumed after the CE run was completed or using a lower voltage.

3.3.7 General maintenance of CE system

The instrument should be maintained every week by cleaning the electrode area and the vial caps, especially when organic solvent additives were used in the run buffer. Partial degradation of the vial cap, which was made of rubber, has caused serious sticking vial problem leading to failure of autosampler and capillary breakage.

Chapter 4 Results and Discussion

4.1 CZE using borate

The selection of electrophoretic run buffer is critical for CE separation. The initial target of this investigation was using an alkaline sodium borate buffer system commonly used in capillary zone electrophoresis (CZE) in the search for optimal separation conditions. As a starting point for the separation of the four pharmacological components in licorice, 50mM sodium tetraborate solution (buffer A) was employed as the running buffer. The results are shown in several electropherograms for the standard mixture and individual compounds. Peak identification is achieved by comparing the migration times of the peaks in the mixture (Fig.12a) and in single compounds (Fig.12b-e). By comparing Fig.12a, c and d, we find that 18α-GA (2) and 18β-GA (3) elute as a single peak. The third and fourth peaks are GL (1) and IQ (4), respectively. A little bump in front of GL (1) may be due to an impurity of IQ (4'). Here, it is worthwhile to note that the first peak has both negative and positive portions, which is attributed to the presence of methanol in the samples. Although methanol does not absorb UV at 254 nm very well, a disturbance in the baseline is usually observed because of the change in refractive index as the solution interface of the sample plug reaches the detector.

As shown in Fig.12, 18α-GA (2) and 18β-GA (3) migrate earlier than GL (1), while GL (1) migrates earlier than IQ (4). The possible reason is attributed to the charges of these compounds in the alkaline pH. According to Fig.1, 18α-GA and 18β-GA will produce

one carboxylate group, GL three carboxylate groups and IQ three phenonate groups. Thus, the number of negative charges under alkaline conditions in descending order is GL, IQ > 18α-GA, 18β-GA. Moreover, the molecular weight of GL is the greatest among the four components. Therefore, their electrophoretic mobilities (negative) which depends on the charge to mass ratio, are in the order of 18α-GA, 18β-GA< GL<IQ. As a result, their net mobilities, which are positive after combining with positive electroosmotic mobility, are in the order of IQ< GL< 18α-GA, 18β-GA, and their migration times are in the order of 18α-GA, 18β-GA< GL<IQ.

To assist in peak identification, we also make use of the information collected by the photodiode array (PDA) detector (190-400 nm). As shown in Fig.13, we observe the information as depicted in the UV contour plots and realize the UV spectra of the peaks in the mixture matches with those in the single compounds. The UV spectra of 18α-GA in Fig.13c was not apparent when the full time scale (0-30 min) was selected. However, when the UV contour plot was expanded in the time scale (i.e. from 5-25 min), the UV profile was observed, as shown in Fig.13c'.

The familiar UV spectra of the four compounds could also be obtained from the PDA profile at the time when the compounds migrated. These spectra which were selected from Fig.12b,c,d,e were given in Fig.14a,b,c,d, respectively. Since we found 254 nm was a wavelength at which the absorbances of all compounds were high, we decided to report electropherograms of subsequent experiments at this wavelength.

The electric current information was also collected during the CE experiments. To illustrate this, the electric current profiles for Fig.12 were shown in Fig.15. It is apparent that the current reaches a fairly constant value shortly after the separation voltage was applied. The current slightly increases at the time (i.e. 10min) when the sample solvent (i.e. water), which is less electrically conducting, migrates out of the capillary. This time is slightly longer than the migration time, $t_{eo,}$ of the sample solvent, and can be correlated to t_{eo} by knowing the total capillary length, L_t (60.2cm), and the distance from the inlet to the detector, L_d (50cm). The current profile is important in trouble-shooting, especially when current loss occurs (see section 3.3.6).

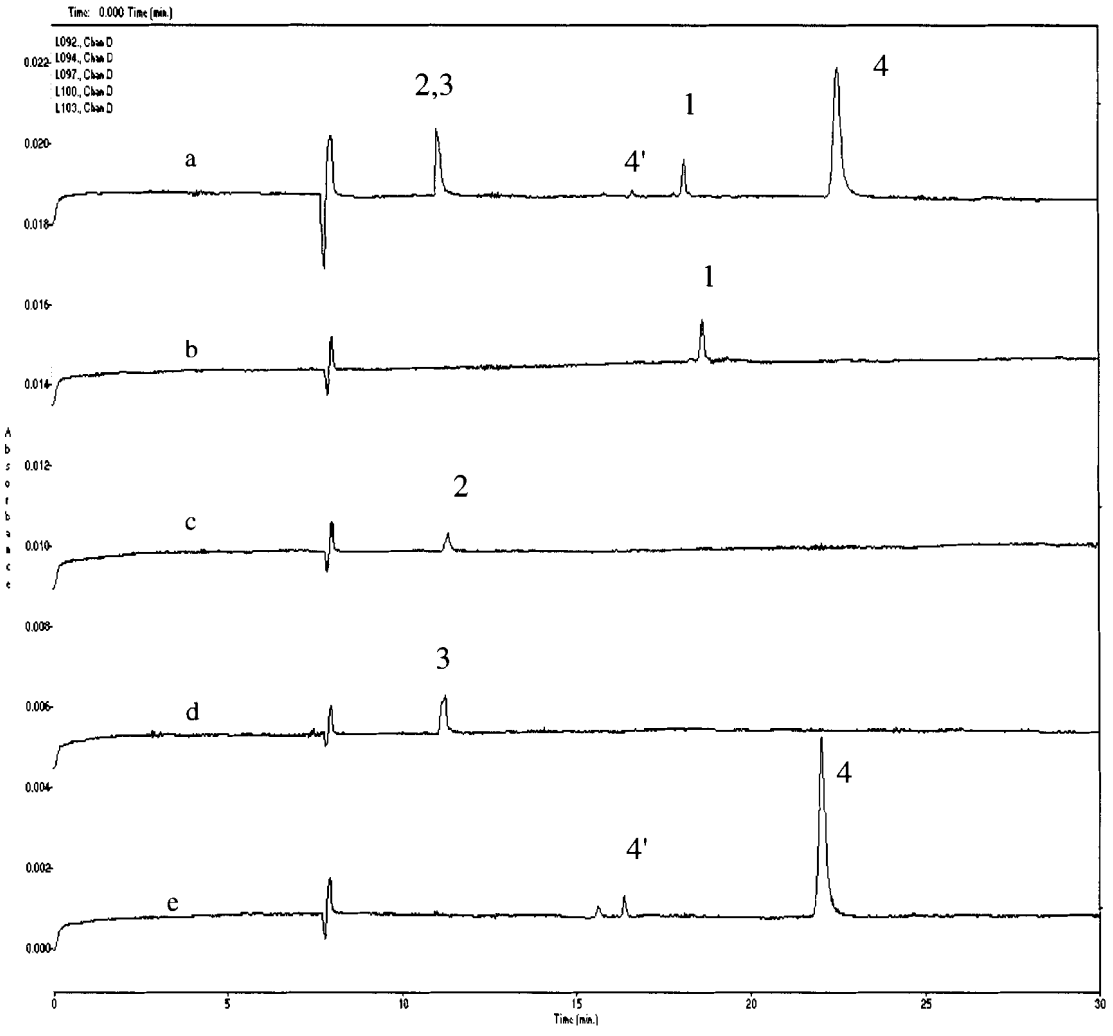

Fig.12 Electropherograms obtained for the separation of GL, 18α-GA, 18β-GA and IQ by CZE. Analytical conditions: 50 mM sodium tetraborate (buffer A); Voltage: 17 kV; Capillary: 50 μm × 60.2 cm; distance to detector: 50 cm; Wavelength: 254 nm.
(a) mixture; (b) GL (1); (c) 18α-GA (2); (d)18β-GA (3); (e) IQ (4 and 4')

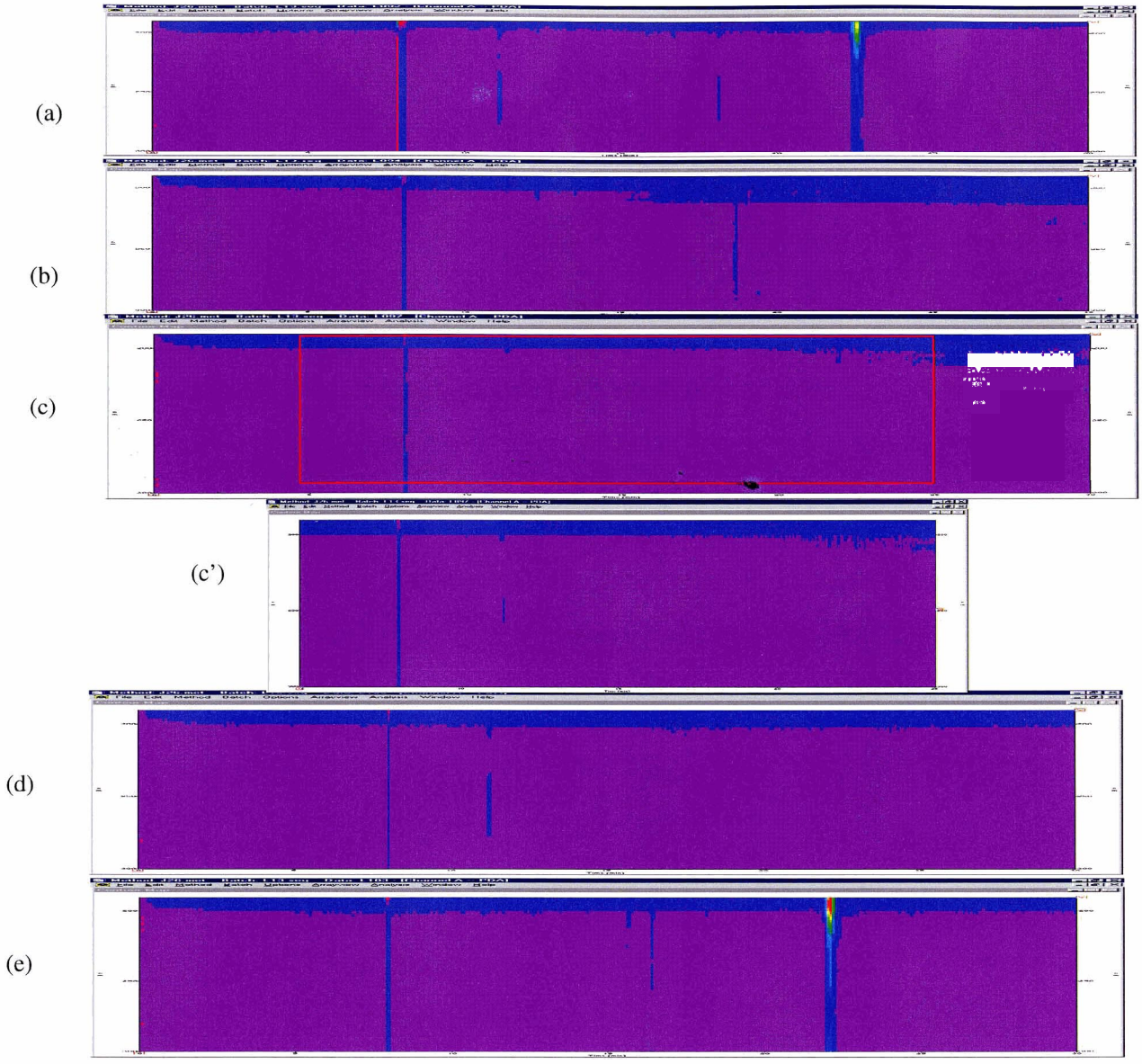

Fig.13 UV contour plots of (a) mixture; (b) GL; (c) 18α-GA; (c') 18α-GA from 5-25 min; (d) 18β-GA and (e) IQ (experimental conditions and matched electropherograms are shown in Fig.11). In all plots, horizontal axis represents time from 0-30 min (except in (c') 5-25 min) and vertical axis represents wavelength from 190 nm (top) to 400 nm (bottom).

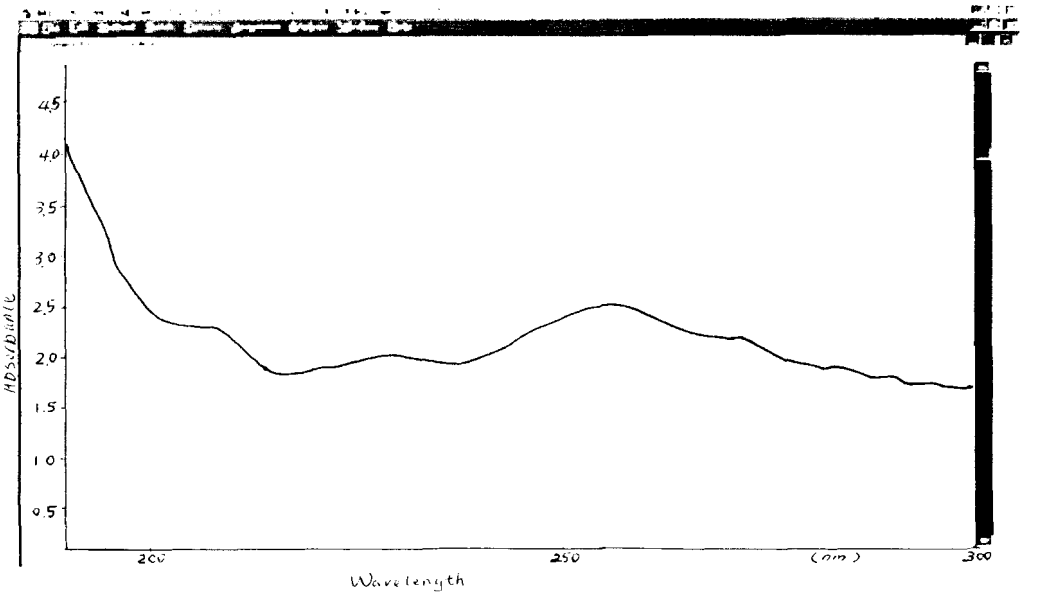

(a)

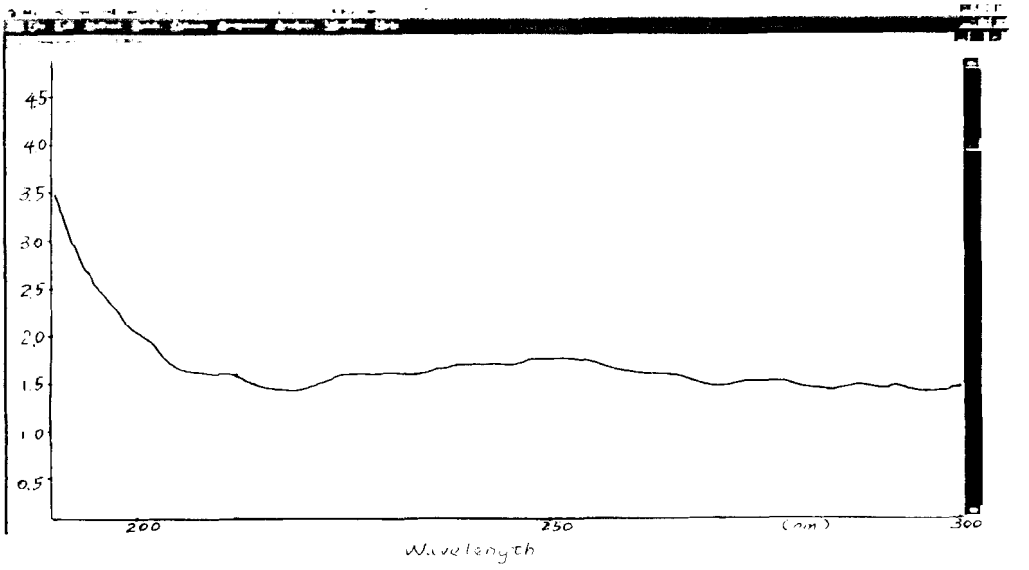

(b)

Fig.14 UV spectra for Fig.12b-e .
(a) for Fig.12b, (b) for Fig.12c.

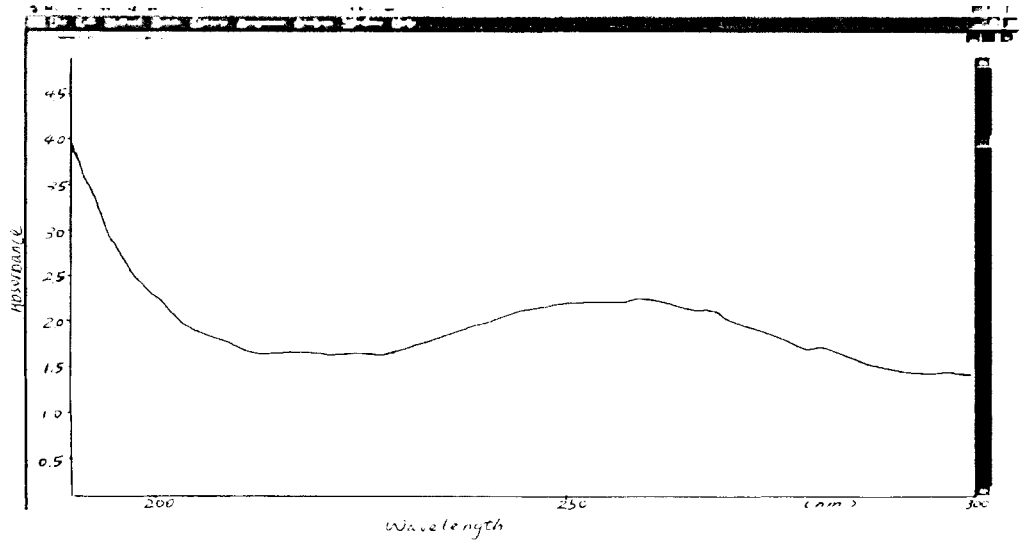

(c)

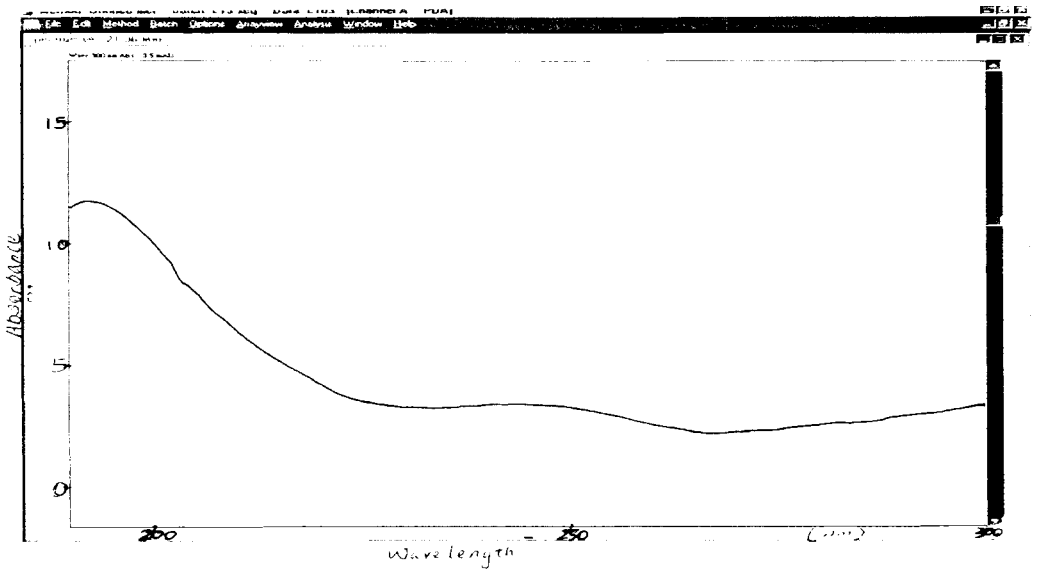

(d)

Fig.14 UV spectra for Fig.12b-e (continued).
(c) for Fig.12d, (d) for Fig.12e.

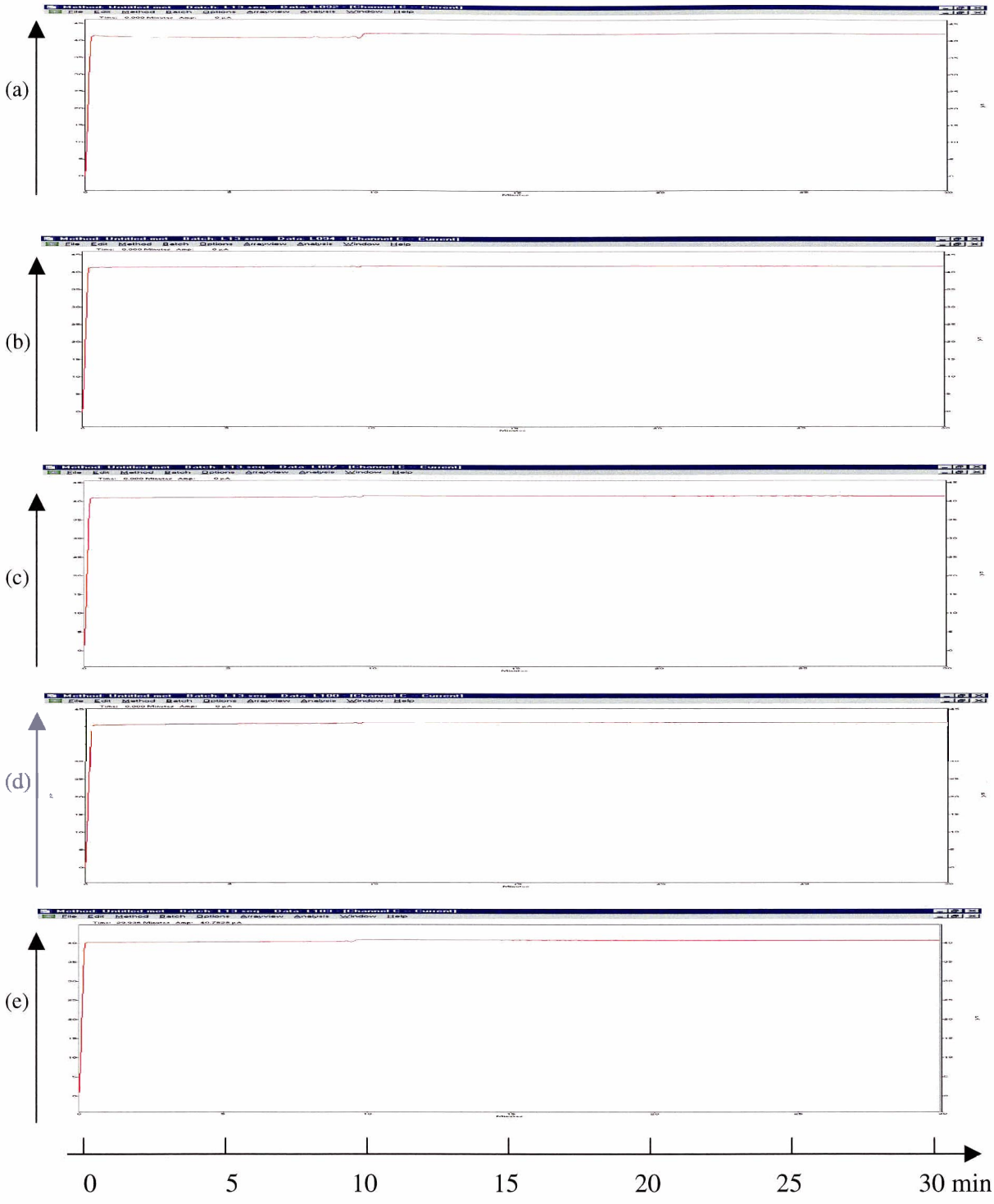

Fig.15 Electric current profiles for Fig.12a-e. (a) mixture; (b) GL; (c) 18α-GA; (d) 18β-GA; (e) IQ. The vertical axis represents current (0-45μA) and the horizontal axis represents time (0-30 min)

The repeatability of CE experiments was also studied. Fig.16a-c represent three consecutive runs for the standard mixture; Fig.16d-f represent three consecutive runs for GL; Fig.16g-i represent three consecutive runs for 18α-GA; Fig.16j-l represent three consecutive runs for 18β-GA; Fig.16m,n,p represent three consecutive runs for IQ. The migration times of these runs are tabulated in Table 2. The relative standard deviations (RSD) of migration time for four components are also shown in Table 2. RSD values are smaller in single compounds as compared to those in the standard mixture (for singles, RSD 0.2-0.5%; for compounds in the mixture, RSD within 1.9%). This may indicates the possibility of matrix effect. In the standard mixture interactions between standard compounds in the mixture.

Electrophoretic mobilities were calculated according to equation 11 and tabulated in Table 2. For single standard, RSDs are between 0.5 to 2.0%; for standard mixture, RSDs are between 0.8 to 1.9%. We found that the RSDs for IQ and GL are reduced when electrophoretic mobilities, instead of migration times, were used. This indicates that part of the variations in migration time is caused by a change in the EOF, which is alleviated when electrophoretic mobility is considered. However, the greater μ_{ep} RSD in 18α-GA and 18β-GA may be resulted, in part, from the short migration time. When the concentration of sodium tetraborate was lower (i.e. 10 mM), the electroosmotic flow was faster, see equations 7a-c. As a result, GL and IQ are not separated, as shown in appendix 2A.

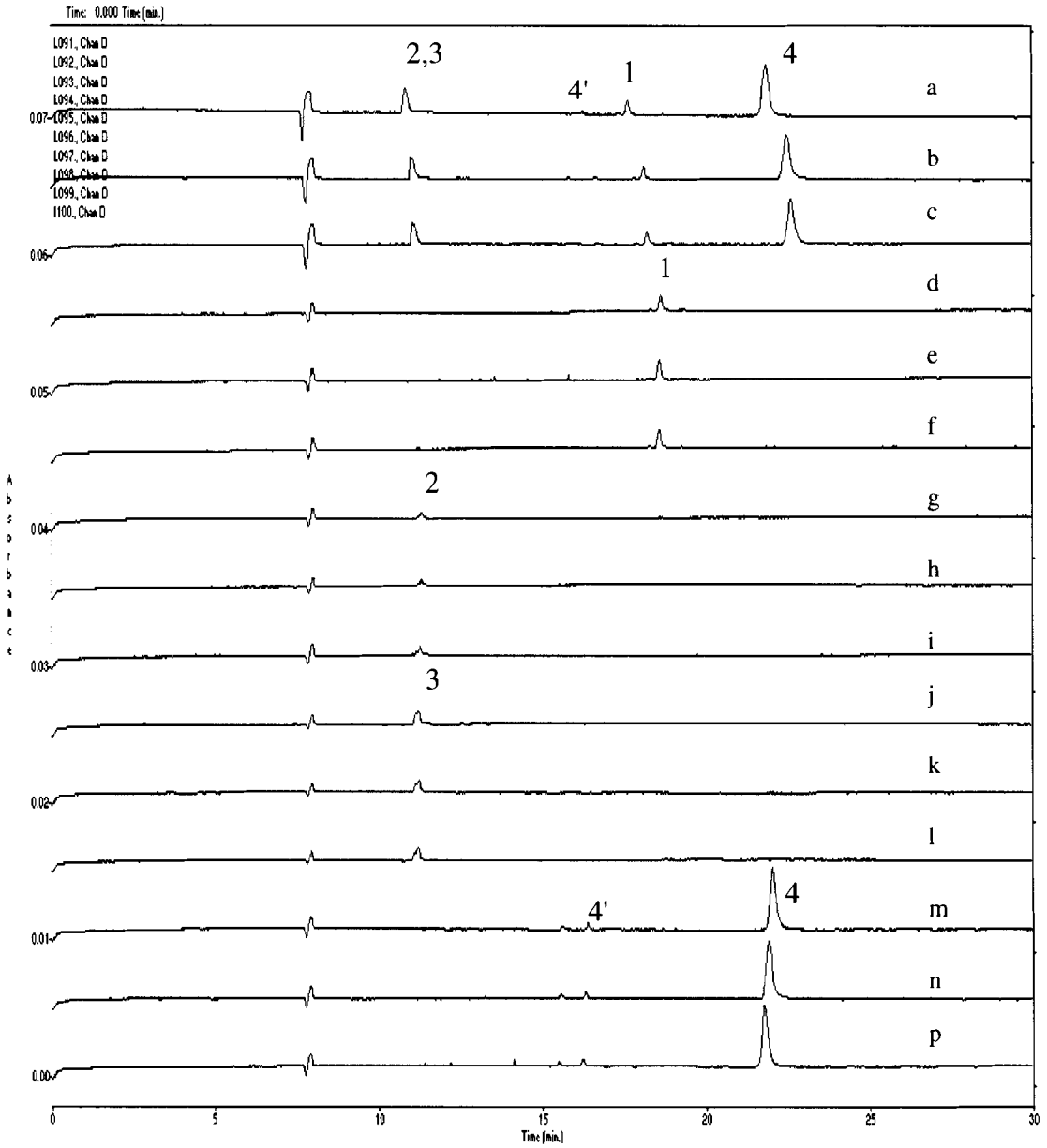

Fig.16 Electropherograms obtained for the repeatability of separation of GL, 18α-GA, 18β-GA and IQ by CZE. Analytical conditions: 50mM sodium tetraborate (buffer A); Voltage: 17kV; Capillary: 50 μm × 60.2 cm; distance to detector: 50 cm; Wavelength: 254 nm.

(a)-(c) mixture; (d)-(f) GL (1); (g)-(i) 18α-GA (2); (j)-(l)18β-GA (3); (m)-(p) IQ (4 and 4')

	GL		18α-GA		18β-GA		IQ	
	in mix	single	in mix	single	in mix	single	in mix	single
Migration Time t_m(min)	17.640	18.687	10.852	11.355	10.852	11.229	21.872	22.039
	18.184	18.603	11.020	11.313	11.020	11.229	22.542	21.913
	18.266	18.603	11.061	11.271	11.061	11.187	22.668	21.830
Average ±RSD	18.03 ± 1.9%	18.63 ± 0.3%	10.98 ± 1.0%	11.31 ± 0.4%	10.98 ± 1.0%	11.22 ± 0.2%	22.36 ± 1.9%	21.93 ± 0.5%
Electrophoretic Mobility (μ_{ep}) (10^{-4} cm^2s^{-1} V^{-1})	-2.17	-2.16	-1.13	-1.17	-1.13	-1.14	-2.50	-2.44
	-2.14	-2.18	-1.09	-1.13	-1.09	-1.14	-2.46	-2.46
	-2.17	-2.16	-1.12	-1.17	-1.12	-1.15	-2.48	-2.47
Average ± RSD	-2.16 ± 0.8%	-2.17 ± 0.5%	-1.11 ± 1.9%	-1.16 ± 2.0%	-1.11 ± 1.9%	-1.14 ± 0.5%	-2.48 ± 0.8%	-2.46 ± 0.6%

Table 2. Repeatability studies for standard solutions of four components separated by CZE using buffer A

(a)

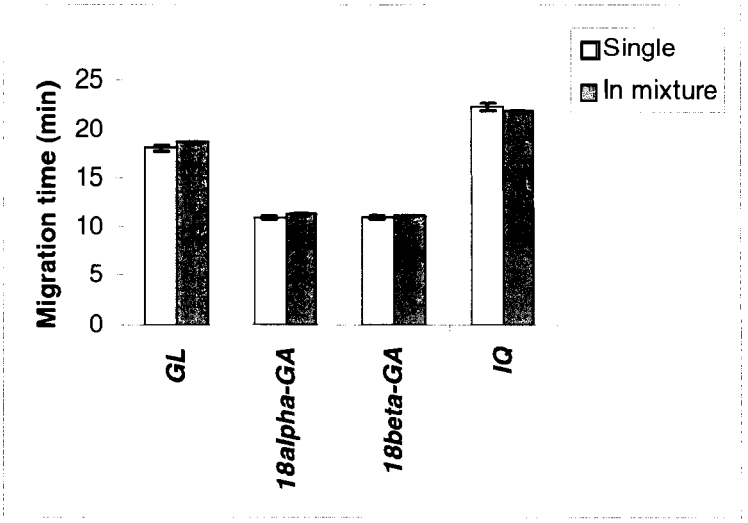

(b)

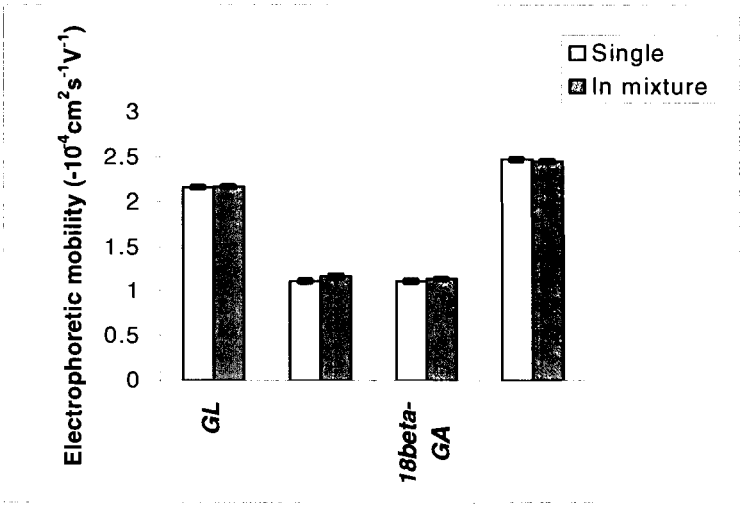

Chart 1. Repeatability studies for standard solutions of four components separated by CZE using buffer A. Data in chart are averages of migration time (a) and electrophoretic mobility (b) in single standard solutions and in mixture from Table 2. Error bars represent SD.

4.2 MECC using SDS

Since 18α-GA and 18β-GA are not separated in buffer A and our goal is to separate all the four compounds, further experiments were conducted by adding an anionic surfactant, sodium dodecyl sulfate (SDS), to the run buffer, leading to the use of the micellar electrokinetic capillary chromatography (MECC) mode. Therefore, SDS (25mM), which was above its critical micelle concentration (CMC) of 8mM [51], was added to buffer A to form buffer B (see Table 1). Micelles of SDS were formed by spontaneous self-association. The mode of CE changed from CZE to MECC.[60] As shown in Fig.17a, three peaks are observed. In comparison of Fig.17a and b, we note that the peak at around 18 min is due to GL. From Fig.17e, there are two prominent peaks resulting from IQ. Migration order for GL and IQ was the same using both buffers A and B. Unfortunately, within a run time of 30 min, no peaks show up for 18α-GA and 18β-GA (see Fig.17a, c and d). Apparently, their migration times were much longer than 30 min. These two diastereoisomers may partition effectively into SDS micelles, i.e. they strongly interact with the interior of the micelles formed by the hydrophobic tails of SDS.[59] This interaction leads to their long migration time. The repeatability of CE run using this method was also shown in Fig.A-3 (see appendix 3). However, when the electroosmotic flow was faster as in less concentrated sodium tetraborate (as given in appendix 2A), 18α-GA and 18β-GA could be observed, though they were not separated (as given in appendix 2B).

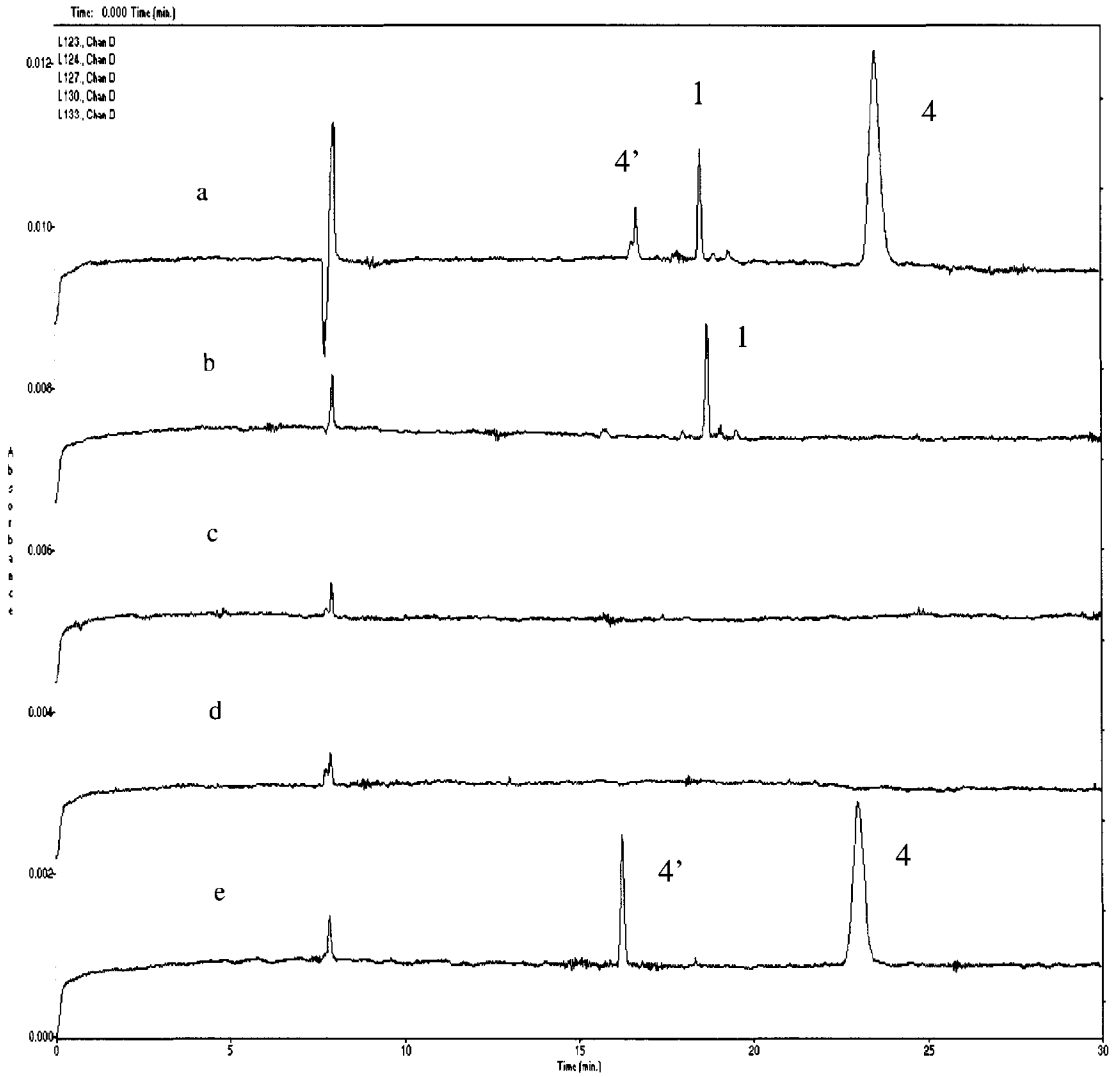

Fig.17 Electropherograms obtained for the separation of GL, 18α-GA, 18β-GA and IQ by MECC (SDS). Analytical conditions: 50 mM sodium tetraborate + 25 mM SDS (buffer B); Voltage: 17 kV; Capillary: 50 μm × 60.2 cm; distance to detector: 50 cm; Wavelength: 254 nm.
(a) mixture; (b) GL (1); (c) 18α-GA (2); (d)18β-GA (3); (e) IQ (4 and 4')

Further increase in SDS concentration from 25 mM to 35 mM worsens the situation by prolonging the analysis time apparently because of even more extensive interaction between the compounds and the micelles. As shown in Fig.18, even the major peak for IQ does not appear. It was because of greater ionic strength of the solution, which decreases zeta potential, leading to a more slowly electroosmotic flow. A compound, such as Sudan III, which shows the migration time of micelles, should have been used to indicate how long the CE should be run to observe, and not to miss, more hydrophobic compounds. Since 30 min was already a long analysis time, no attempt has been made to extend the CE run time so as to see the peaks due to 18α -GA and 18β-GA.

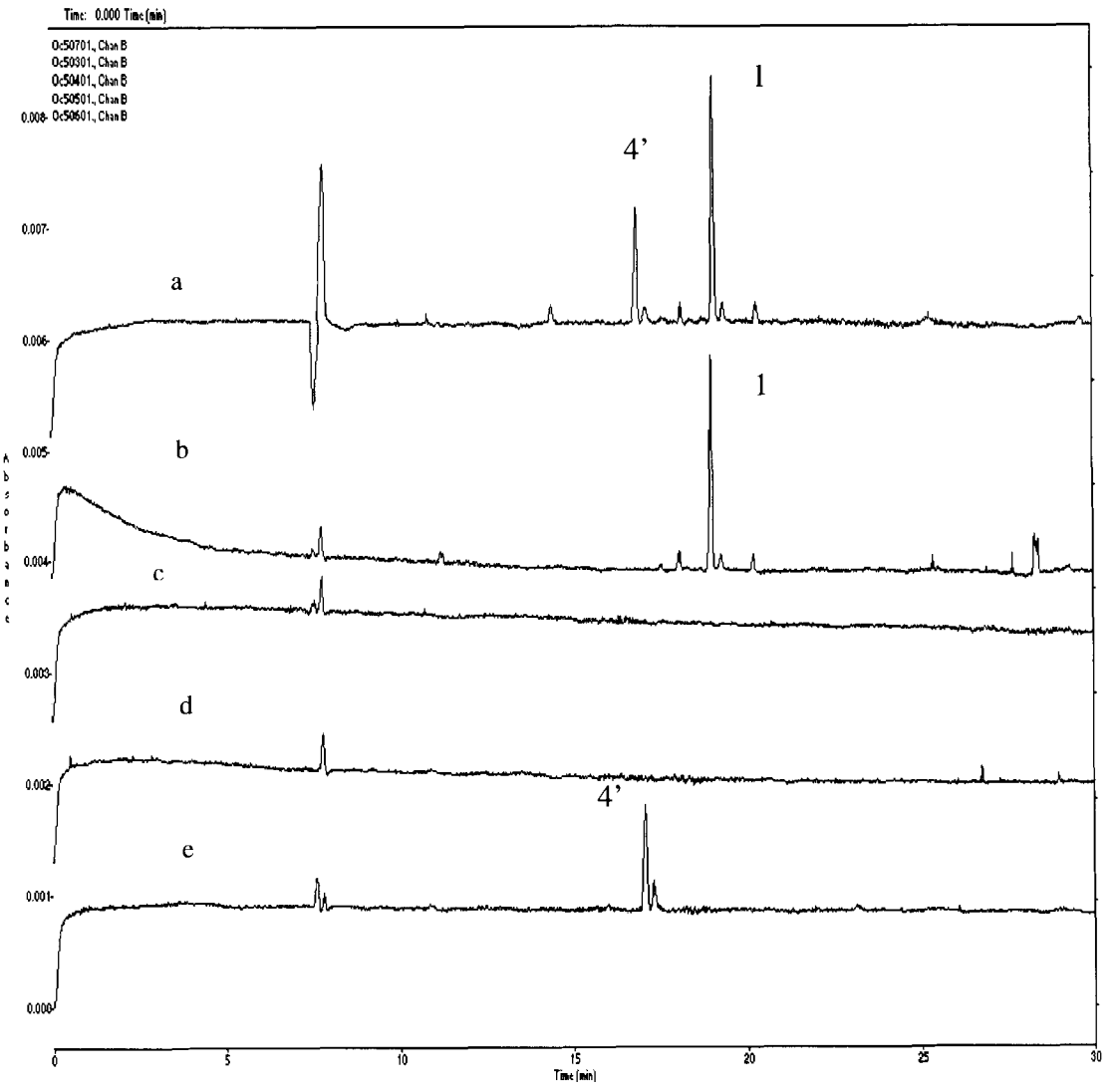

Fig.18 Electropherograms obtained for the separation of GL, 18α-GA, 18β-GA and IQ by MECC (SDS). Analytical conditions: 50 mM sodium tetraborate + 35 mM SDS (buffer Q); Voltage: 17 kV; Capillary: 50 μm × 60.2 cm; distance to detector: 50 cm; Wavelength: 254 nm.

(a) mixture; (b) GL (1); (c) 18α-GA (2); (d)18β-GA (3); (e) IQ (4 and 4'). Note that another component from IQ (4) did not appear by 30 min.

4.3 CD-MECC (SDS)

Since 18α-GA and 18β-GA are diastereomers, their chemical separation is not straightforward as illustrated by the two buffer systems previously described. In principle, two diastereomers, which have different mobilities resulted from molecular shape differences, can be separated from each other by CE using a non-chiral buffer system. However, such difference does not guarantee that it is great enough to permit separation. It is because the difference in the mobilities of ionized diastereoisomers in solution are affected and maybe masked by their solvation shells. Therefore, analytically useful differences in diastereoisomer mobilities are not expected to occur frequently.

In order to achieve the separation of 18α-GA and 18β-GA, a chiral selector cyclodextrin (CD) was added to the run buffer in the MECC mode. CD is usually used as an effective chiral additive in CE because of its ability to form inclusion complexes with a variety of molecules.[53] Because of the low cost of β-CD (versus γ-CD) and the greater cavity size (versus α-CD), β-CD was selected in this work. Fig.19 shows the electrophoregrams using buffer C, which was prepared with a final concentration of 20 mM β-CD added to buffer B (see Table 1). In Fig 19a, b and e, two peaks of IQ (4,4') show up earlier, while the peak of GL (1) shows up later. In addition, GL appears as a fronting peak. For the mixture as shown in Fig.19a, a broad tailing peak shows up. However, in single standard runs, no 18α-GA and 18β-GA peaks show up even within 40 min which was already longer than the usual run time of 30 min.

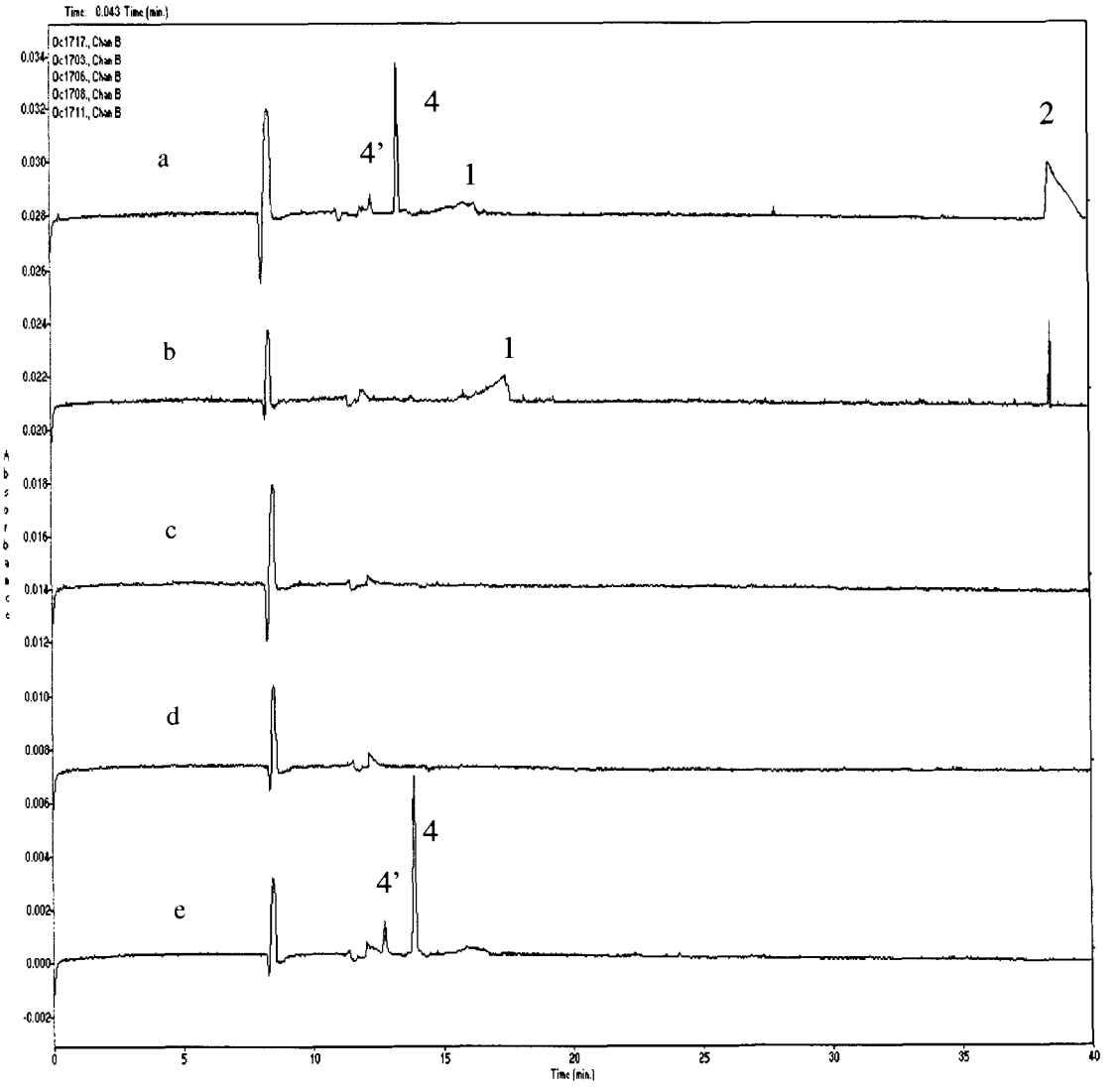

Fig.19 Electropherograms obtained for the separation of GL, 18α-GA, 18β-GA and IQ by CD-MECC. Analytical conditions: 50 mM sodium tetraborate + 25 mM SDS + 20 mM β-CD (buffer C); Voltage: 17 kV; Capillary: 50 μm × 60.2 cm; distance to detector: 50 cm; Wavelength: 254 nm.
(a) mixture; (b) GL (1); (c) 18α-GA (2); (d)18β-GA (3); (e) IQ (4 and 4')

An interesting observation is that the migration order for GL and IQ using buffer C is reversed in comparison of using buffers A and B. GL migrates later in buffer C, as compared to buffer A and B. The possible explanation is that IQ is smaller in size and maybe more easily gets inside the cavity of β-CD than GL does. As a result, IQ migrates faster than GL. Meanwhile, because of neutral properties of β-CD, the IQ-β-CD inclusion complex migrates close to EOF. Since no 18α-GA and 18β-GA peaks were observed in this buffer, it is concluded that 18α-GA and 18β-GA, still interact with SDS more strongly than with β-CD. The SDS micelles, which are negatively charged, migrates very slowly. Therefore, 18α-GA and 18β-GA did not appear within 40min, though one of them did appear in the mixture. So, we explore various ways to reduce the analysis time.

It is known that by using a higher voltage, faster EOF and shorter migration time occur (see equation 11). This is illustrated in Fig.20a in which the experiment was performed under similar conditions as in Fig.19 except that a higher voltage of 25 kV, instead of 17 kV, was employed for separation. Single standard electropherograms for Fig.20a are given in Fig.B-4 and Fig.B-5 in appendix 8. In this experiment, a crude separation of 18α-GA and 18β-GA was observed as two broad tailing peaks within 20 min. In this case, 18α-GA migrates earlier than18β-GA. This is due to the fact that 18α-GA is rod-shaped (Fig.1b), which may fit in the cavity of β-CD better than 18β-GA which is L-shaped. So, 18α-GA interacts more strongly with β-CD and migrates earlier.

In addition, another drawback of this method is the high current produced by a higher voltage (25 kV). The value of current increased from 93.2 ± 2.5 μA (17 kV) to 145.2 ±

5.0 μA (25 kV). Such a high current has led to the Joule heating problem even though there is coolant circulating around the capillary. Excessive Joule heating can have undesirable effects on both resolution and analyte stability. Another problem is the outgassing or boiling of the buffer. If the Joule heating can not be dissipated easily, boiling bubbles will be produced so that the capillary was blocked, thus causing loss of current. In order to solve this problem, a lower voltage was used. However, with decreased voltage, the analysis time was increased greatly (i.e. longer than 40 min, see Fig.20). In order to decrease analysis time, the shorter effective capillary detection length (10.2 cm from the detector to the outlet) and a lower voltage (10 kV) were used, with results shown in Fig.20b. The sample was injected from the outlet end and a reverse polarity (i.e. -10kV) was used. It should be noted that the total capillary length was not changed at all because the same capillary was used. Since a lower voltage was used, lower current, and hence, less heat was resulted. Fig.20b illustrates the electropherogram of the separation of four components. Separation was achieved within 20 min. Nevertheless, fronting peak of GL and tailing peaks of 18α-GA and 18β-GA still exist because the same run buffer (i.e. buffer C) was used. Component identification for Fig.20b is given in Fig.B-5 in appendix 8.

Although under the CD-MECC mode, four components of licorice were separated, the efficiency of the method was not satisfactory because of the tailing peaks of 18α-GA and 18β-GA and fronting peak of GL. This phenomenon is termed electrodispersion. The appearance of fronting and tailing peaks occurred when β-CD was added to the buffer. The addition of β-CD decreases the conductivity and electrophoretic mobility of the run

buffer. As regard to the reason for the changes of buffer mobility by adding β-CD, it is because β-CD is a neutral compound, which decreases the conductivity of the run buffer, leading to slower electrophoretic mobility. Thus, GL zone has a higher conductivity than the running buffer, it has a higher electrophoretic mobility than the latter. Then the front edge of the GL solute zone, which diffuses in the direction of migration, encounters a higher electric field on entering the less conducting buffer zone. This causes the diffusing solute to accelerate away from the solute zone, which results in zone fronting.[61] Conversely, the occurrence of tailing peak [61] is because 18α-GA and 18β-GA at the trailing edge diffuses into the running buffer and they also encounters an increase in electric field, but now in the same direction of migration and accelerates back into the solute zone.

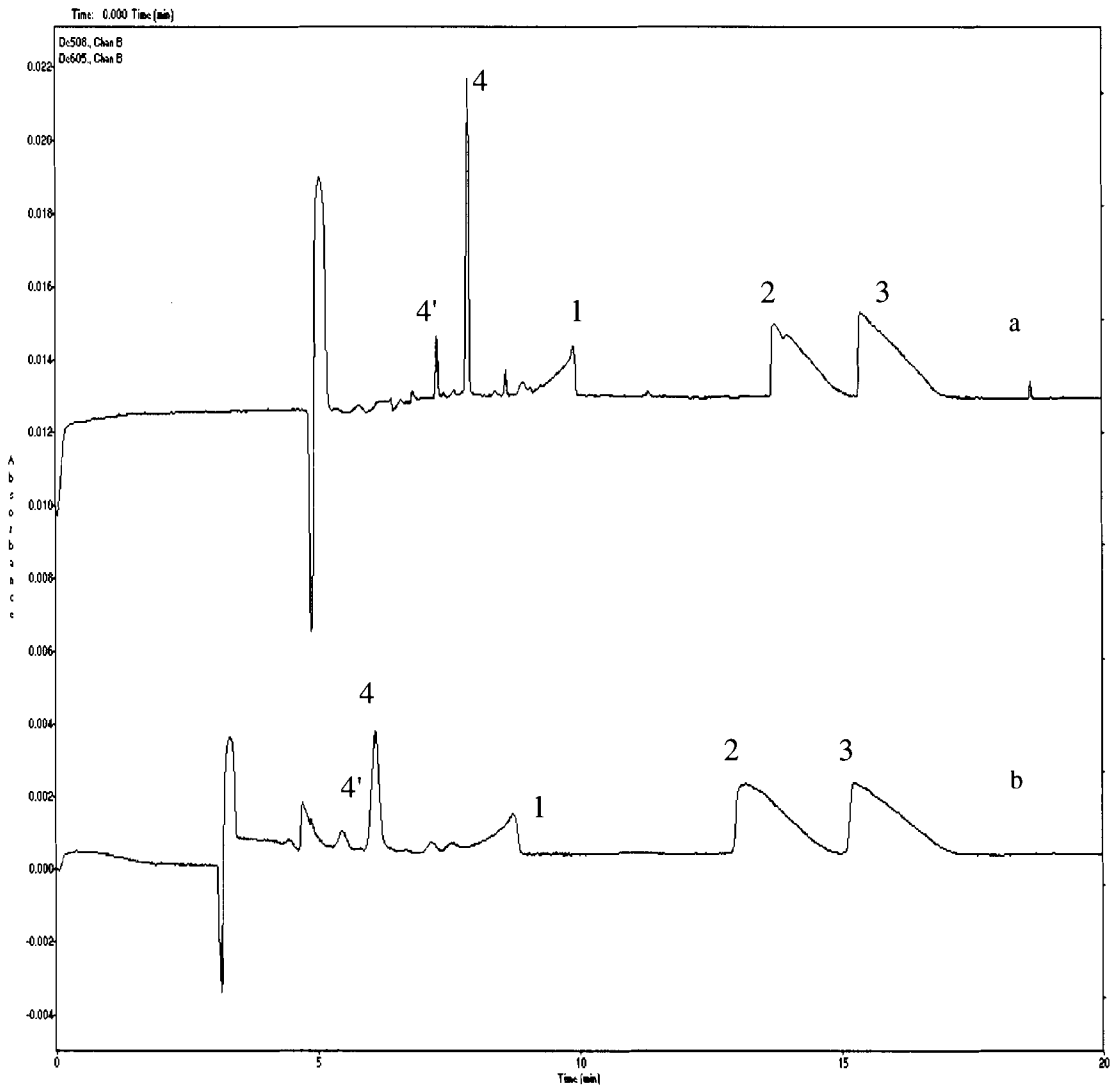

Fig.20 Electropherograms comparison at different analytical conditions. Analytical conditions: 50 mM sodium tetraborate + 25 mM SDS + 20 mM β-CD (buffer C); Voltage: 25kV; Capillary: 75 μm × 60.2 cm; distance to detector: 50 cm; Wavelength: 254 nm. The only difference is:
(a) 25 kV, 50 cm; (b) 10 kV, 10.2 cm.
Components identification of a and b are given in Fig.B-4 and Fig.B-5 (in appendix 8), respectively.

4.4 CD-MECC with organic modifiers

The addition of methanol to the run buffer was attempted to improve efficiency, i.e., to reach baseline separation and peak symmetry. The effect of the organic solvent is based on the competition of the solvent and the chiral selector for the analytes and on the influence of the solvent on the micelles.[62,63] [Here, although a capillary with a different internal diameter (75μm) was used, we found that a greater internal diameter did not affect separation resolution, except that a higher current was produced, see appendix 4].

Fig.21 shows the effect of the addition of methanol to the buffer on the separation of four components of licorice. All four components separated completely, though the peak of GL is still fronting. Moreover, as illustrated, 18α-GA and 18β-GA behave very differently from Fig.20b that 18α-GA and 18β-GA migrate faster than IQ. As expected, on addition of organic modifier to the buffer electrolyte, the electroosmotic flow decreases. The migration time of EOF marker [64] increased from around 4 min (Fig.20b) to 5 min (Fig 21a) when methanol (15%, v/v) was added to the buffer C to form buffer E. This is caused by a decrease in zeta potential and a decreased magnitude of the ratio of dielectric constant to viscosity of the buffer.[61] The reduced electroosmotic flow allowed adequate time for the small differences in mass-to-charge ratio to result in complete separation of 18α-GA and 18β-GA. Herein, 18α-GA and 18β-GA migrate the fastest among the four components. Thus, larger 18α-GA and 18β-GA are able to interact with the cavity of β-CD and migrate at the speed of neutral β-CD.

Since the improvement on peak symmetries of the two diastereomers was so impressive with buffer E, we decided to launch a systematic study of the effect of different amounts of methanol on separation. As shown in Fig.22b, by using 10% methanol in the buffer, an insufficient peak resolution of GL and 18α-GA and 18β-GA resulted and the peak symmetry of the latter two stereoisomers were still poor. By using 15% methanol, a sufficient separation with good peak symmetry of 18α-GA and 18β-GA and IQ was obtained (Fig.22c). Although the migration times of the two components increase with an increase in the proportion of methanol contained in the run buffer, the resolution of the two components remained roughly the same (see Appendix 5A for resolution calculation) using equation 12. Indeed, the most effective separation of these components was achieved when 15% of methanol was added to the run buffer leading to the maximum resolution of 2.4 (see Appendix 5). The impressive or unusual improvement when 5% more MeOH was added is not clear (see Appendix 6).

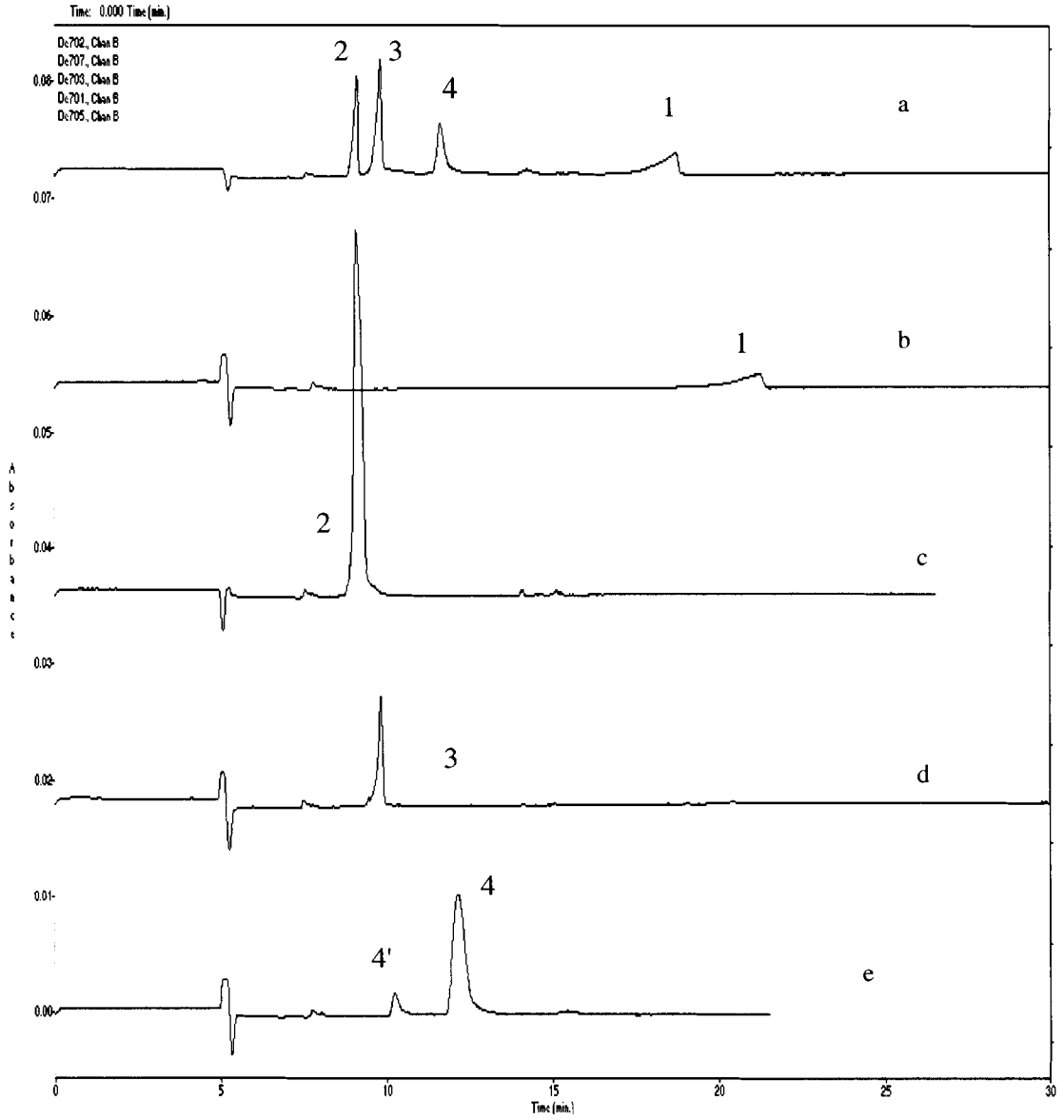

Fig.21 Electropherograms obtained for the separation of GL, 18α-GA, 18β-GA and IQ by CD-MECC. Analytical conditions: 50 mM sodium tetraborate + 25 mM SDS + 20 mM β-CD + 15% MeOH (buffer E); Voltage: 10kV; Capillary: 75 μm × 60.2 cm; distance to detector: 10.2 cm; Wavelength: 254 nm.
(a) mixture; (b) GL (1); (c) 18α-GA (2); (d)18β-GA (3); (e) IQ (4 and 4')

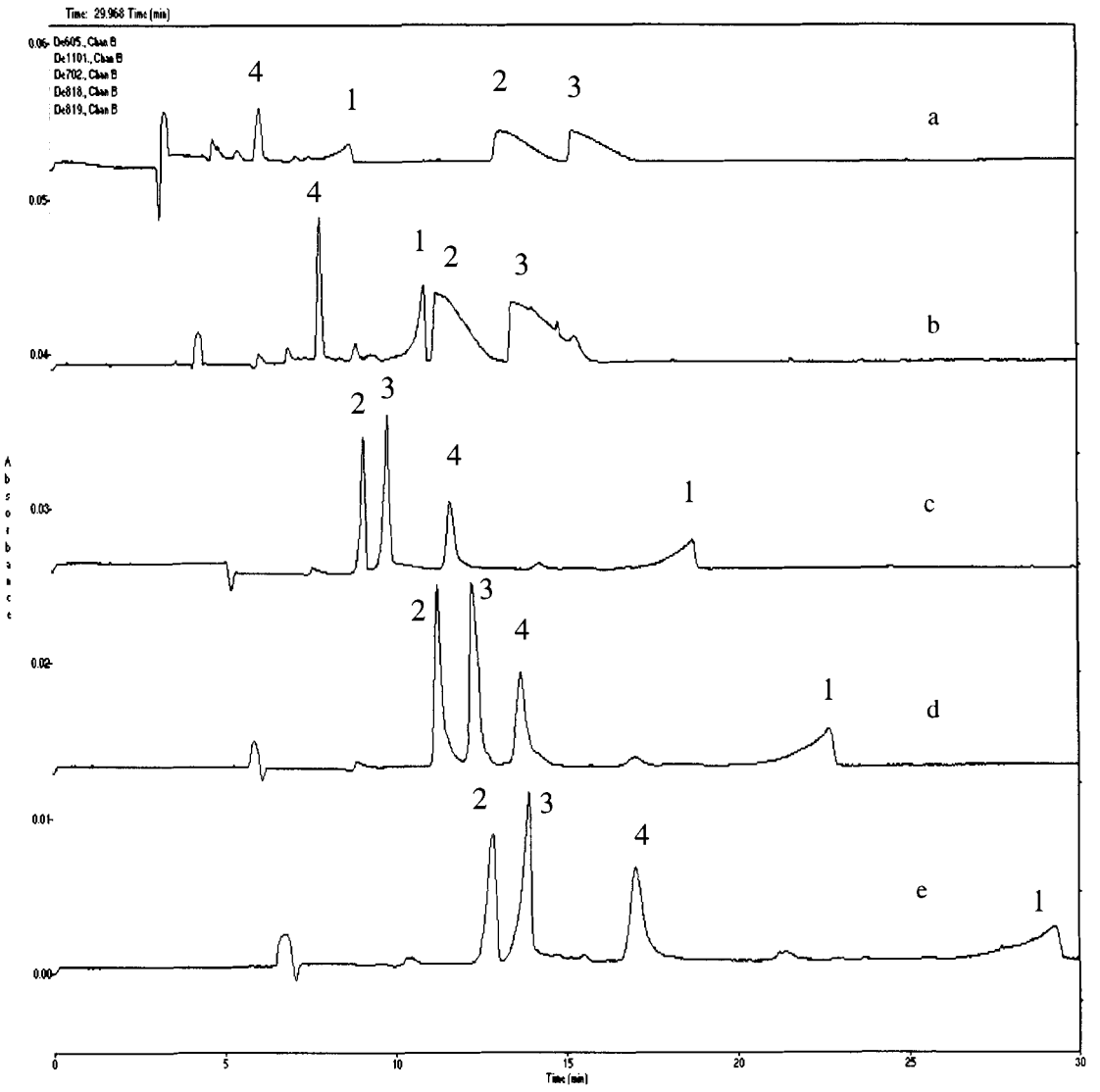

Fig.22 Electropherograms obtained to study the effect of different methanol percentage in run buffer on the separation of GL, 18α-GA, 18β-GA and IQ by CD-MECC.
Analytical conditions: 50 mM sodium tetraborate + 25 mM SDS + 20 mM β-CD; Voltage: 10kV; Capillary: 75 μm × 60.2 cm; distance to detector:10.2 cm; Wavelength: 254 nm.
(a) 0% MeOH (buffer C); (b) 10% MeOH (buffer D); (c) 15% MeOH (buffer E); (d) 20% MeOH (buffer F); (e) 25% MeOH (buffer G). Component identification for a, b and c are given in Fig.19b, Fig.B-6 and Fig.20, respectively. Single standard electropherograms were not performed for d and e, as component identification became obvious.

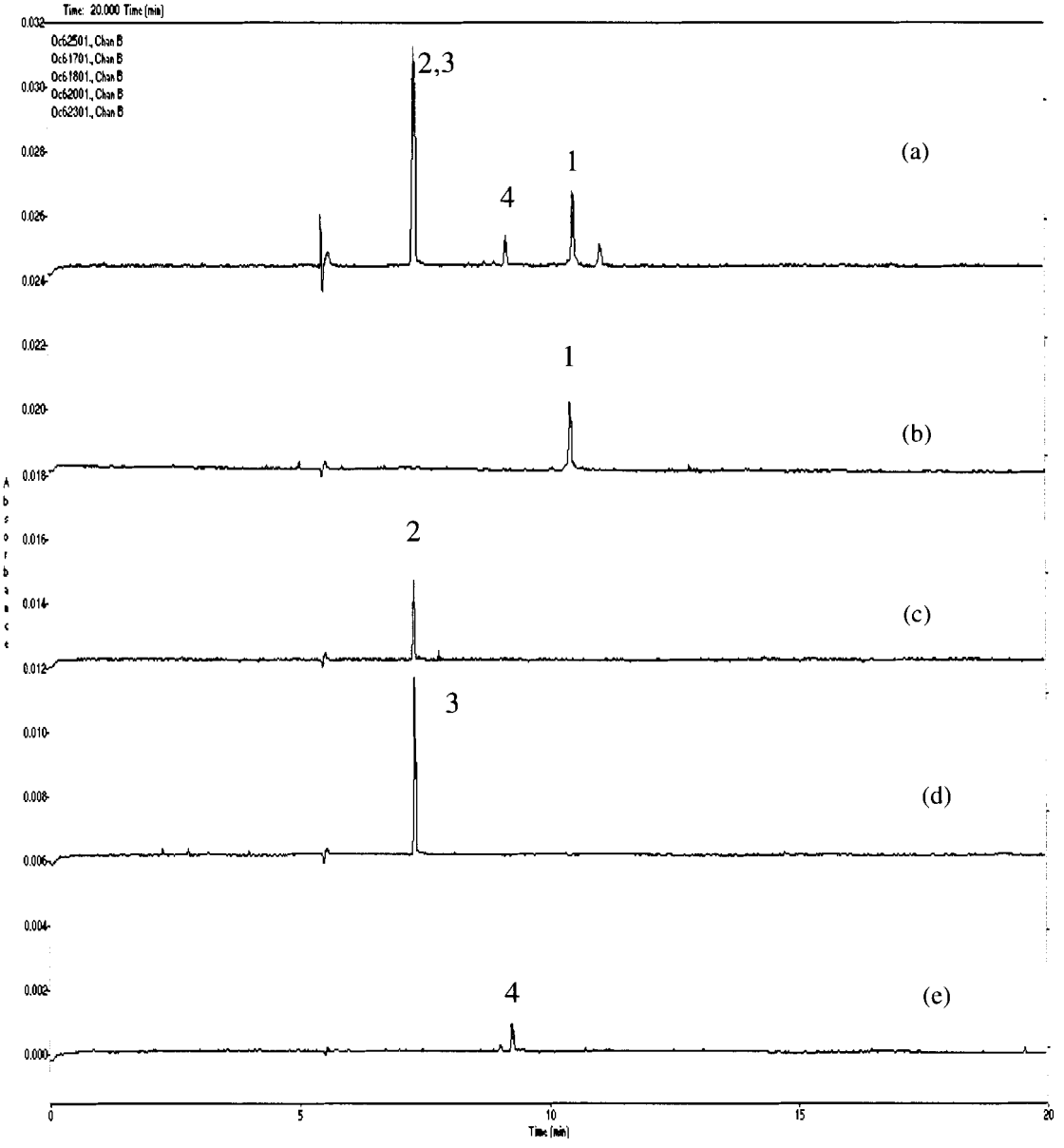

Fig.23 Electropherograms obtained for the separation of GL, 18α-GA, 18β-GA and IQ by MECC (SC). Analytical conditions: 10 mM sodium tetraborate + 25 mM SC (buffer H); Voltage: 17kV; Capillary: 50 μm × 60.2 cm; distance to detector: 50 cm; Wavelength: 254 nm.
(a) mixture; (b) GL (1); (c) 18α-GA (2); (d)18β-GA (3); (e) IQ (4 and 4')

4.5 MECC-SC

Next, we study another micelle-sodium cholate SC or bile salt [65] to see if we can simplify the buffer system.

The structures and aggregation properties of SC micelles (see Fig. 8) are very different from those of SDS micelles. SC forms smaller primary micelles with aggregation numbers between two and ten. At higher SC concentrations, secondary micelles with much larger aggregation numbers might be formed. The aggregation process of SC or bile salt has been a controversial matter. There are two theories about the formation of SC micelle.[66-69] One assumes that aggregation is primarily due to interaction of the hydrophobic backbones of the bile salts molecules (back-to-back model), leaving the polar hydroxyl functional groups in contact with water. The other is face-to-face model, in which a dimer formation at premicellar concentration as a result of hydrogen bonding interaction between the hydroxyl groups of two bile salts molecules. In this model, hydroxyl groups of the steroid ring backbone are oriented towards the core of the micelle.

As shown in Fig.23, a buffer (buffer H, see Table 1) with 25 mM SC in 10 mM borate at pH 8.5 was used. 18α- GA and 18β- GA migrated earlier than GL and IQ, which were in contrary to their behavior in SDS-based buffer system. This suggests that 18α- GA and 18β- GA did not interact with SC very much. As mentioned above, SC is more polar than SDS because of hydroxyl groups. This reconciles the fact that the two diastereoisomers are more hydrophobic than GL and IQ. Moreover, since GL is more polar than IQ, GL

interacts more strongly with the polar SC by formation of hydrogen bond. Therefore, IQ migrates earlier than GL.

10 mM borate was used in these studies as different from 50 mM borate used previously. But it has been shown that the effect of a lower borate concentration only result in shorter migration time without change in resolution. (See Appendix 2A) The capillary of internal diameter of 75 μm has been used, but there is no effect on separation, except that the current is higher, see appendix 4.

4.6 CD-MECC-SC

In order to improve the separation of two diastereoisomers, β-CD was added to buffer H to form buffer I (see Table 1).[70] A sufficient separation for the four components was obtained in about 10 min. (see Fig.24) The migration order (in increasing migration time) is 18α-GA, 18β-GA, IQ (2 components) and GL. In contrast to the SDS-mediated system, a faster separation was now obtained under the same capillary length and voltage conditions, the separation time decreased from 30 mins to 10 mins. The efficiency and resolution were improved greatly, especially for GL, the distortion of fronting peak existed in the SDS-mediated system was less severe. Another advantage of this system over the SDS -mediated system is the buffer composition was simplified. The number of constituents of buffer was three. The resolution between 18-GA and 18-GA was determined. (See appendix 5). In both SDS and SC systems, peak asymmetry of GL is unsatisfactory.

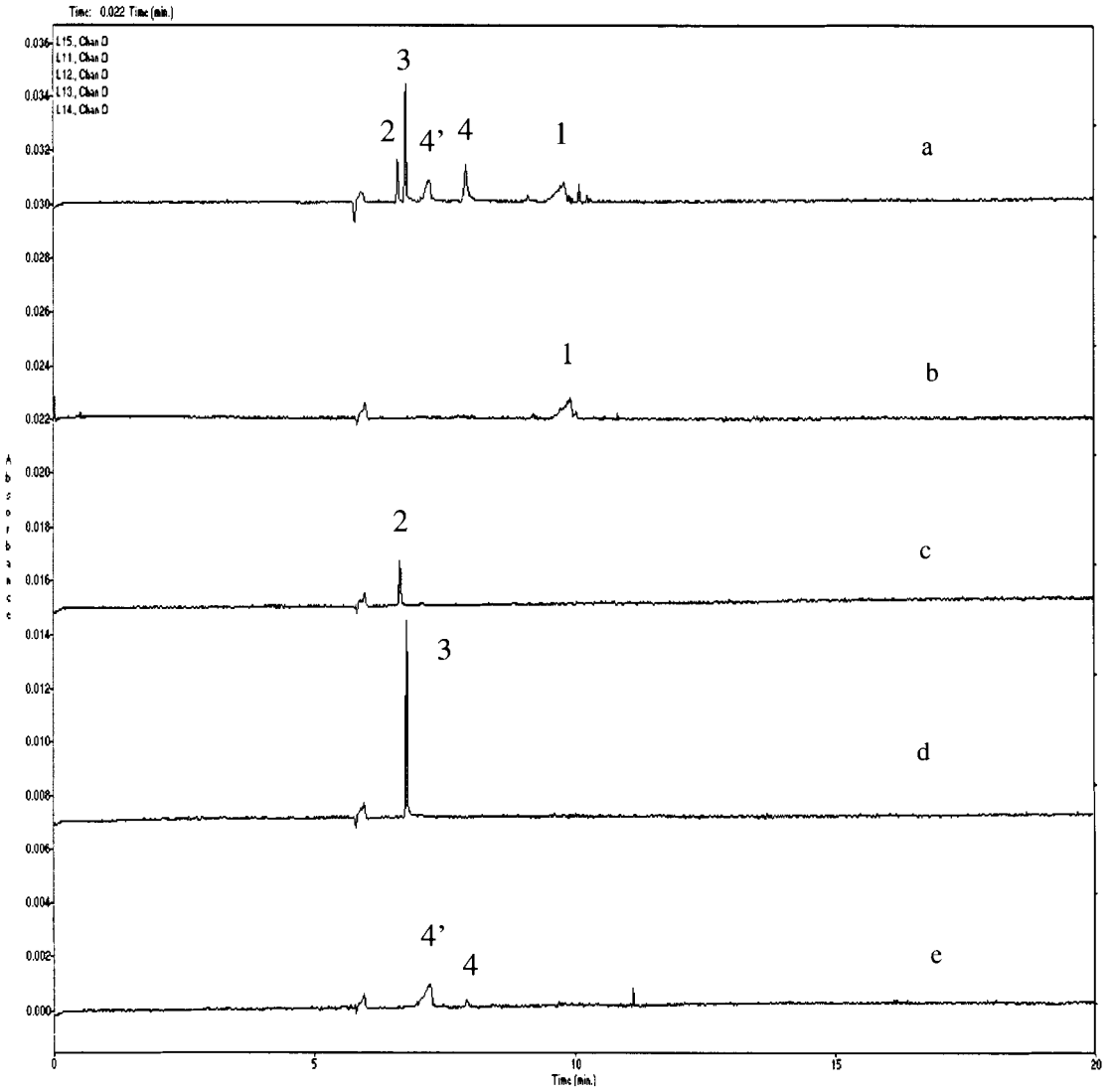

Fig.24 Electropherograms obtained for the separation of GL, 18α-GA, 18β-GA and IQ by CE. Analytical conditions: 10 mM sodium tetraborate + 25 mM SC + 20 mM β-CD (buffer I); pH: 8.5; Voltage: 17kV; Capillary: 75 μm × 60.2 cm; distance to detector: 50 cm; Wavelength: 254 nm.
(a) mixture; (b) GL (1); (c) 18α-GA (2); (d)18β-GA (3); (e) IQ (4 and 4')

4.7 Optimization of analytical conditions (CD-MECC-SC)

Since the buffer system involving SC produced better separation resolution and peak symmetry than the system using SDS, we decided to perform some studies on optimizing this buffer system by variations in pH, temperature and MeOH content.

4.7.1 pH Effect

The pH value of the electrolyte solution is an important parameter in CE separation.[71] In general, separation in electrophoresis is based on differences in electrophoretic mobilities of the analytes, which in turn depend on their size (r) and net charge (q) (see equation 6). The net charge of the ion is dependent on the degree of ionization, as determined by the difference in pKa value of the analytes (due to acid or basic functional groups) and pH of the solution. If the ionizable functional groups of the analytes are weak acids or bases (pKa for IQ is 7.86 ± 0.35, for GA is 4.71 ± 0.20) and their pKa are close to pH, any slight change in pH of the buffer will result in a strong influence on the net charge of the analytes.

In addition, the charge of the capillary wall surface and the zeta potential (ξ) are influenced by buffer pH (see equation 7b). When constant-concentration buffers are used, μ_{eo} decreases with pH for a strong base-weak acid type buffer.[48] As expected, the ionic strength of buffer increased with increasing pH, which result in decreasing electrical

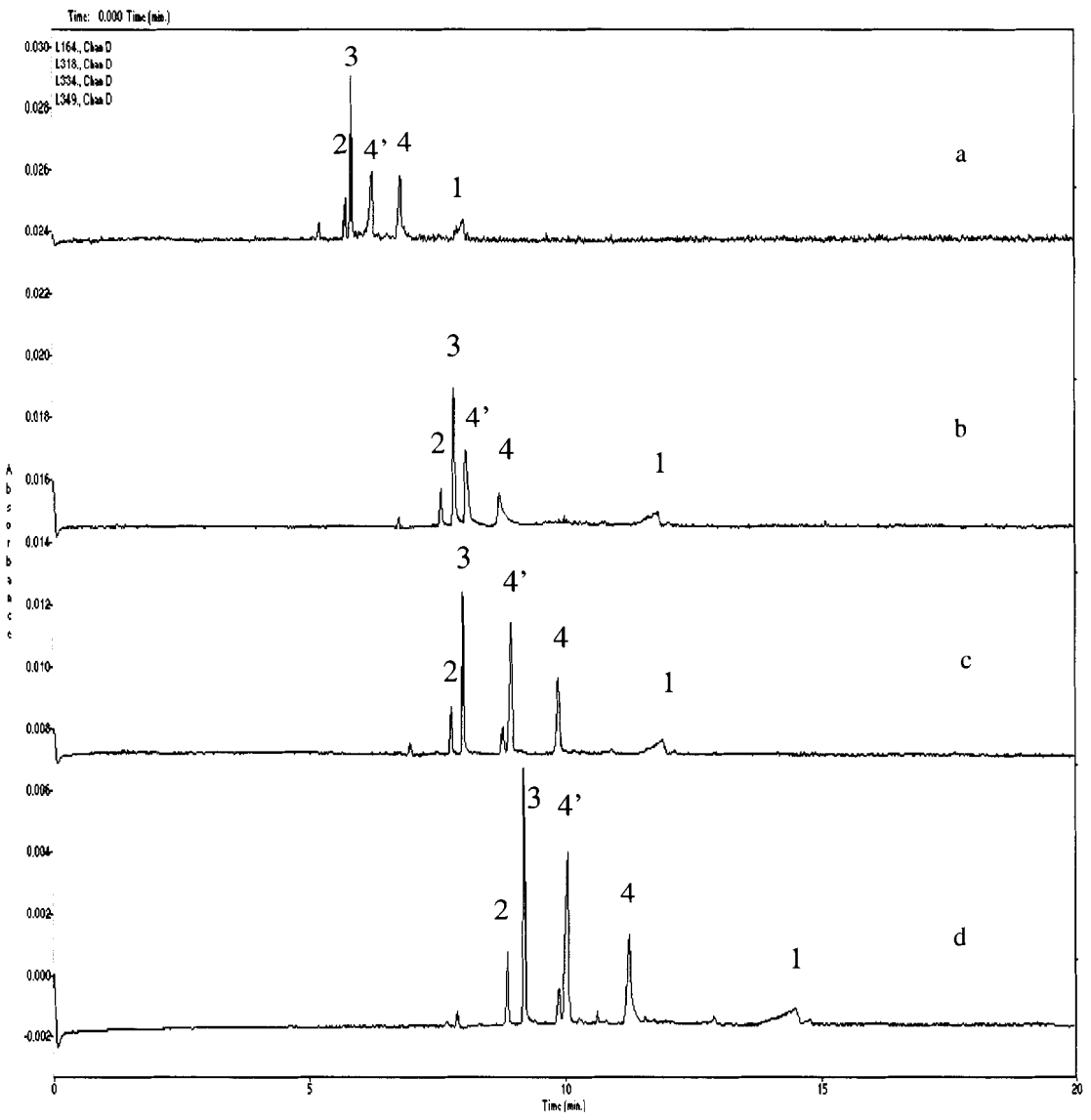

Fig.25 Electropherograms obtained to study the effect of different pH of run buffer on the separation of GL, 18α-GA, 18β-GA and IQ by CD-MECC. Analytical conditions: 10 mM sodium tetraborate + 25 mM SC + 20 mM β-CD; Voltage: 17kV; Capillary: 50 μm × 60.2 cm; distance to detector: 50 cm; Wavelength: 254 nm.
(a) pH 8.5 (buffer I); (b) pH 9.0 (buffer J); (c) pH 9.5 (buffer K); (d) pH 10.0 (buffer L)
For component identification of (a), see Fig.24.

double-layer thickness and further decreased zeta potential and EOF. Fig. 25 shows the the effect of buffer pH on the electrophoretic mobility of 18α-GA, 18β-GA, IQ and GL obtained in the pH range 8.5 to 10.0 with an applied voltage of 17 kV by employing 10 mM sodium tetraborate-25 mM SC-20 mM β-CD buffer. The migration time increased.[72,73] Although increasing pH did result in an increase in separation efficiency and resolution (see appendix 5), the increases were not very great.. While separation resolution is enhanced with the pH increment, a sufficient separation has been obtained at pH 8.5 with adequate efficiency and fast analysis speed. It is interesting to note that a small peak appeared in front of peak 4' in both Fig. 25c and d, and also the ratio of peak 4' and 4 in Fig. 25a is larger than in Fig. 25 b, c, d. The reason may be attributed to the degradation of IQ. From the chemical structure of IQ (see Fig. 1d), it is obviously that under alkaline conditions, hydroxyl groups of IQ are easy to be oxidized as ketones sequencely. So, with increasing pH and elongation time, more IQ is degraded so that stepwisely we observe that ratio changes and new peaks appear. Despite this, separation of the four components was achieved successfully. Therefore, for the separation of 18α-GA, 18β-GA, GL and IQ, buffer with pH 8.5 was considered to be the optimal pH.

4.7.2 Temperature Effect

It has been reported that temperature considerably affects resolution, efficiency and analysis time.[74] Therefore, temperature effect was investigated between 20°C and 40°C in the presence of 10 mM sodium tetraborate- 25 mM SC- 20 mM β-CD buffer (buffer I, pH 8.5). As shown in Fig 26, the migration time of all components decreased with increasing temperature of the capillary. At 20°C, analysis was completed in 10 min. At 40°C,

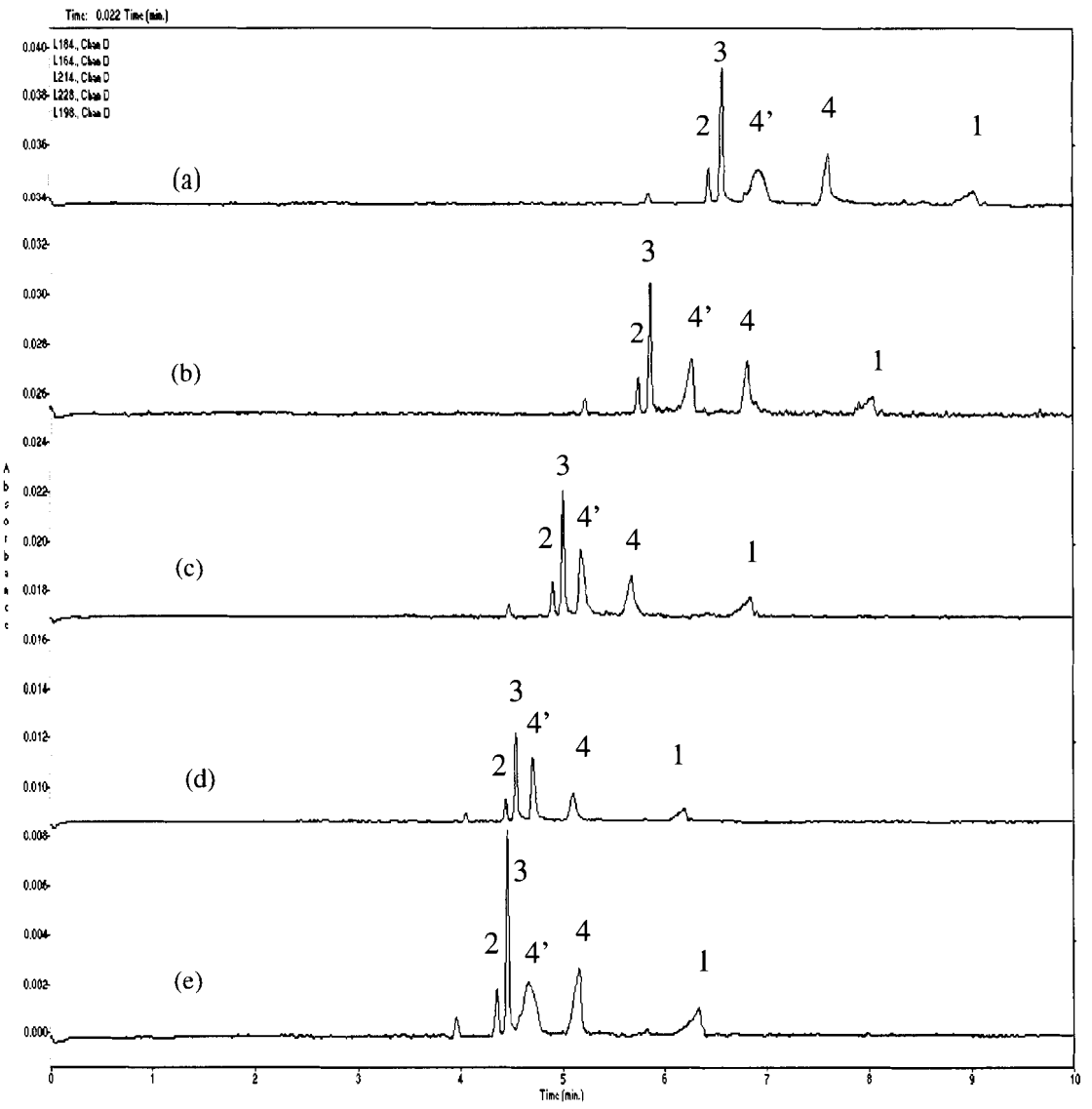

Fig.26 Electropherograms obtained to study the effect of different temperature of capillary on the separation of GL, 18α-GA, 18β-GA and IQ by CD-MECC. Analytical conditions: 10 mM sodium tetraborate + 25 mM SC + 20 mM β-CD (buffer I); pH 8.5; Voltage: 17kV; Capillary: 50 μm × 60.2 cm; distance to detector: 50 cm; Wavelength: 254 nm; temperature of capillary at (a) 20°C; (b) 25°C; (c) 30°C; (d) 35°C; (e) 40°C
For component identification of (b), see Fig.24.

analysis was completed within 7 min. This behavior is attributed to viscosity decrease at elevated temperature, resulting in higher electrophoretic and electroosmotic mobilities (see equations 6 and 7), with the latter being to a greater extent. Additionally, from the resolution calculations (see Appendix5), we have known that at 25°C, the resolution for peaks 2 and 3 is the greatest. Hence, the use of capillary temperature at 25°C was considered as optimal for rapid separation and high efficiency.

4.7.3 Effect of Organic modifier

The effect of the addition of methanol to the buffer on the separation of four components was studied. Fig.27 a, b, c and d shows the electropherograms obtained when 0,10,15 and 20% of MeOH were added in the run buffer I (see Table 1). The single standard electropherograms for Fig.27b, c and d are given in Fig.B-9, B-10 and B-11, respectively, in appendix 8. As expected, on addition of organic modifier to the run buffer, the electroosmotic flow (EOF) decreases as a result of a decrease in zeta potential (ξ) and a decreased viscosity of the buffer (η). At 25°C, the viscosity of water is 0.890 mPa.s and methanol 0.544 mPa.s. As illustrated, with an increase in the proportion of methanol (0-20%) contained in the buffer solution, the migration time and the electrophoretic mobilities (EPF) of all components increased significantly. Moreover, 18α -GA and 18β-GA coelute when MeOH is present in the run buffer. Since 18α -GA and 18β-GA could not be resolved when MeOH was added. It is because 18α-GA and 18β-GA were separated even though MeOH was absent. In addition, the peak shape for GL improved greatly with a symmetric peak replacing a fronting peak when MeOH was added. The

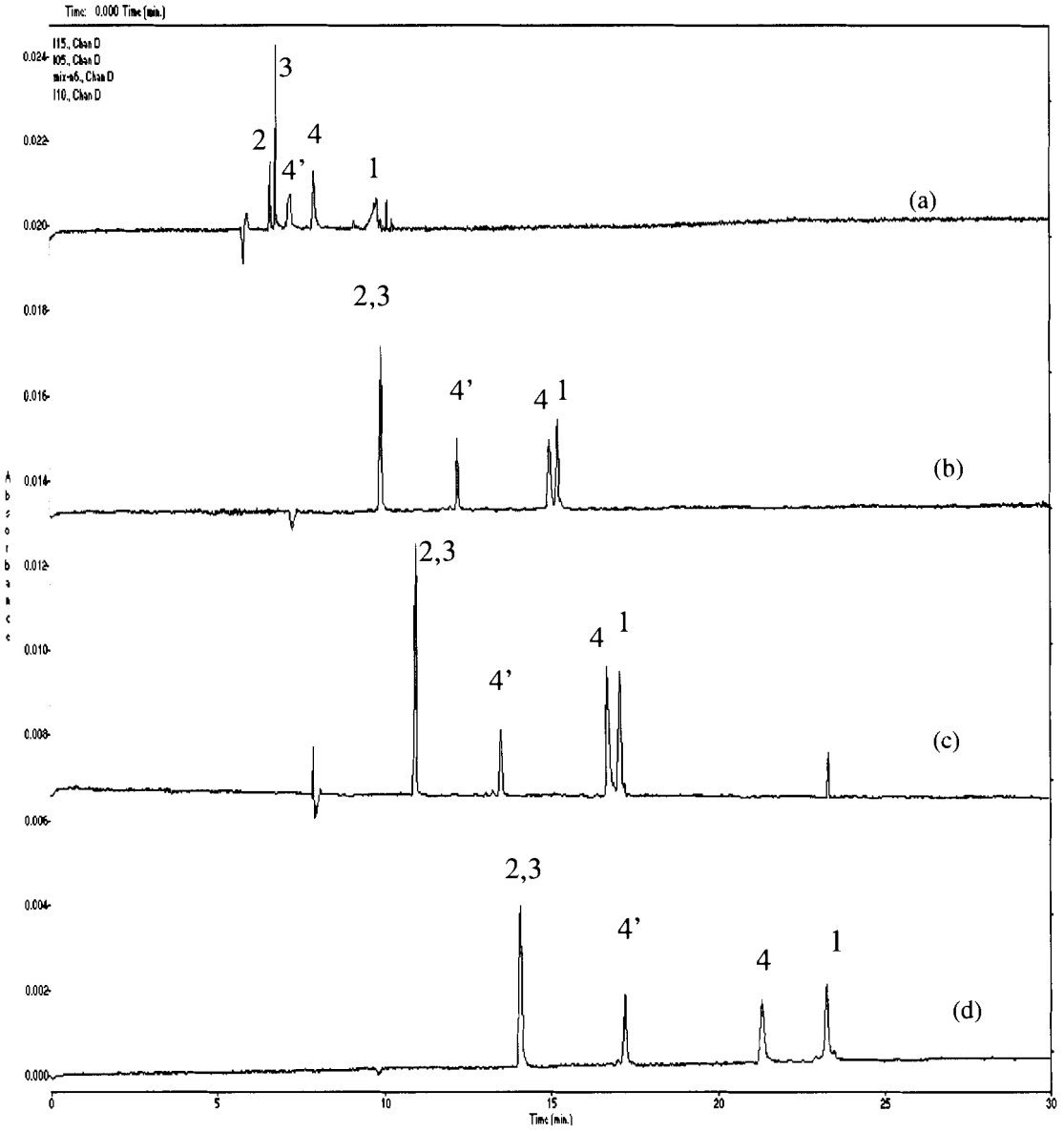

Fig. 27. Electropherograms obtained to study the effect of different percentage of methanol in run buffer on the separation of GL, 18α-GA, 18β-GA and IQ by CD-MECC. Analytical conditions: 10 mM sodium tetraborate + 25 mM SC + 20 mM β-CD (buffer I); pH 8.5; Voltage: 17kV; Capillary: 50 μm × 60.2 cm; distance to detector: 50 cm; Wavelength: 254 nm; temperature at 25°C (a) 0% (buffer I); (b) 10% (buffer M); (c) 15% (buffer N); (d) 20% (buffer P)
For component identification of (a), (b), (c), (d), see Fig.24, B-9, B-10, B-11, respectively.

possible reason is that MeOH helps to solvate GL. Again this does not reconcile with the fact that SC could have been added in the CD-MECC (SDS system, Fig.22) because GL always gave a fronting peak. Therefore, SC should not have been added in the previous work.

4.7.4 Repeatability

We conclude that the optimized buffer is buffer I which contains 10 mM sodium tetraborate, 25 mM SC and 20 mM β-CD.

Precision was evaluated by measuring repeatability of migration times. Repeatability of the method was determined by performing 11 consecutive runs of standard mixture containing the four substances. In Table 3, relative standard deviation (RSD) values are given for migration times of the selected components. In all cases, RSDs range from 0.4-0.7% for migration time, which showed that precision of migration time was satisfactory.

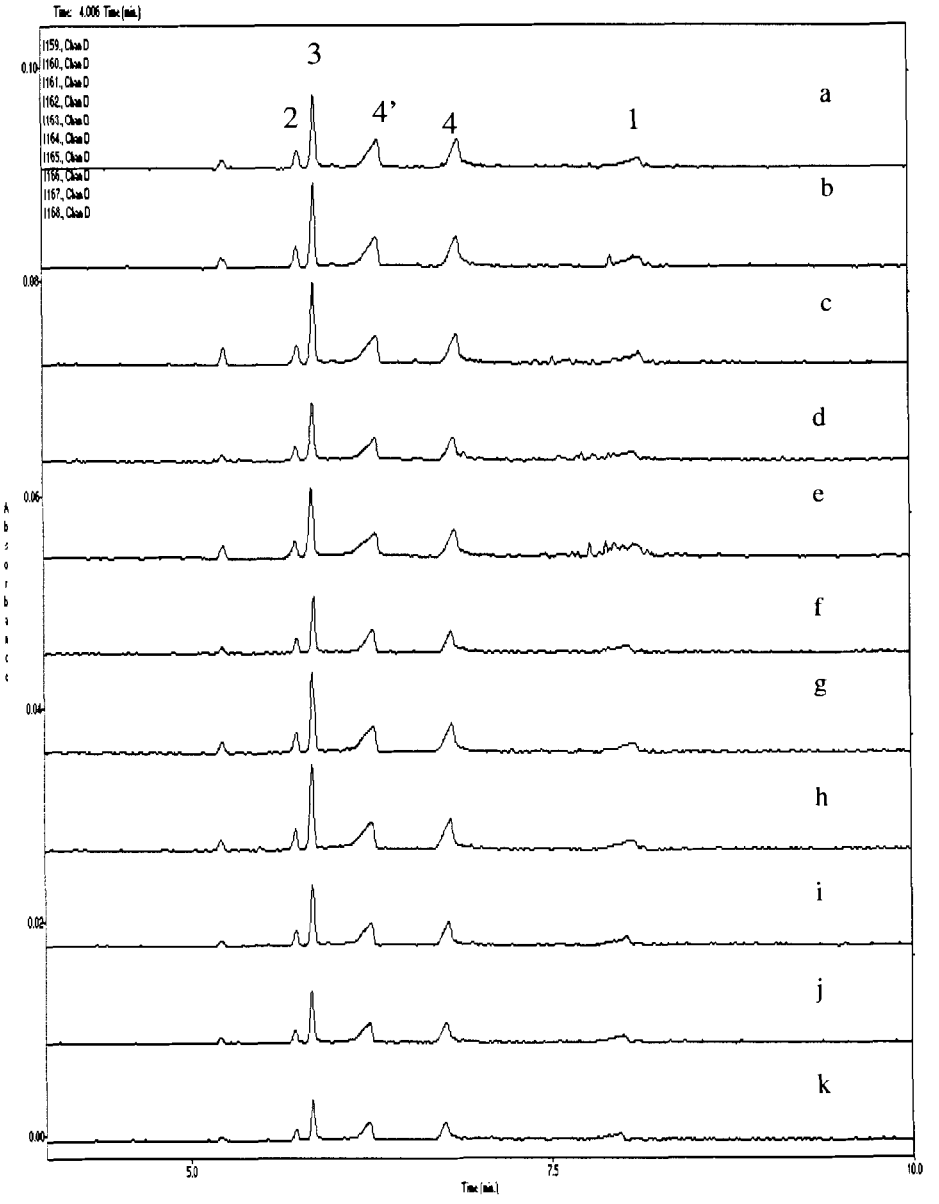

Fig.28 Electropherograms obtained for the repeatability on the separation of GL, 18α-GA, 18β-GA and IQ by CD-MECC. Analytical conditions: 10 mM sodium tetraborate + 25 mM SC + 20 mM β-CD (buffer I); pH 8.5; Voltage: 17kV; Capillary: 50 μm × 60.2 cm; distance to detector: 50 cm; Wavelength: 254 nm; temperature at 25°C

Electrophero -gram	EOF (min)	GL (min)	18α-GA (min)	18β-GA (min)	IQ (min)	
a	5.237	8.128	5.782	5.908	6.285	6.872
b	5.237	8.087	5.782	5.908	6.327	6.830
c	5.237	8.126	5.782	5.866	6.327	6.872
d	5.237	8.045	5.740	5.866	6.285	6.830
e	5.237	8.087	5.782	5.866	6.285	6.830
f	5.237	8.087	5.782	5.866	6.243	6.788
g	5.196	8.045	5.782	5.866	6.243	6.788
h	5.196	8.045	5.698	5.824	6.285	6.788
i	5.196	8.003	5.656	5.824	6.243	6.746
j	5.196	8.003	5.698	5.824	6.243	6.746
k	5.196	7.961	5.698	5.824	6.201	6.746
Average ±RSD	5.2±0.4%	8.1±0.6%	5.7±0.7%	5.9±0.5%	6.3±0.6%	6.8±0.6%

Table 3. Repeatability of migration time of all components using the optimum method. Refer to Fig.30 for the electropherograms

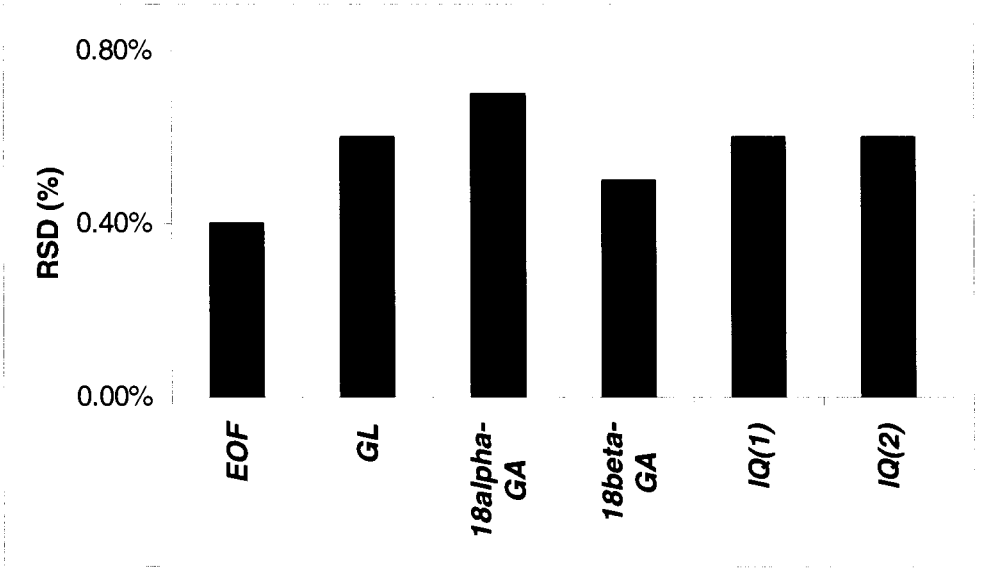

Chart 2. Repeatability of migration time of all components under the optimum method.

4.8 CE analysis of raw and roasted licorice

It is widely accepted in TCM that the pharmacological effects of raw and roasted licorice are different. Therefore, the optimized buffer (i.e., buffer I) was used to examine these herbal samples in order to find out the chemical basis for the difference in pharmacological effects.

The use of methanol may not have extracted the highly water-soluble GL. Moreover, in TCM, licorice root is usually extracted using boiled water or wine and used as a decoction (herbal soup). Therefore, extraction of licorice root with water and ethanol has clinical relevance. We compare extracts of raw and roasted licorice obtained by MeOH, ethanol and water.

Fig.29 shows the electropherograms of raw and roasted licorice extracted with methanol. The roasted sample was prepared from the same batch of raw licorice. From Fig.29a, b and c, we observed that there are some differences between the composition of the raw and roasted licorice samples extracted in methanol. It is apparent that peak II and III were more abundant in raw licorice (see Fig.29b). However, because of shift in EOF as determined from the characteristic methanol peaks, it is difficult to conclude that peak I, II, III and IV correspond to peak 3, 4',4 and 1 in the standard mixture, respectively. (see Fig.29a and b). It is estimated that EOF shift may be caused by the different composition file in raw and roasted licorice sample, which may affect the zeta potential due to possible different wall adsorption effect. Since comparison of migration times between

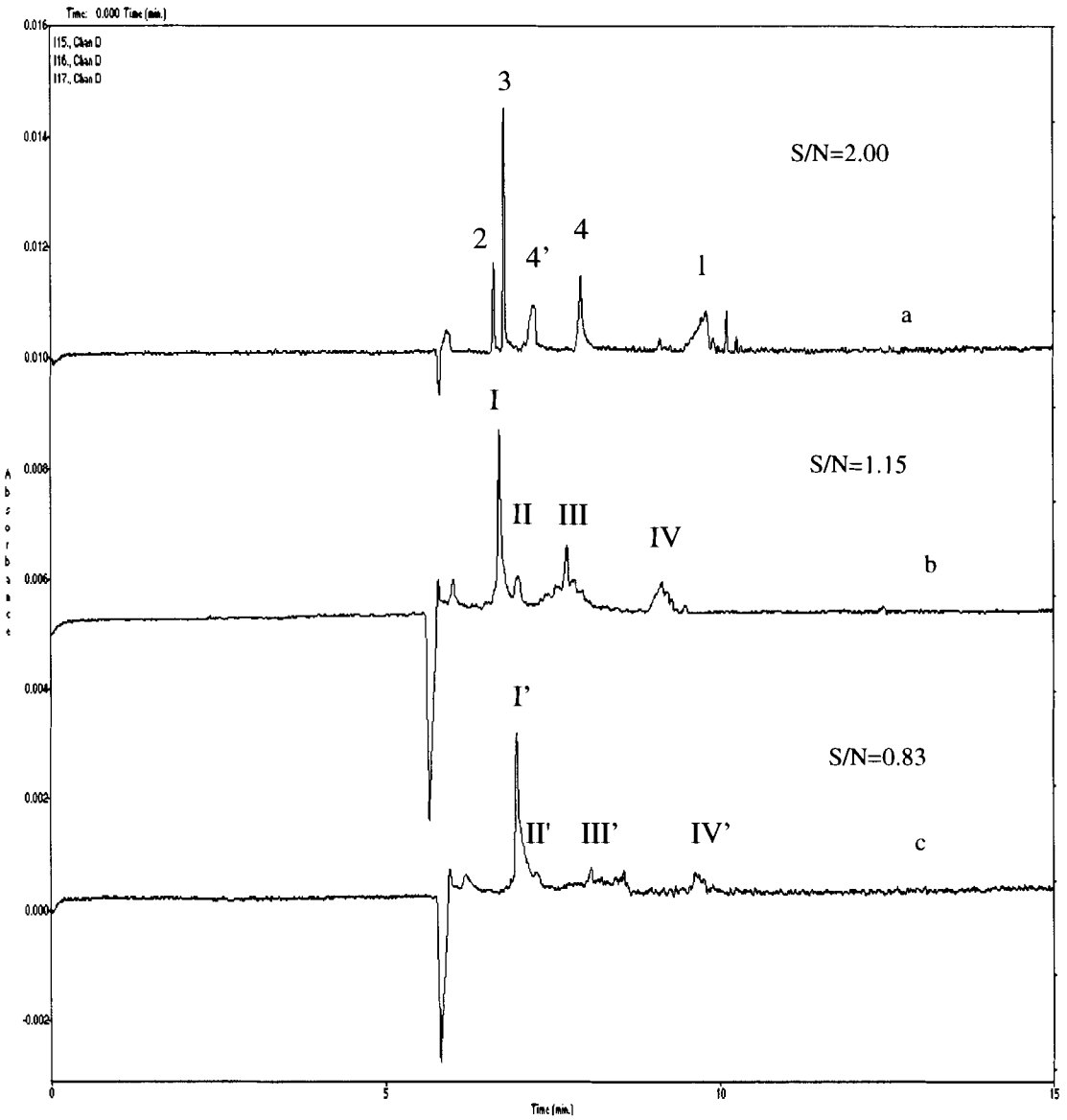

Fig.29 Electropherograms obtained for the separation of licorice components in raw licorice(S4a) and roast licorice (S4b) samples by CD-MECC. Analytical conditions: 10 mM sodium tetraborate + 25 mM SC + 20 mM β-CD (buffer I); pH 8.68; Voltage: 17kV; Capillary: 50 μm × 60.2 cm; distance to detector: 50 cm; Wavelength: 254 nm; temperature at 25°C (a) standard mixture; (b) raw licorice, extracted by methanol (S4a); (c) roasted licorice, extracted by methanol (S4b)

(a)

(b)

(c)

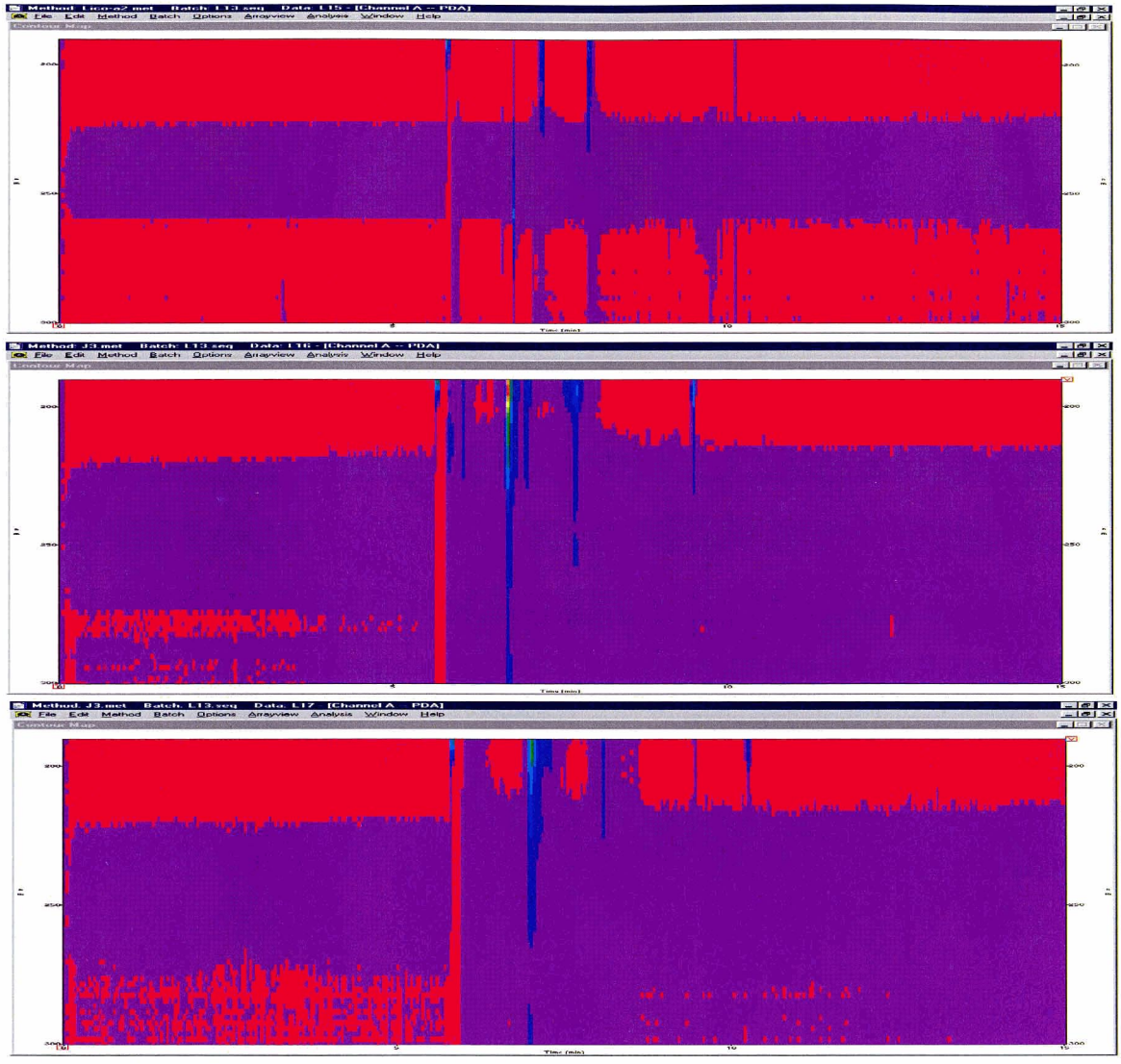

Fig.30 UV contour plots for Fig.29. Analytical conditions: 10 mM sodium tetraborate + 25 mM SC + 20 mM β-CD (buffer I); pH 8.68; Voltage: 17kV; Capillary: 50 μm × 60.2 cm; distance to detector: 50 cm; Wavelength: 254 nm; temperature at 25°C (a) standard mixture; (b) raw licorice, extracted by methanol; (c) roasted licorice, extracted by methanol In all plots, horizontal axis represents time from 0 to15 min and vertical axis represents wavelength from 190 nm (top) to 400 nm (bottom)

samples and standards is not a conclusive method, especially when there is shift in migration time, we resort to the use of full UV contours collected by the photodiode array (PDA) detector.[75] See section 4.1 and Fig.13 for the discussion on UV contour data. As shown in Fig. 30, we notice that the UV contour of peak I does not match that of either peak 2 or 3. However, the UV contours of peak II and III do match with those of peak 4' and 4 of IQ, respectively. Since these 2 peaks become less prominent in Fig. 29c, we conclude that IQ is less in roasted licorice, as compared to raw licorice. Furthermore, the UV contour of peak IV does not match that of peak 1 (GL), which is normally a major ingredient in licorice. Spiking should have been performed to provide more evidence for component identifications.

Extractions using ethanol were also performed on raw and roasted licorice, and their electropherograms were shown in Fig.31b and c, respectively. Here the peaks due to the presence of ethanol appeared (as negative peaks). Although there were shifts in migration times, the reduction in sizes of peaks corresponding to peaks II and III were also observed. A new observation is that peak IV is reduced in roasted licorice to a large extent in ethanol extracts (Fig.31 b and c) as compared to the water extracts (Fig.31 d-g). Moreover, we found that peak II in ethanol is reduced in roasted licorice (Fig.31 b and c), which is to a greater extent than in the methanol extracts (Fig.29b and c). On the other hand, we found that peak III in water extracts (Fig.31d and e) is reduced to a less extent than in the methanol extracts (Fig.29b and c). Since these water extracts of licorice samples did not contain methanol or ethanol, the characteristic EOF peaks did not appear. Therefore, methanol was added to these water extracts. However, as shown in Fig. 31f

and g, even after methanol was added to the water extracts, the characteristic methanol peaks did not show up. This may be because methanol was not added enough. Nevertheless, Fig. 31d and e resemble Fig. 31f and g, respectively. This comparison should have been more conclusive if (a) an internal standard had been used to eliminate the variations in injection sample size. (b) normalization to the amount of the herbal sample was performed.

Again, Fig.32 shows the UV contours for the identification of the major component. It was found that the major component I is neither 18α-GA or 18β-GA. Although the CE method has been optimized for separation of 18α-GA and 18β-GA, such a method has led to the co-migration of a major component with the two pharmacologically different stereoisomers. Accordingly we also used other buffers to examine the composition profile of licorice extracts (see Appendix 10).

Although the original hypothesis was to prove that raw and roast licorice have different amount of 18α-GA and 18β-GA, our findings indicate that there are other differences (i.e. IQ). Future work will be performed to test the hypothesis.

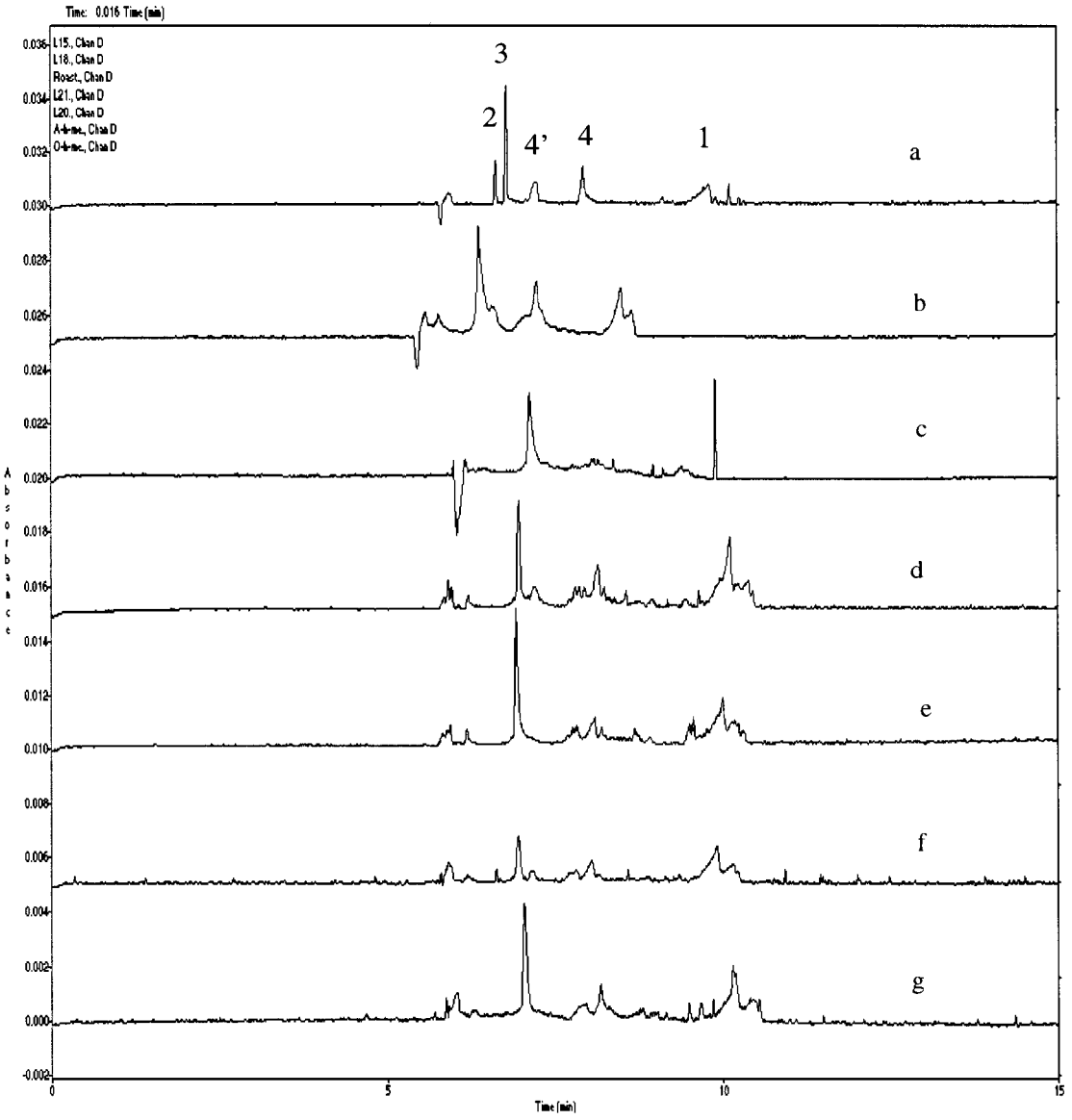

Fig.31 Electropherograms obtained for the separation of licorice components in raw licorice (S4a) and roast licorice (S4b) samples by CD-MECC.
Analytical conditions: 10 mM sodium tetraborate + 25 mM SC + 20 mM β-CD (buffer I); pH 8.68; Voltage: 17kV; Capillary: 50 μm × 60.2 cm; distance to detector: 50 cm; Wavelength: 254 nm; temperature at 25°C (a) standard mixture; (b) raw licorice, extracted by ethanol; (c) roasted licorice, extracted by ethanol; (d) raw licorice, extracted by water; (e) roasted licorice, extracted by water; (f) raw licorice, extracted by water with added methanol; (g) roasted licorice, extracted by water with added methanol

(a)

(b)

(c)

(d)

(e)

(f)

(g)

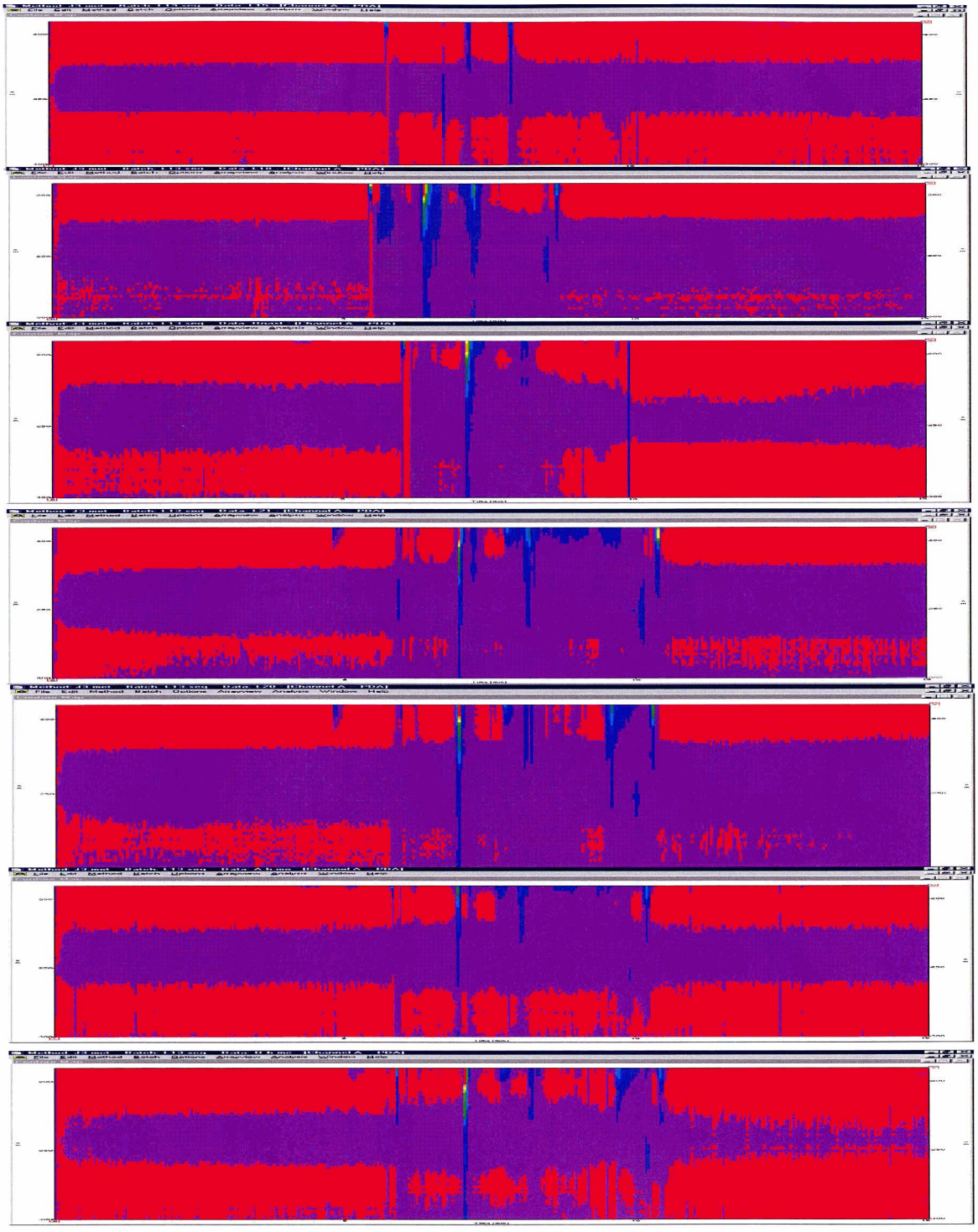

Fig. 32 UV contour plots for Fig. 31. For analytical conditions and legends, see Fig. 31. In all plots, horizontal axis represents time from 0 to 15 min and vertical axis represents wavelength from 190 nm (top) to 400 nm (bottom).

Chapter 5 Conclusion and future work

GL, 18α -GA, 18β-GA and IQ are four bioactive components existing in the licorice root and each of them has different pharmacological effects. Separation of GL, 18α -GA, 18β-GA and IQ extracted from raw and roasted licorice root by various modes of capillary electrophoresis has been investigated in this study. Although separation of the components in licorice samples has been previously reported, most methods focus on one or two of the four components by HPLC or GC. CE methods are seldom employed. In addition, since 18α-GA and 18β-GA are two diastereoisomers, separation for them was more difficult. To date, no literature has been found for their separation by CE. Furthermore, study on the difference of the four components in raw and roasted licorice samples has not been reported. In present research, for the first time, the simultaneous separation of above four components in one CE run has been reported. In addition, different CE modes have been investigated to select the optimal separation conditions.

Different modes of CE have been done to achieve optimal baseline resolution. Preliminary experiments started with CZE mode with 50 mM sodium tetraborate buffer. Methanol was added to the sample solution as a marker of EOF. Only GL and IQ were separated. Methanol as a neutral compound is supposed to be a good marker for EOF theoretically, but from our study, we found that the peak uncertainty of methanol may bring up some difficulties for the component identification. Therefore, in the future, we suggest that mesityl oxide (4-methyl-3-penta-2-one) as shown in Fig. 33 should be used

instead of methanol as the EOF marker because mesityl oxide has strong and stable absorbance at UV range due to its conjugated group.

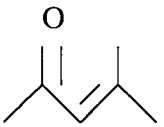

Fig. 33 Chemical structure of mesityl oxide

MECC mode was employed to reach separation of the four components. Two kinds of micelle systems have been investigated. More hydrophobic 18α -GA and 18β-GA, which interacted with SDS strongly, did not show up within the usual 30 min analysis time. Increasing SDS concentration, worsen the situation by prolonging the analysis time. As a chiral selector, the addition of β-CD improved the separation of 18α-GA and 18β-GA, but they migrate very slowly, and with tailing peaks. Although IQ and GL were separated thoroughly, GL was a fronting peak. Methanol was employed as an organic modifier to improve the peak symmetry. By addition of methanol more hydrophobic 18α-GA and 18β-GA competitively dissolve in methanol instead of combining with SDS. Thus, 18α-GA and 18β-GA migrate at EOF rather than at SDS speed, which migrates very slowly. Consequently, the tailing peaks were solved. The effect of different amounts of methanol was also investigated. The results showed that 15% methanol produced satisfactory results. A desired separation was achieved by 50 mM sodium tetraborate-20 mM CD-25 mM SDS-15% methanol-MECC system at pH8.5.

The separation was also performed on another micelle system: SC. By using the SC micelle system, the analysis time was decreased greatly from 30 min to 10 min. In order to achieve chiral separation, β-CD was added to the buffer. A complete separation was obtained by using 50 mM sodium tetraborate-20 mM β-CD-25 mM SC. Moreover, the effects of pH, temperature and the amount of organic modifier on separation were investigated systematically. The optimum analytical conditions were pH8.5 at 25°C, and without the use of any organic modifier. The SC micelle system has two advantages over the SDS micelle system. First, the baseline separation of four licorice compounds was achieved within 10 mins instead of 30 mins. Second, the buffer system is simpler without the use of organic solvents. The repeatability study gave satisfactory results with RSD of 0.4-0.7%.

In both buffer systems, the peak shape of GL is not symmetric in the electrophoregrams. It has been reported that the addition of methanol may improve peak shape. But, in our study, we did not see great improvement on the peak shape of GL by changing the amount of methanol.

Future work includes systematic investigation of the effects of different concentration of sodium tetraborate, SDS, SC and CD on the improvement of peak shape of GL.

The raw and roasted licorice roots have also been investigated in this study. Both of them were extracted with methanol, water and ethanol. The extracts were analyzed under the optimum separation conditions. In the beginning, we hypothesized that the difference in

the pharmacological effect of raw and roasted licorice was based on the different amounts of 18α-GA and 18β-GA. However, through our study, we found that there was some other difference such as the amount of IQ. And also, the difference depended on the different extraction methods too.

Future work includes thorough investigation on the effects of different roasting conditions (temperature, time, and the amount of honey) on the herbal compound composition, quantitation of several components in licorice. An internal standard should also be used to assist quantitation.

Chapter 6 Appendix

Appendix 1a Method File

Data files are created using method j3.met. A program consisted of rinse, injection and separation is used. The capillary is rinsed with methanol, water, and conditioned with 0.1 M NaOH, then rinsed with water again, finally filled with run buffer. Inject sample by 0.5 psi for 5 s. Separation is performed by using 17 kV for 30 min. Sample is detected by PDA detector, in which wavelength of 214 nm and 254 nm are chosen.

Time Program (Instrument #1) - [P/ACE MDQ]

File Edit Options View Window Help

Initial Conditions

Cartridge: 25.0 °C
Sample: 4.0 °C
Power: (no data collection)
Max = 9.00 W
Voltage: (no data collection)
Max = 30.00 KV
Current: Channel C
Max = 300.00 µA
Peak Detect

Change...

PDA Detector Initial Conditions

Scan Data: Channel A
Data Rate: 4.0
Channel 1: Channel B
Use Reference Channel: No
Wavelength: 214
Bandwidth: 10
Channel 2: Channel D
Use Reference Channel: No
Wavelength: 254

#	Time (min)	Event	Value	Duration	Inlet Vial	Outlet Vial	Summary	
1		Rinse - Pressure	20.0 psi	1.00 min	BI:A5	BO:B1	fwd	rinsed with methanol (j3.met)
2		Rinse - Pressure	20.0 psi	1.00 min	BI:A1	BO:B1	fwd	rinsed with water
3		Rinse - Pressure	20.0 psi	1.00 min	BI:A3	BO:B1	fwd	conditioned with 0.1 M NaOH
4		Rinse - Pressure	20.0 psi	1.00 min	BI:A1	BO:B1	fwd	rinsed with water
5		Rinse - Pressure	20.0 psi	1.00 min	BI:C3	BO:B1	fwd	filled with run buffer
6		Inject - Pressure	0.5 psi	5.0 sec	SI:A2	BO:B1	override o.k., fwd	sample injected
7	0.00	Separate - Voltage	17.0 KV	30.00 min	BI:C3	BO:C3	0.17 min Ramp, normal polarity	separation
8								

Method file (j3.met)

Appendix 1b Batch File

In order to automate the measurement, a batch file (L14.seq) is employed to perform 20 runs continually. In this sequence file, the method file, sample injection inlet and outlet vials, rinse inlet and outlet vials, separation vials are set.

The sample ID is set automatically when the first was input. In method column, one method can be chosen from any setup method list, but all the 20 runs must have the same method. Filenames if not specially state, are the same as "sample ID". Sample injection inlet and outlet vials, rinse inlet and outlet vials, separation vials are set the same as in setting up method.

Batch file (L14.seq)

Method J3.met Batch L14.seq Data A-n1

File Edit Method Batch Options Areaview Analysis Window Help

Batch L14.seq

Run #	Run Type	Reps	Sample ID	Method	Filename	Level	Sample Amt.	ISTD Amt.
1	Unknown	1	1136	j3.met	1136	0	1	
2	Unknown	1	1137	j3.met	1137	0	1	
3	Unknown	1	1138	j3.met	1138	0	1	
4	Unknown	1	1139	j3.met	1139	0	1	
5	Unknown	1	1140	j3.met	1140	0	1	
6	Unknown	1	1141	j3.met	1141	0	1	
7	Unknown	1	1142	j3.met	1142	0	1	
8	Unknown	1	1143	j3.met	1143	0	1	
9	Unknown	1	1144	j3.met	1144	0	1	
10	Unknown	1	1145	j3.met	1145	0	1	
11	Unknown	1	1146	j3.met	1146	0	1	
12	Unknown	1	1147	j3.met	1147	0	1	
13	Unknown	1	1148	j3.met	1148	0	1	
14	Unknown	1	1149	j3.met	1149	0	1	
15	Unknown	1	1150	j3.met	1150	0	1	
16	Unknown	1	1151	j3.met	1151	0	1	
17	Unknown	1	1152	j3.met	1152	0	1	
18	Unknown	1	1153	j3.met	1153	0	1	
19	Unknown	1	1154	j3.met	1154	0	1	
20	Unknown	1	1155	j3.met	1155	0	1	
21								

Appendix 2 Effect of concentration of sodium tetraborate on the separation of four licorice components by CZE

(A) Borate only

See Fig A-1 for the comparison between two runs using (a) 10 mM (buffer R) and (b) 50 mM sodium tetraborate (buffer A).

We notice that the EOF is faster and hence migration times are shorter when 10 mM sodium tetraborate buffer is used. This is attributed to the fact the zeta potential is greater in a lower ionic strength buffer, leading to a faster EOF, see equation 7a-c.The current profiles are also given in Fig C-1 (see Appendix 9). We notice that the current is lower in the case of 10 mM sodium tetraborate.

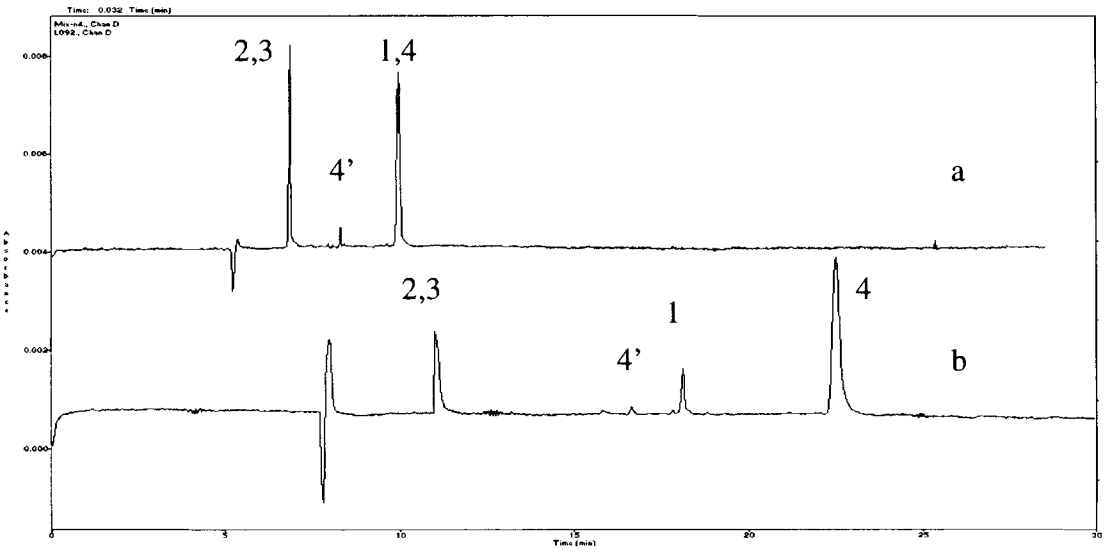

Fig.A-1 Effect of concentration of sodium tetraborate on the separation of four licorice components by CZE. Analytical conditions: Voltage: 17 kV; Capillary: 50 μm × 60.2 cm; distance to detector: 50 cm; Wavelength: 254 nm. (a) 10 mM sodium tetraborate; (b) 50 mM sodium tetraborate
GL (1); 18α-GA (2); 18β-GA (3); IQ (4 and 4')
Component identification for a and b are given in Fig B-1 and Fig 11, respectively. See C-1 for current profiles.

(B) Borate and SDS

See Fig.A-2 for the comparison between two runs using (a) 10 mM sodium tetraborate and 25 mM SDS (buffer T) and (b) 50 mM sodium tetraborate and 25 mM SDS (buffer B).

We notice that the migration times are shorter in buffer T as explained in (A).
As shown in Fig C-2 in Appendix 9, we see the current in buffer T is lower.

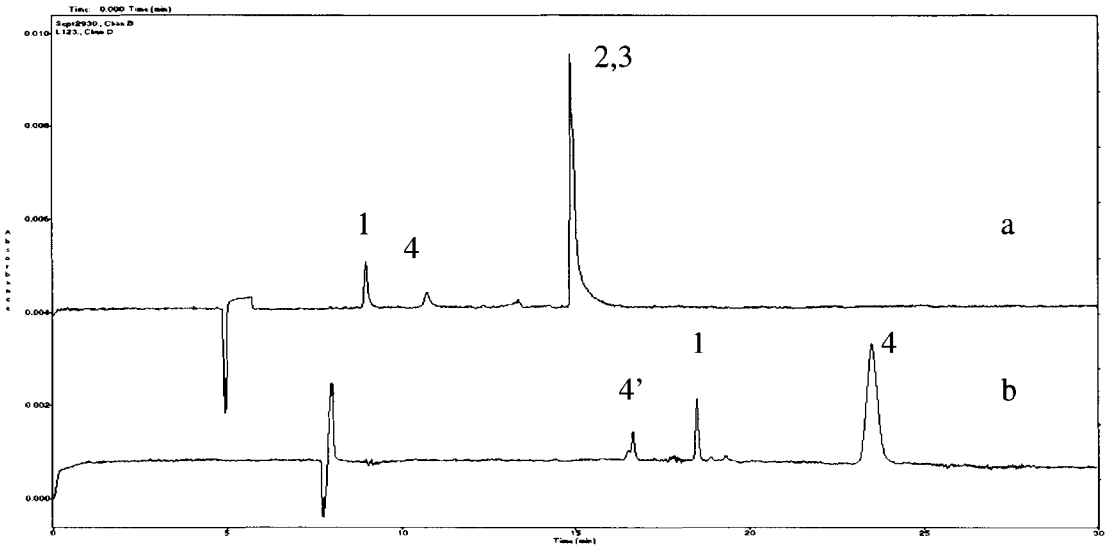

Fig.A-2 Effect of concentration of sodium tetraborate on the separation of four licorice components by MECC. Analytical conditions: Voltage: 17 kV; Capillary: 50 μm × 60.2 cm; distance to detector: 50 cm; Wavelength: 254 nm. (a) 10 mM sodium tetraborate + 25 mM SDS; (b) 50 mM sodium tetraborate + 25 mM SDS
GL (1); 18α-GA (2); 18β-GA (3); IQ (4 and 4'). See Fig.C-2 for current.

Appendix 3 Repeatability study of triplicate separation of licorice components using buffer B

See Fig A-3 for the repeatability study of triplicate separation of licorice components using buffer B. Repeatability is in general satisfactory, except in (a).

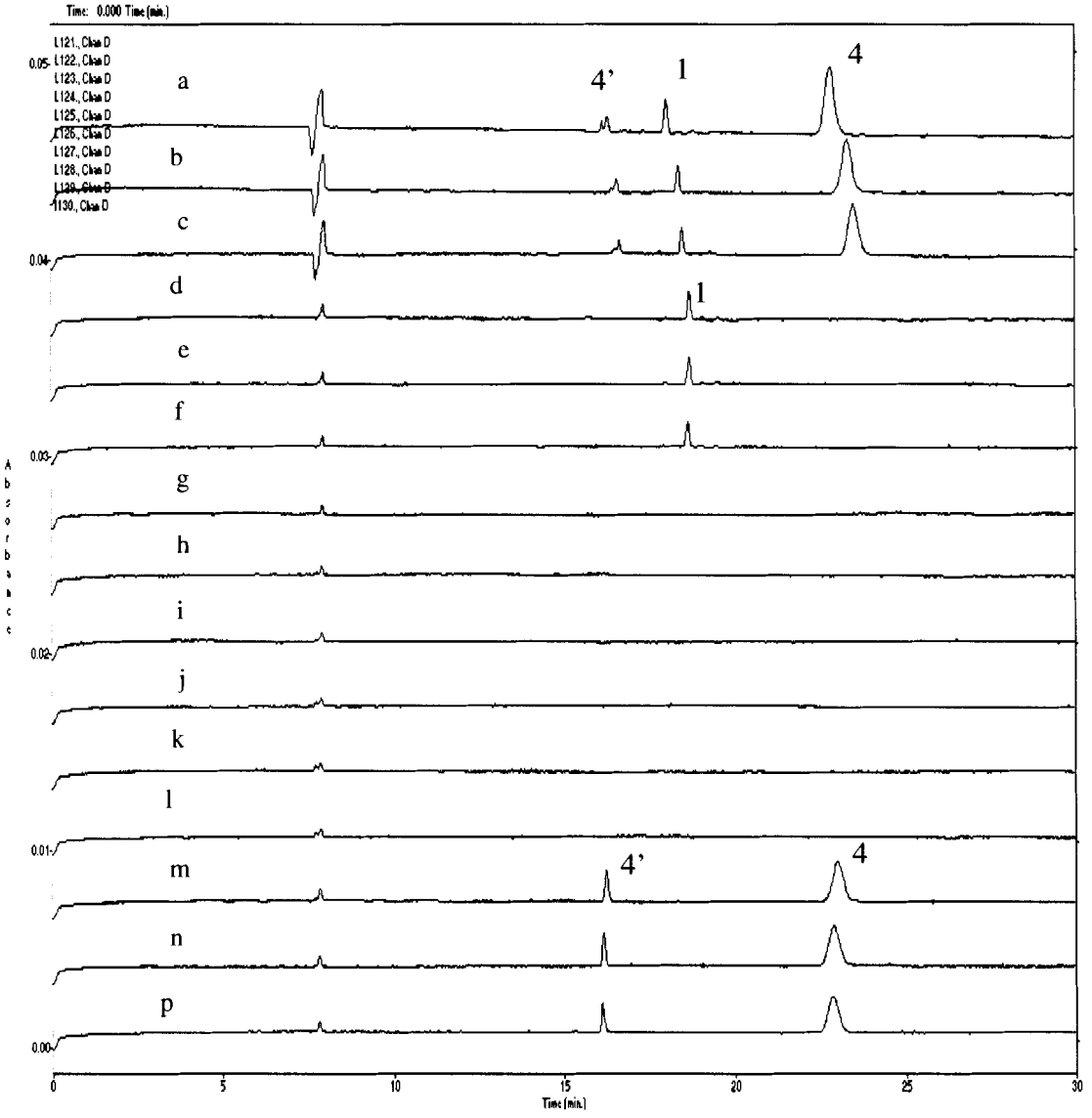

Fig.A-3 Electropherograms obtained for the repeatability of separation of GL, 18α-GA, 18β-GA and IQ by MECC (SDS). Analytical conditions: 50mM sodium tetraborate + 25mM SDS (buffer B); Voltage: 17kV; Capillary: 50 μm × 60.2 cm; distance to detector: 50 cm; Wavelength: 254nm.
(a)-(c) mixture; (d)-(f) GL (1); (g)-(i) 18α-GA (2); (j)-(l)18β-GA (3); (m)-(p) IQ (4 and 4')

Appendix 4 Effect of internal diameter of capillary on separation of licorice components by CZE

See Fig A-4 for the comparison between two runs using capillary i.d. of (a) 50 μm and (b) 75 μm .

We notice that migration times for all peaks are shorter in 50 μm (Fig A-4b). But compounds 2,3 and 1,4 remains unseparated. But an additional compound migrates earlier than the peak where compounds 1 and 4 co-migrate.

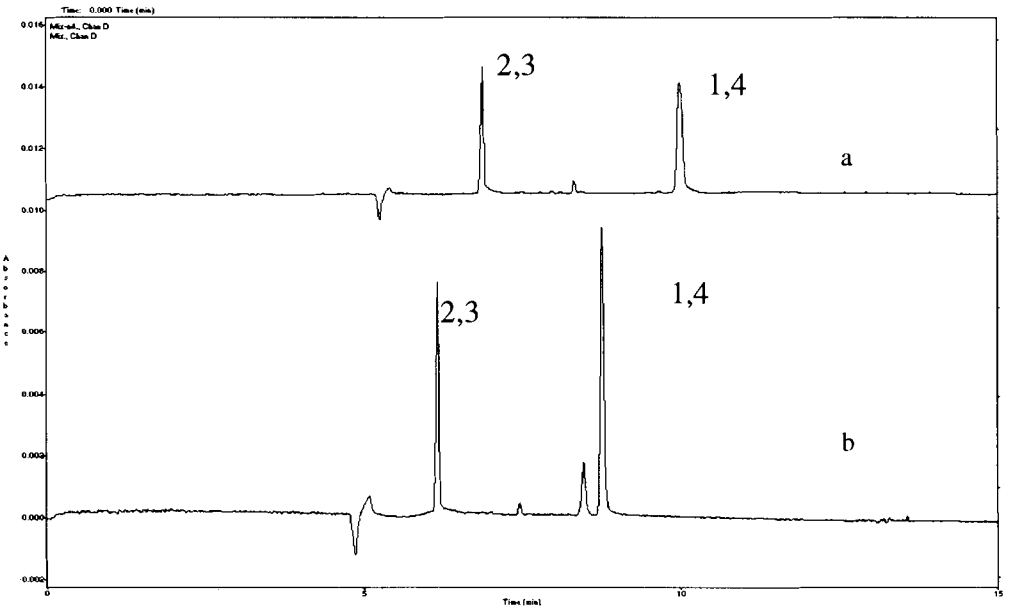

Fig.A-4 Effect of different inner diameter of capillary on the separation of four licorice components by CZE. Analytical conditions: 10 mM sodium tetraborate (buffer R); Voltage: 17 kV; Wavelength: 254 nm. (a) Capillary: 75 μm × 60.2 cm; distance to detector: 50 cm; (b) Capillary: 50 μm × 60.2 cm; distance to detector: 50 cm;
GL (1); 18α-GA (2); 18β-GA (3); IQ (4 and 4')
Component identification for a and b are given in Fig B-1 and Fig B-3, respectively in Appendix 8. See Fig C-3 for current profiles (see Appendix 9).

Appendix 5 Resolution calculations

Resolution of separation between peaks were calculated according to equation 12.

Appendix 5A pH effect on resolution in CD-MECC (SC)

	Peak	t1(s)	t2(s)	w1(cm)	wt1(s)	w2(cm)	wt2(s)	R
Fig.25a	2,3	5.76	5.88	0.15	0.04	0.35	0.09	1.80
	3,4'	5.88	6.28	0.35	0.09	0.65	0.17	3.04
	4,4'	6.28	6.83	0.65	0.17	0.55	0.15	3.46
	4,1	6.83	8.06	0.55	0.15	0.80	0.21	6.78
Fig.25b	2,3	7.61	7.88	0.20	0.08	0.30	0.12	2.76
	3,4'	7.88	8.10	0.30	0.12	0.45	0.17	1.53
	4,4'	8.10	8.78	0.45	0.17	0.50	0.19	3.73
	4,1	8.78	11.86	0.50	0.19	1.50	0.58	8.02
Fig.25c	2,3	7.81	8.03	0.20	0.08	0.30	0.12	2.17
	3,4"	8.03	8.82	0.30	0.12	0.30	0.12	6.58
	4",4'	8.82	8.96	0.30	0.12	0.30	0.12	1.15
	4',4	8.96	9.90	0.30	0.12	0.50	0.20	5.80
	4,1	9.90	11.96	0.50	0.20	1.35	0.54	5.52
Fig.25d	2,3	8.89	9.21	0.15	0.08	0.20	0.10	3.59
	3,4"	9.21	9.89	0.20	0.10	0.25	0.13	5.79
	4",4'	9.89	10.07	0.25	0.13	0.30	0.16	1.23
	4',4	10.07	11.29	0.30	0.16	0.35	0.18	7.20
	4,1	11.29	14.53	0.35	0.18	1.75	0.91	5.93

Note: R is resolution
t1 and t2 represent the migration times for the two peaks.
w1 and w2 represent the peak width in centimeter for the two peaks, while wt1 and wt2 represent the peak width in second for the two peaks.

Greatest resolution for components 2 and 3 is found in Fig 25d, i.e. pH=10.0.

Appendix 5B Temperature effect on resolution in CD-MECC (SC)

	Peak	t1(s)	t2(s)	w1(cm)	wt1(s)	w2(cm)	wt2(s)	R
Fig.26a	1,2	6.45	6.57	0.35	0.10	0.35	0.10	1.19
	2,3	6.57	6.93	0.35	0.10	0.75	0.21	2.28
	3,4	6.93	7.61	0.75	0.21	0.60	0.17	3.54
	4,5	7.61	9.05	0.60	0.17	0.65	0.19	8.06
Fig.26b	1,2	5.76	5.88	0.15	0.04	0.35	0.09	1.80
	2,3	5.88	6.28	0.35	0.09	0.65	0.17	3.04
	3,4	6.28	6.83	0.65	0.17	0.55	0.15	3.46
	4,5	6.83	8.06	0.55	0.15	0.80	0.21	6.78
Fig.26c	2,3	4.91	5.02	0.55	0.11	0.70	0.13	0.88
	3,4'	5.02	5.19	0.70	0.13	1.15	0.22	0.97
	4',4	5.19	5.69	1.15	0.22	1.15	0.22	2.25
	4,1	5.69	6.85	1.15	0.22	1.25	0.24	5.03
Fig.26d	2,3	4.46	4.56	0.50	0.09	1.15	0.20	0.68
	3,4'	4.56	4.72	1.15	0.20	1.95	0.34	0.59
	4',4	4.72	5.12	1.95	0.34	1.95	0.34	1.19
	4,1	5.12	6.20	1.95	0.34	1.30	0.22	3.88
Fig.26e	2,3	4.37	4.47	0.65	0.11	0.70	0.12	0.82
	3,4'	4.47	4.47	0.70	0.12	1.10	0.19	1.27
	4',4	4.67	5.16	1.10	0.19	1.95	0.34	1.86
	4,1	5.16	6.33	1.95	0.34	2.00	0.35	3.37

Note: R is resolution
t1 and t2 represent the migration times for the two peaks.
w1 and w2 represent the peak width in centimeter for the two peaks, while wt1 and wt2 represent the peak width in second for the two peaks.

Greatest resolution for components 2 and 3 is found in Fig 26b, i.e. temperature=25°C

Appendix 6 Effect of different methanol percentage in CD-MECC (SDS)

See Fig A-5 for the effect of different methanol percentage in the run buffer. We found that 18α–GA and 18β-GA did not migrate faster than IQ.

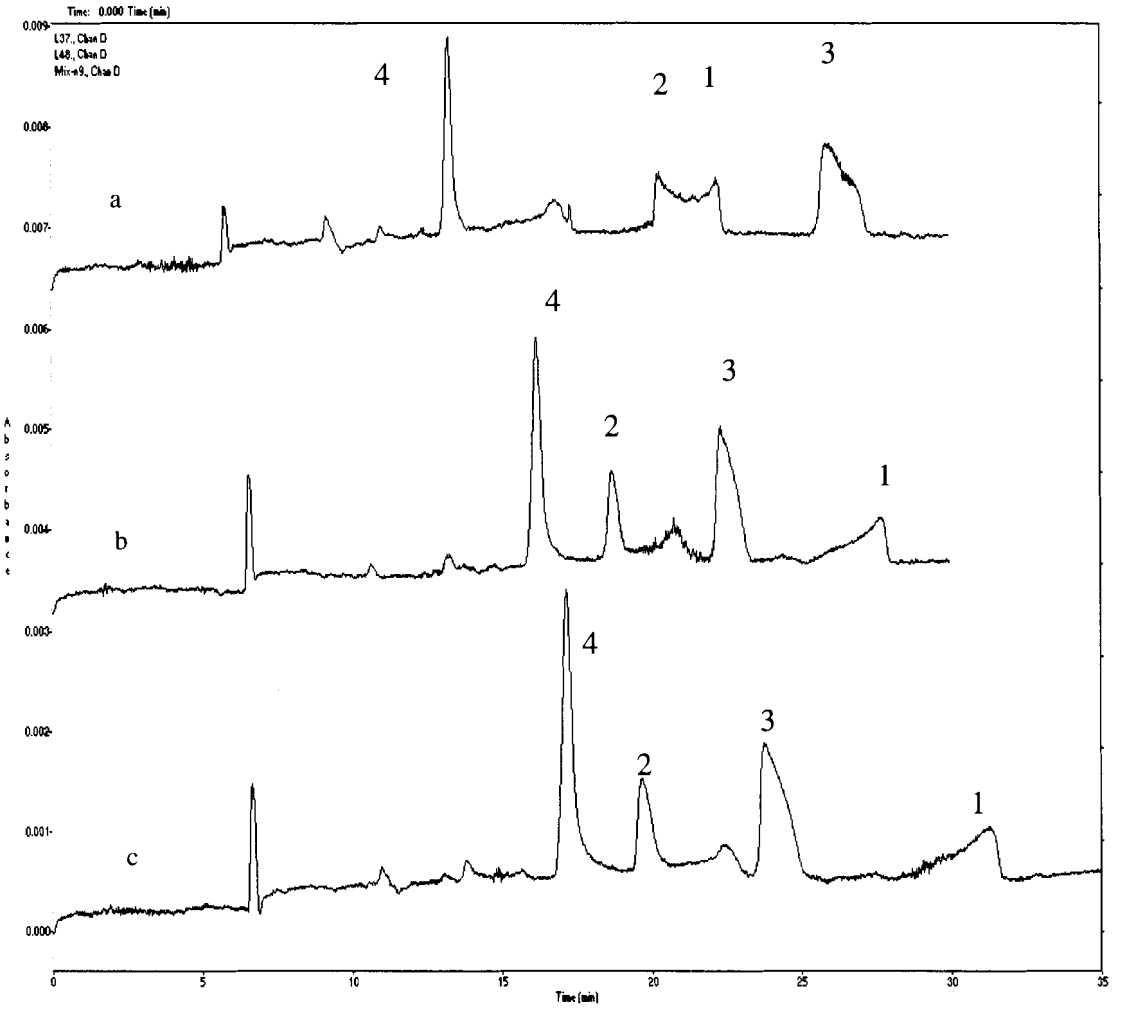

Fig.A-5 Electropherograms obtained for the effect of different percentage of MeOH on the separation of GL, 18α-GA, 18β-GA and IQ by CD-MECC. Analytical conditions: 50 mM sodium tetraborate + 25 mM SDS + 20 mM β-CD; Voltage: 10kV; Capillary: 50 μm × 60.2 cm; distance to detector: 10.2 cm; Wavelength: 254 nm; pH 8.5; temperature at 25°C; Amount of methanol: (a) 15% (buffer E); (b) 20% (buffer F); (c) 30% (buffer G) GL (1); 18α-GA (2); 18β-GA (3); IQ (4 and 4') Component identification for a and b are given in Fig B-7 and Fig B-8, respectively. Single standard electropherograms were not obtained for c, as peak identification became obvious.

Appendix 7 Separation using the borate-SC-SDS-CD system

(A) The effect of methanol

Fig.A-6 is the electropherograms for the effect of different percentage of MeOH by using buffer W. Resolution increased as MeOH content increased.

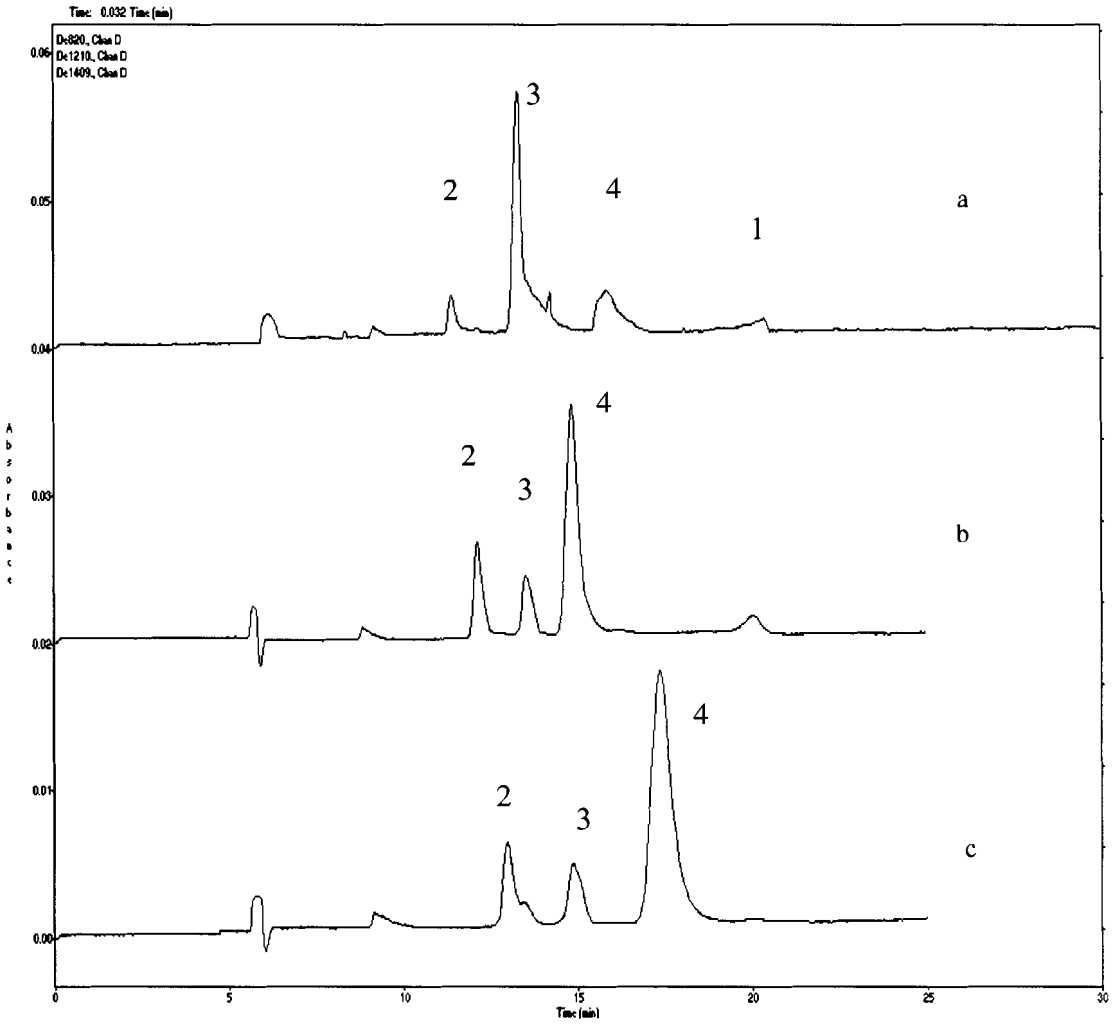

Fig.A-6 Electropherograms obtained for the effect of different percentage of MeOH on the separation of GL, 18α-GA, 18β-GA and IQ by CD-MECC. Analytical conditions: 50 mM sodium tetraborate + 25 mM SDS + 20 mM β-CD + 10 mM SC; Voltage: 10kV; Capillary: 75 μm × 60.2 cm; distance to detector: 10.2 cm; Wavelength: 254 nm; pH 8.5; temperature at 25°C; Amount of methanol in run buffer:(a) 20%; (b) 25%; (c) 30%

(B) The effect of temperature

Fig.A-7 shows the electropherograms for the effect of two different temperatures by using buffer S. EOF was faster at a higher temperature and analysis time was shortened, as shown in (b). But in (a), a better resolution is obtained.

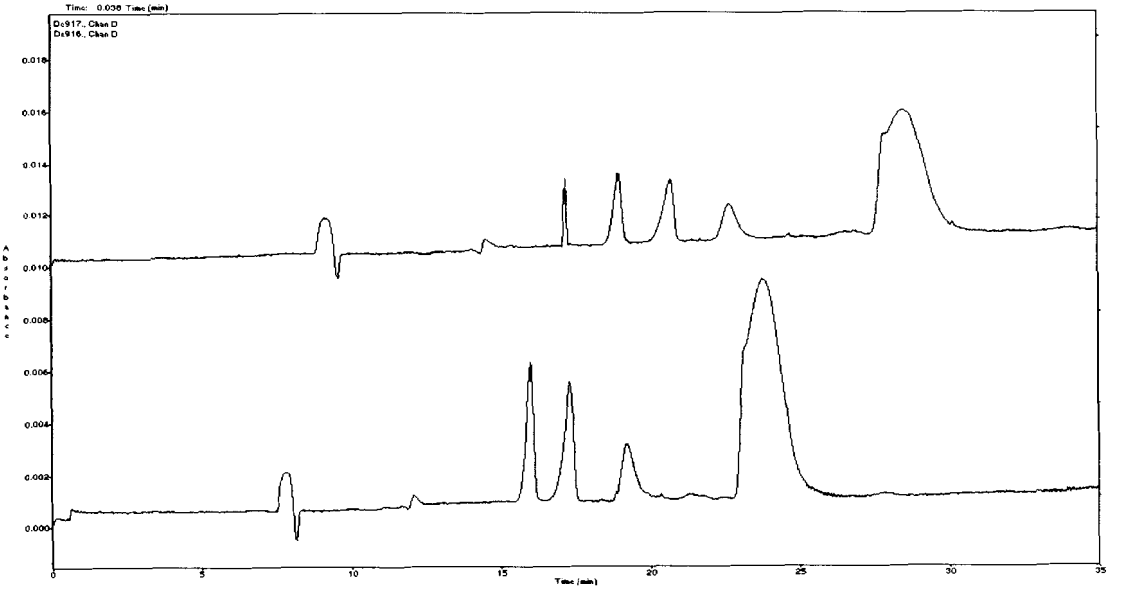

Fig.A-7 Electropherograms obtained for the effect of different temperature on the separation of GL, 18α-GA, 18β-GA and IQ by CD-MECC. Analytical conditions: 50 mM sodium tetraborate + 25 mM SDS + 20 mM β-CD + 10 mM SC + 30% MeOH; Voltage: 10kV; Capillary length: 10.2 cm; Wavelength: 254 nm; pH 8.5; temperature at (a) 20°C; (b) 25°C

Appendix 8 Electropherograms of single standards for component identification

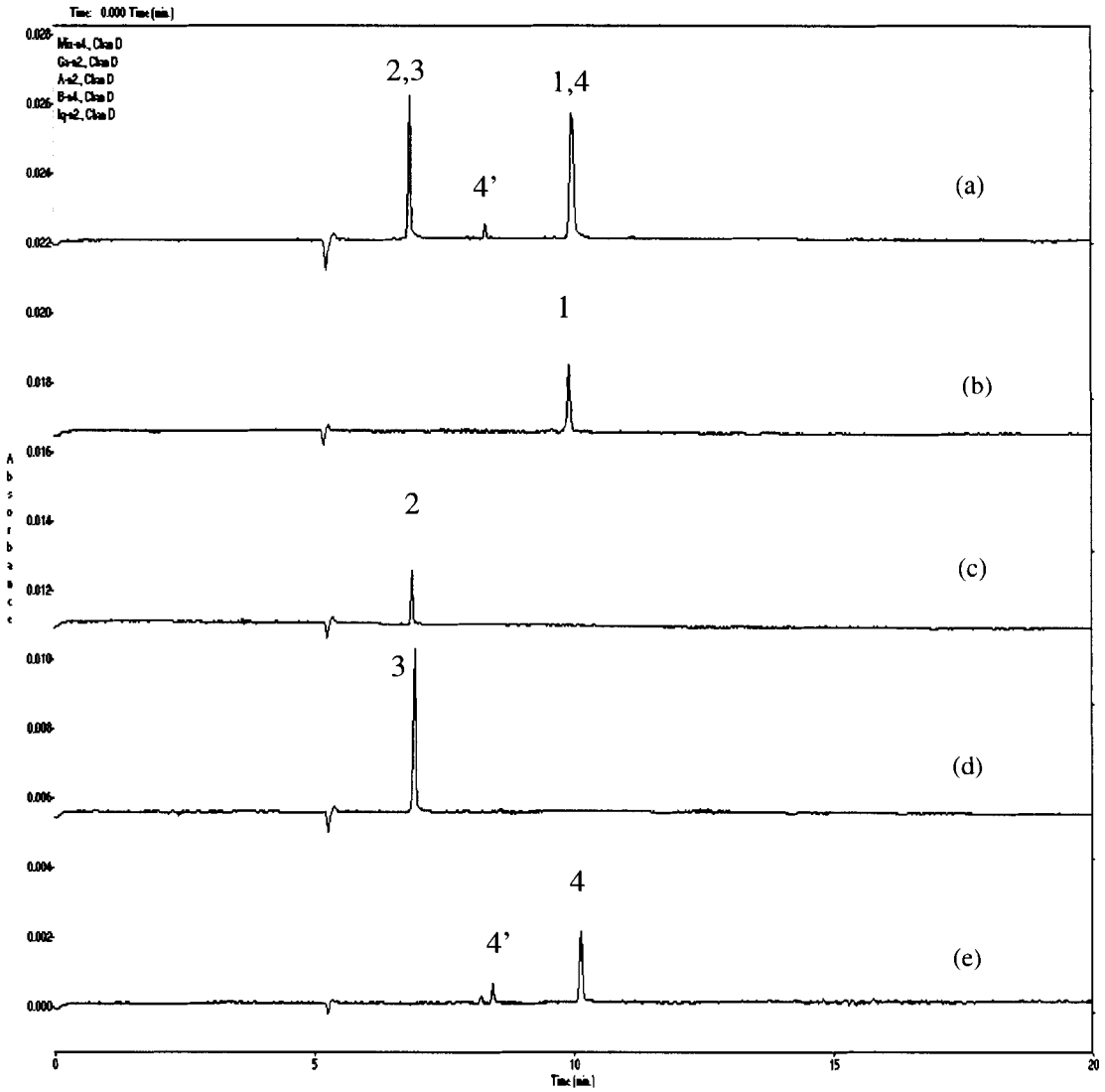

Fig.B-1 Electropherograms obtained for the separation of four conpounds derived from licorice by CZE. Analytical conditions: 10 mM sodium tetraborate (buffer R); Voltage: 17kV; Capillary: 75 μm × 60.2 cm; distance to detector: 50 cm; Temperature of capillary: 25 °C; Wavelength: 254nm.
(a) mixture; (b) GL (1); (c) 18α-GA (2); (d)18β-GA (3); (e) IQ (4 and 4')

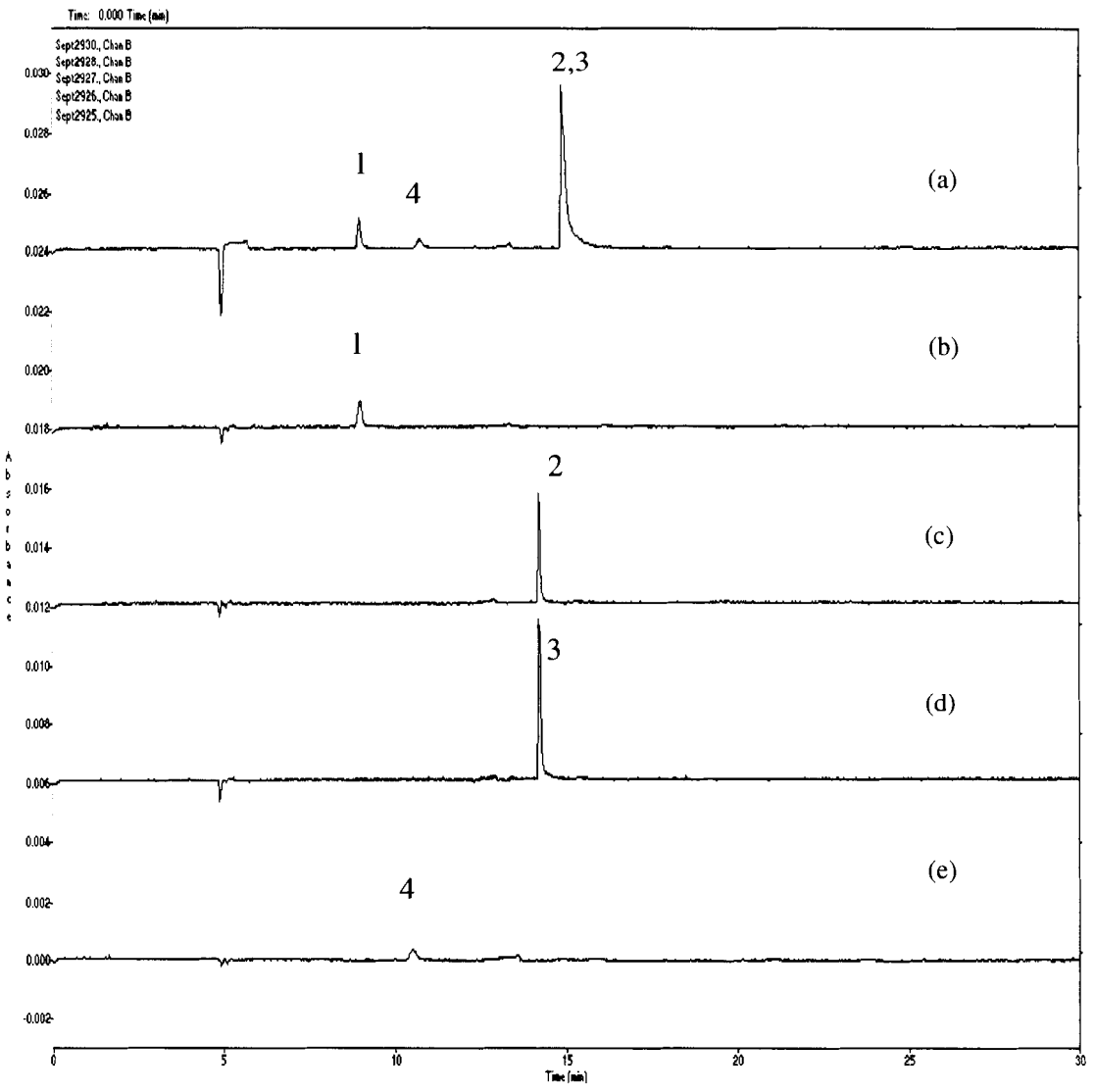

Fig.B-2 Electropherograms obtained for the separation of four compounds derived from licorice by MECC. Analytical conditions: 10 mM sodium tetraborate + 25 mM SDS (buffer T); Voltage: 17kV; Capillary: 75 μm × 60.2 cm; distance to detector: 50 cm; Temperature of capillary: 25 °C; Wavelength: 254nm.
(a) mixture; (b) GL (1); (c) 18α-GA (2); (d)18β-GA (3); (e) IQ (4 and 4')

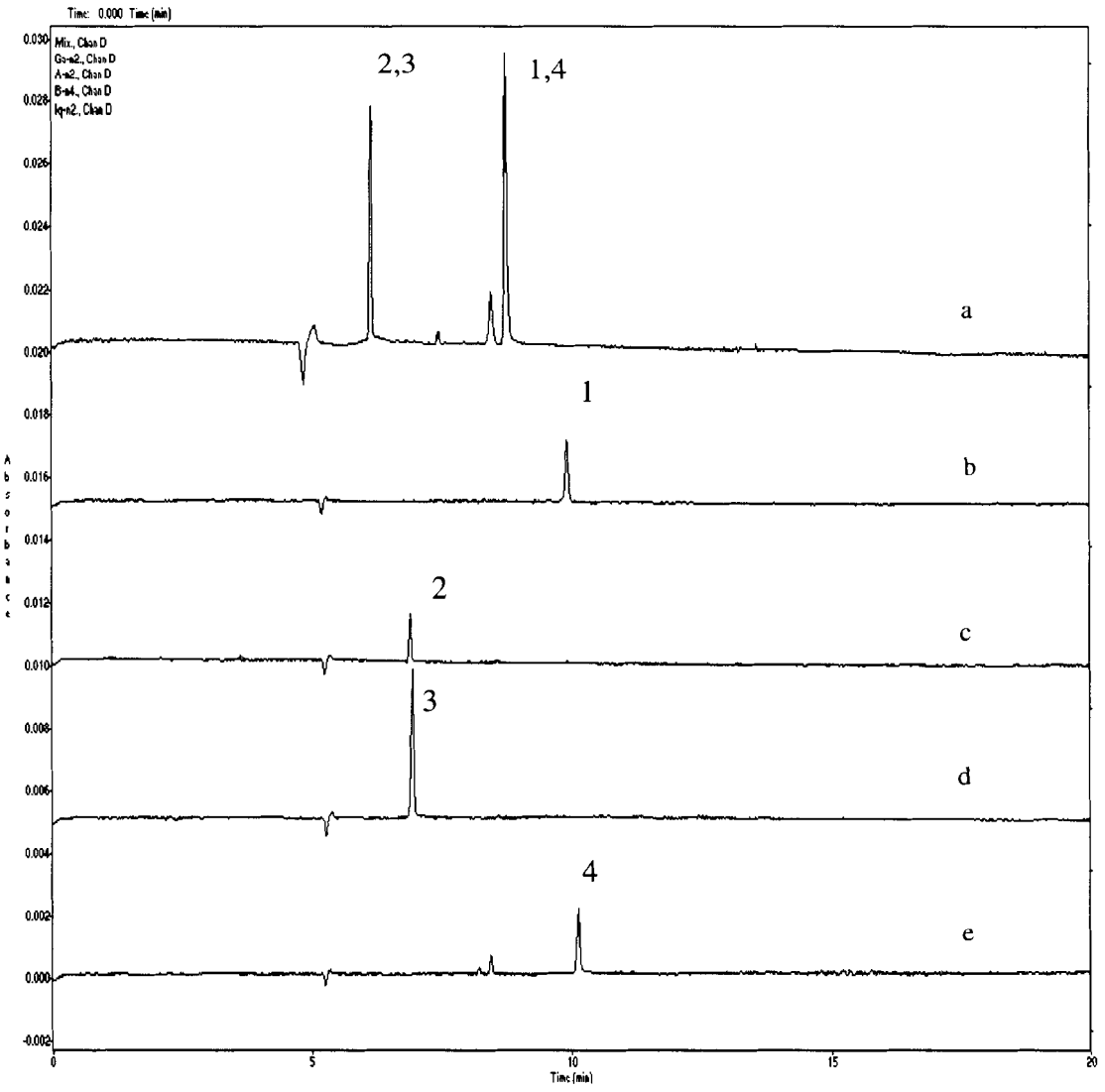

Fig.B-3 Electropherograms obtained for the separation of four compounds derived from licorice by CZE. Analytical conditions: 10 mM sodium tetraborate (buffer R); Voltage: 17kV; Capillary: 50 μm × 60.2 cm; distance to detector: 50 cm; Temperature of capillary: 25 °C; Wavelength: 254nm.
(a) mixture; (b) GL (1); (c) 18α-GA (2); (d)18β-GA (3); (e) IQ (4 and 4')

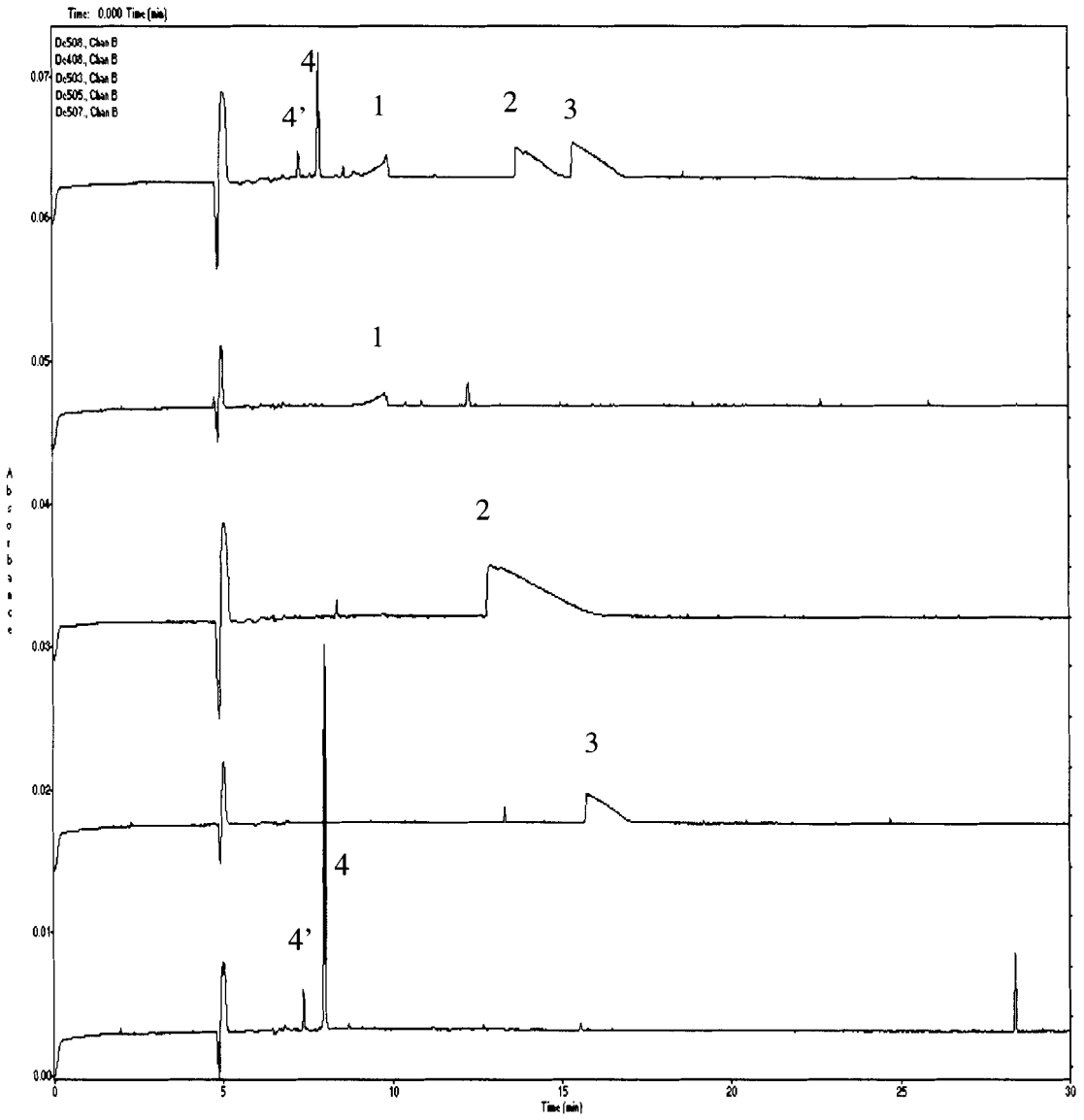

Fig.B-4 Electropherograms obtained for the separation of GL, 18α-GA, 18β-GA and IQ by CD-MECC. Analytical conditions: 50 mM sodium tetraborate + 25 mM SDS + 20 mM β-CD (buffer C); Voltage: 25kV; Capillary: 75 μm × 60.2 cm; distance to detector: 50 cm; Wavelength: 254 nm.
(a) mixture (b) GL (1); (c) 18α-GA (2); (d)18β-GA (3); (e) IQ (4 and 4')

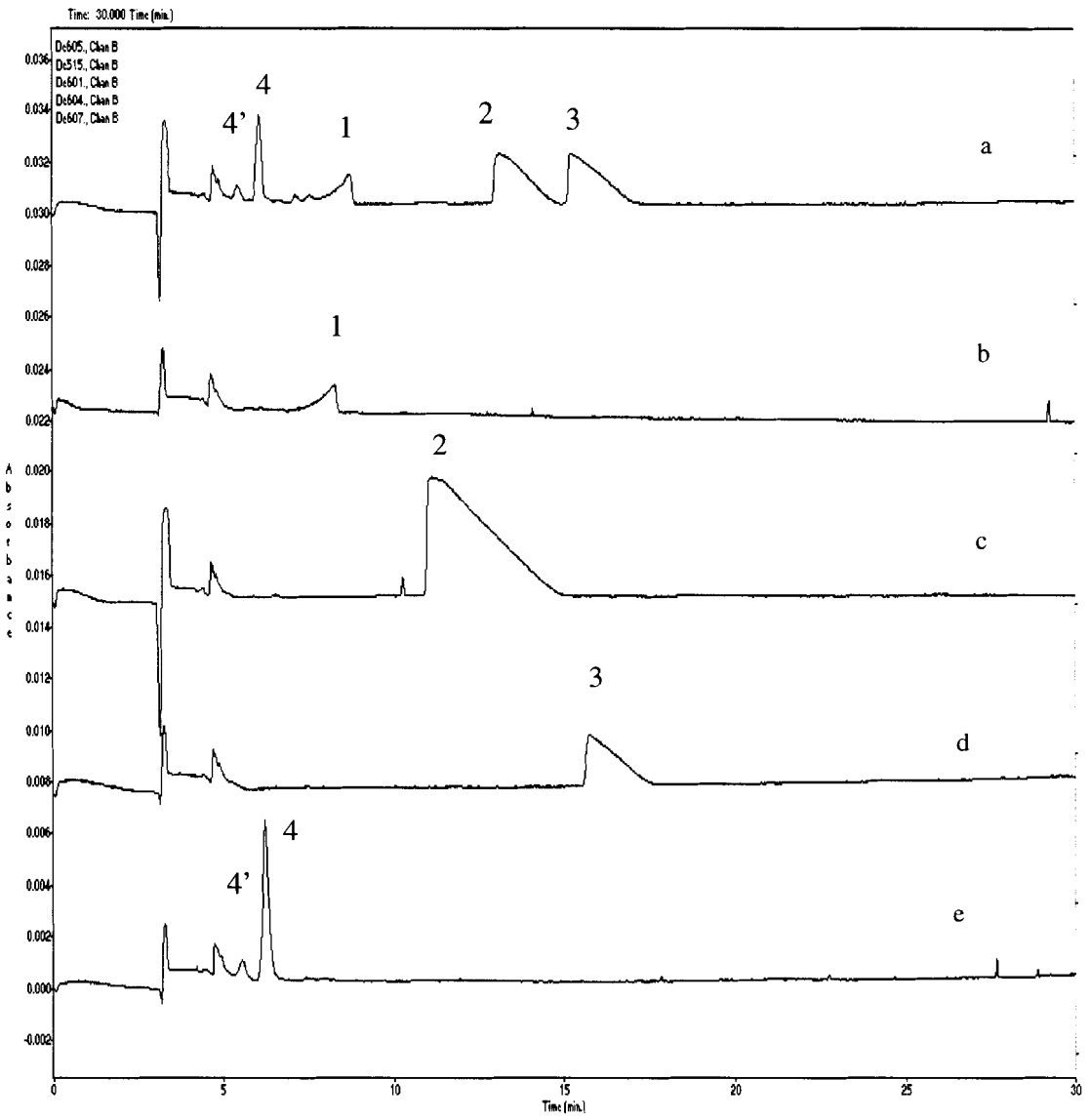

Fig.B-5 Electropherograms obtained for the separation of GL, 18α-GA, 18β-GA and IQ by CD-MECC. Analytical conditions: 50 mM sodium tetraborate + 25 mM SDS + 20 mM β-CD (buffer C); Voltage: 10kV; Capillary: 75 μm × 60.2 cm; distance to detector: 10.2 cm; Wavelength: 254 nm.
(a) mixture; (b) GL(1); (c) 18α-GA (2); (d)18β-GA (3); (e) IQ (4 and 4')

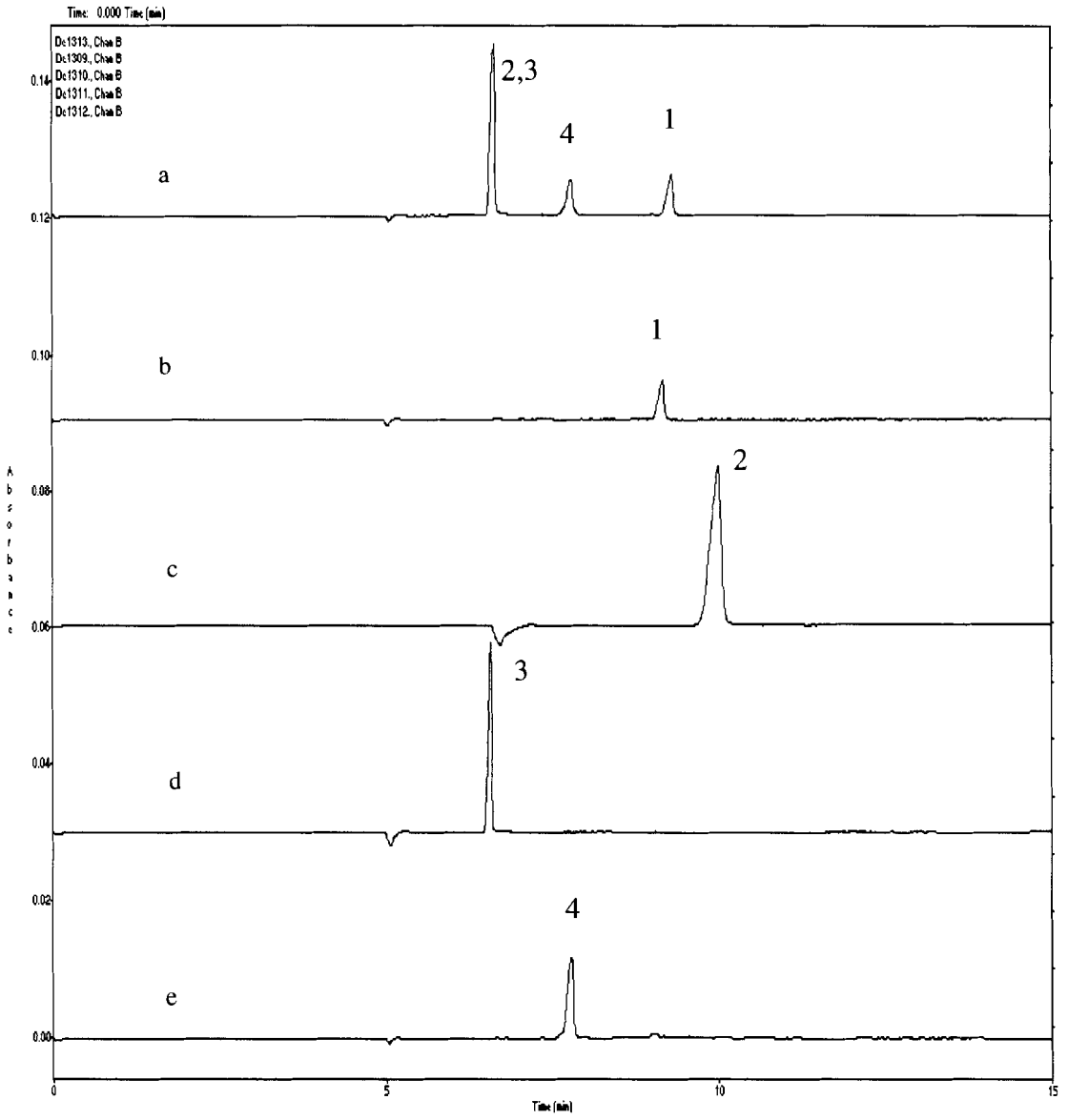

Fig.B-6 Electropherograms obtained for the separation of GL, 18α-GA, 18β-GA and IQ by CD-MECC. Analytical conditions: 50mM sodium tetraborate + 25 mM SDS + 20 β-CD + 10 mM SC + 25% MeOH; Voltage: 10kV; Capillary: 75 μm × 60.2 cm; distance to detector: 10.2 cm; Wavelength: 254nm.
(a) mixture; (b) GL (peak 1); (c) 18α-GA (peak 2); (d) 18β-GA (peak 3); (e) IQ (peak 4 and peak 4')

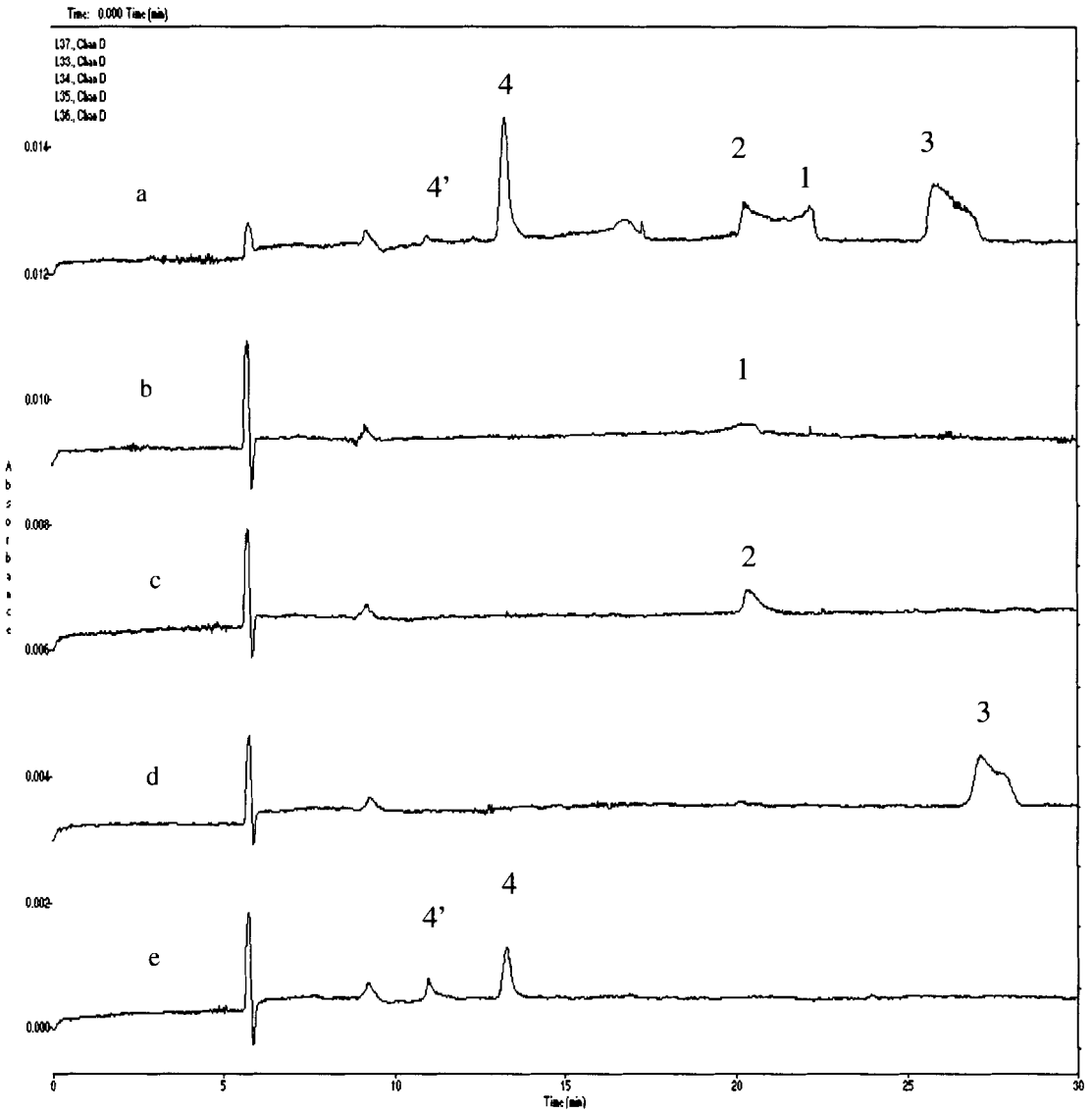

Fig.B-7 Electropherograms obtained for the separation of GL, 18α-GA, 18β-GA and IQ by CD-MECC. Analytical conditions: 50 mM sodium tetraborate + 25 mM β-CD + 25 mM SDS + 15% MeOH (buffer E); Voltage: 10kV; Capillary: 75 μm × 60.2 cm; distance to detector: 10.2 cm; Wavelength: 254nm.
(a) mixture; (b) GL (peak 1); (c) 18α-GA (peak 2); (d)18β-GA (peak 3); (e) IQ (peak 4 and peak 4')

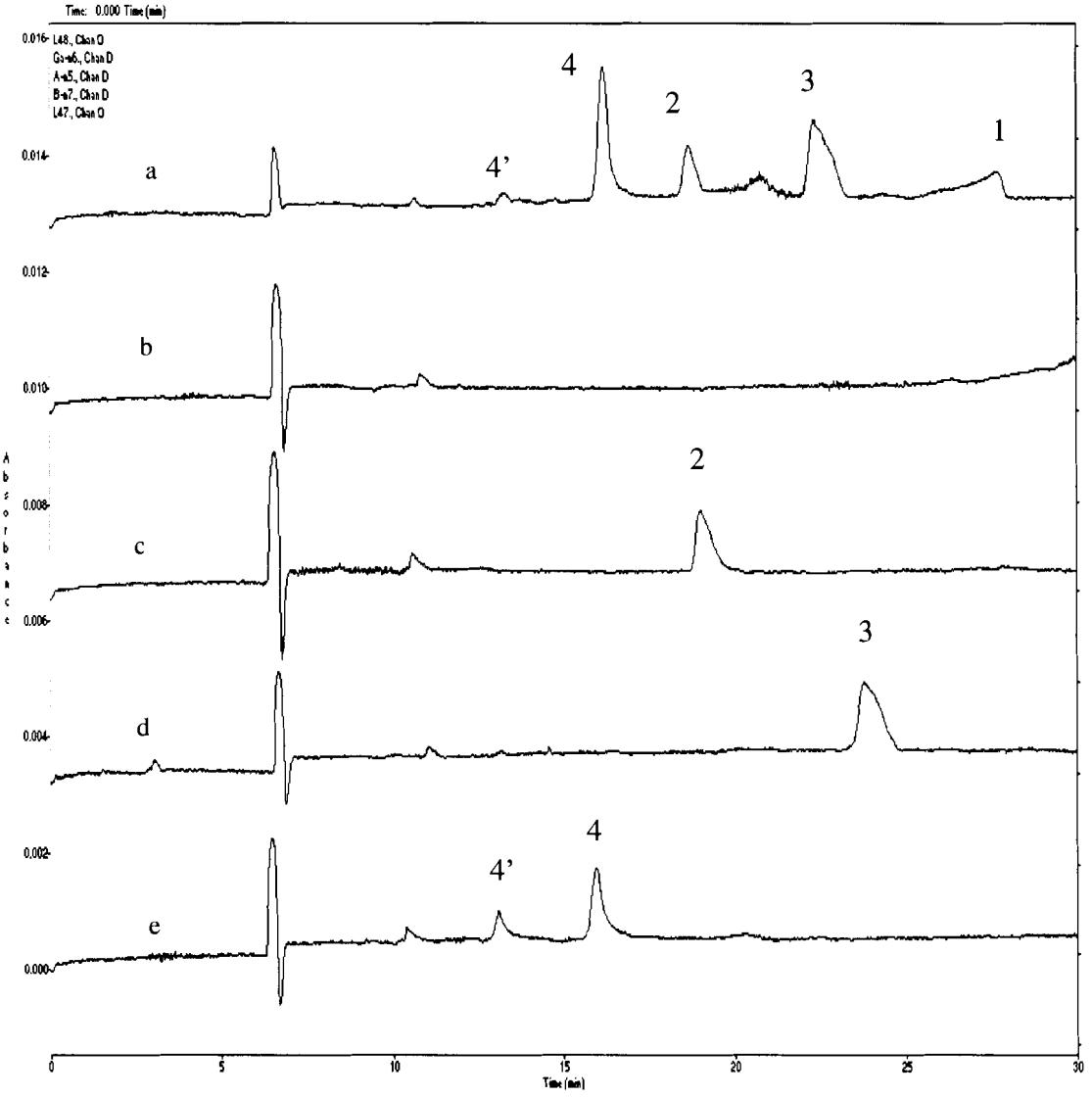

Fig.B-8 Electropherograms obtained for the separation of GL, 18α-GA, 18β-GA and IQ by CD-MECC. Analytical conditions: 50 mM sodium tetraborate + 25 mM β-CD + 25 mM SDS + 20% MeOH (buffer F); Voltage: 10kV; Capillary: 75 μm × 60.2 cm; distance to detector: 10.2 cm; Wavelength: 254nm.
(a) mixture; (b) GL (peak 1); (c) 18α-GA (peak 2); (d)18β-GA (peak 3); (e) IQ (peak 4 and peak 4')

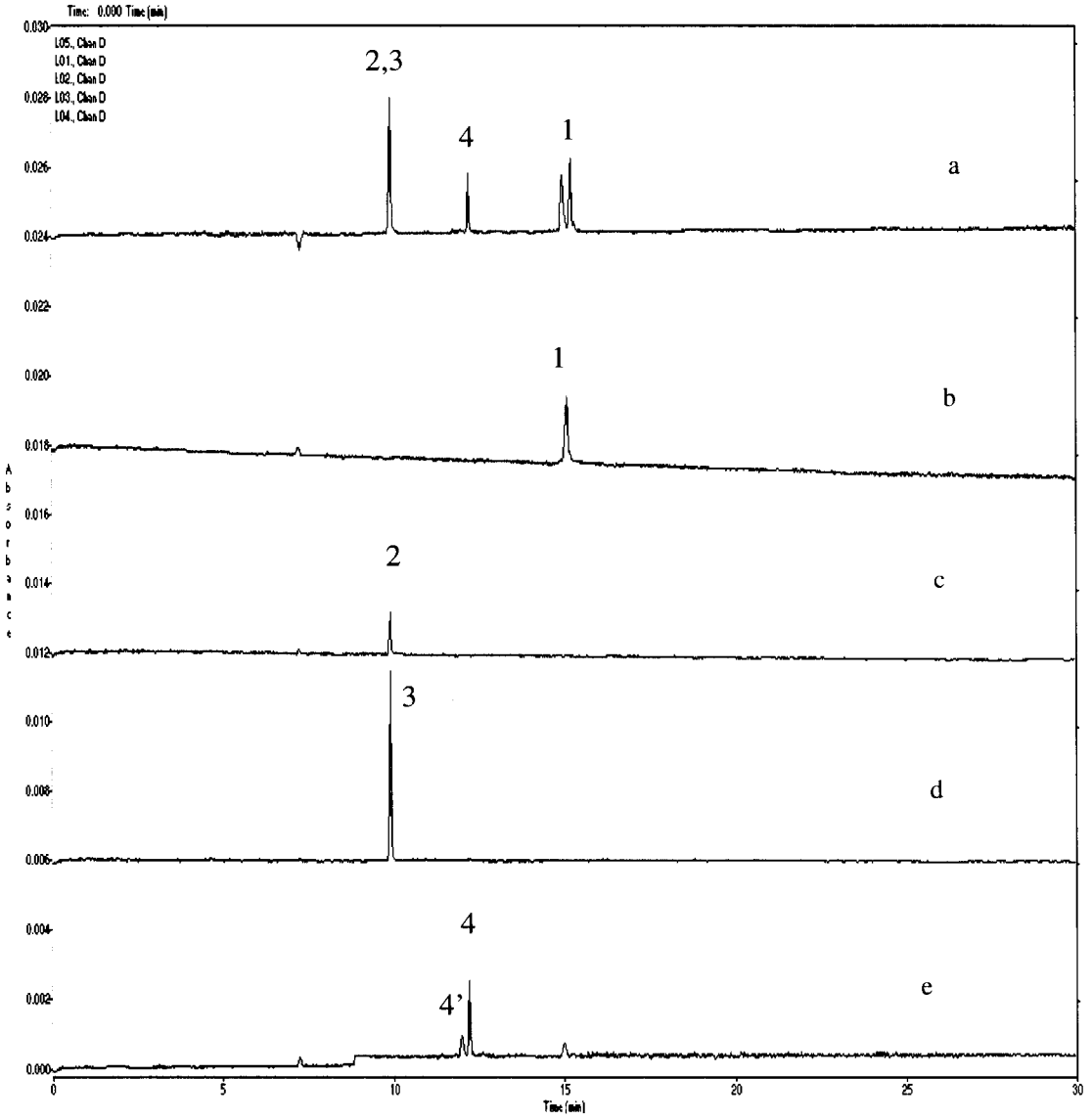

Fig.B-9 Electropherograms obtained for the effect of different percentage of MeOH in run buffer on the separation of GL, 18α-GA, 18β-GA and IQ by CD-MECC. Analytical conditions: 10 mM sodium tetraborate + 25 mM SC + 20 mM β-CD + 10% MeOH (buffer M); Voltage: 17kV; Capillary: 75 μm × 60.2 cm; distance to detector: 50 cm; Wavelength: 254nm.
(a) mixture; (b) GL (1); (c) 18α-GA (2); (d)18β-GA (3); (e) IQ (4 and 4')

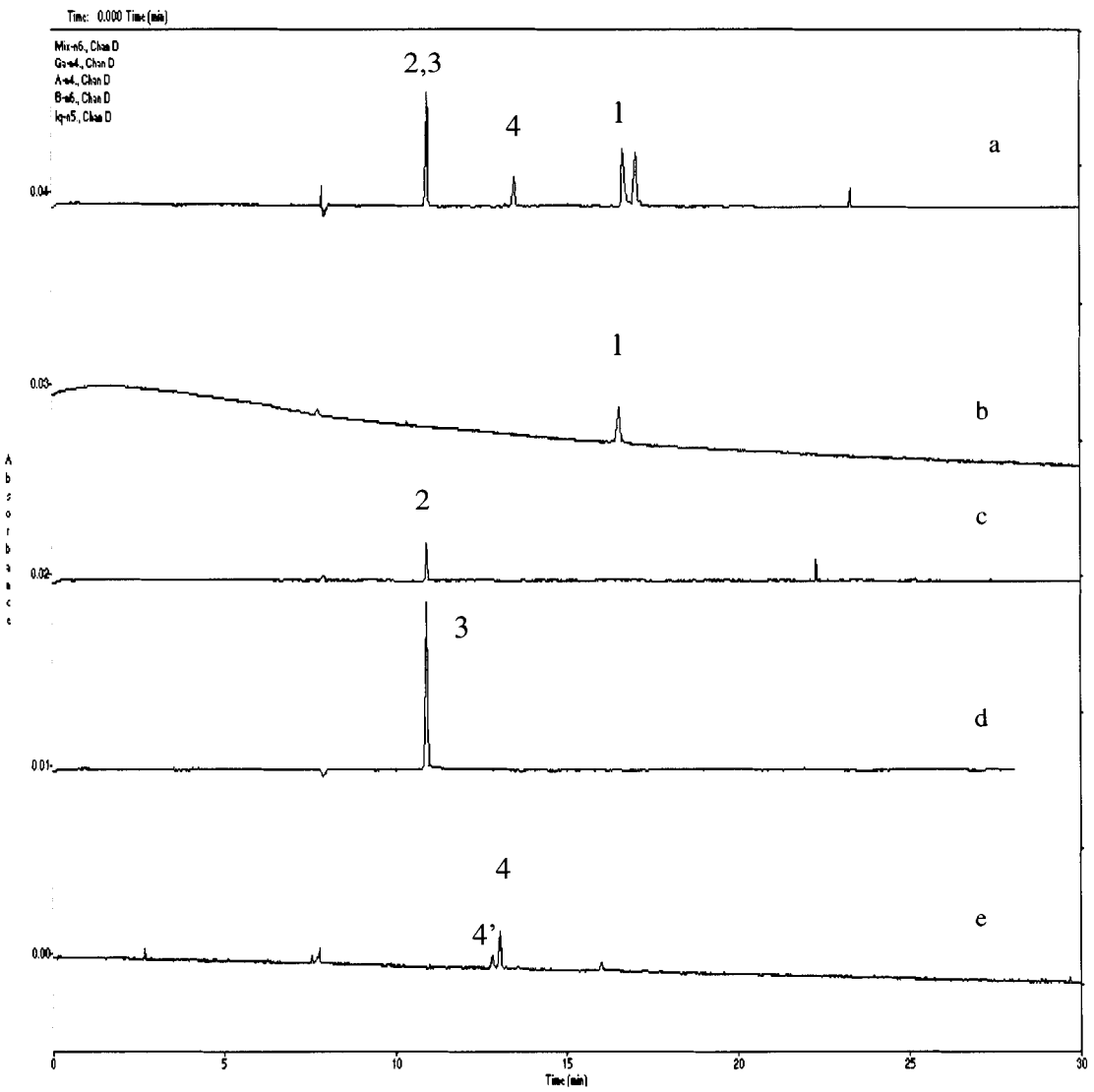

Fig.B-10 Electropherograms obtained for the effect of different percentage of MeOH in run buffer on the separation of GL, 18α-GA, 18β-GA and IQ by CD-MECC. Analytical conditions: 10 mM sodium tetraborate + 25 mM SC + 20 mM β-CD + 15% MeOH (buffer N); Voltage: 17kV; Capillary: 75 μm × 60.2 cm; distance to detector: 50 cm; Wavelength: 254nm.
(a) mixture; (b) GL (1); (c) 18α-GA (2); (d)18β-GA (3); (e) IQ (4 and 4')

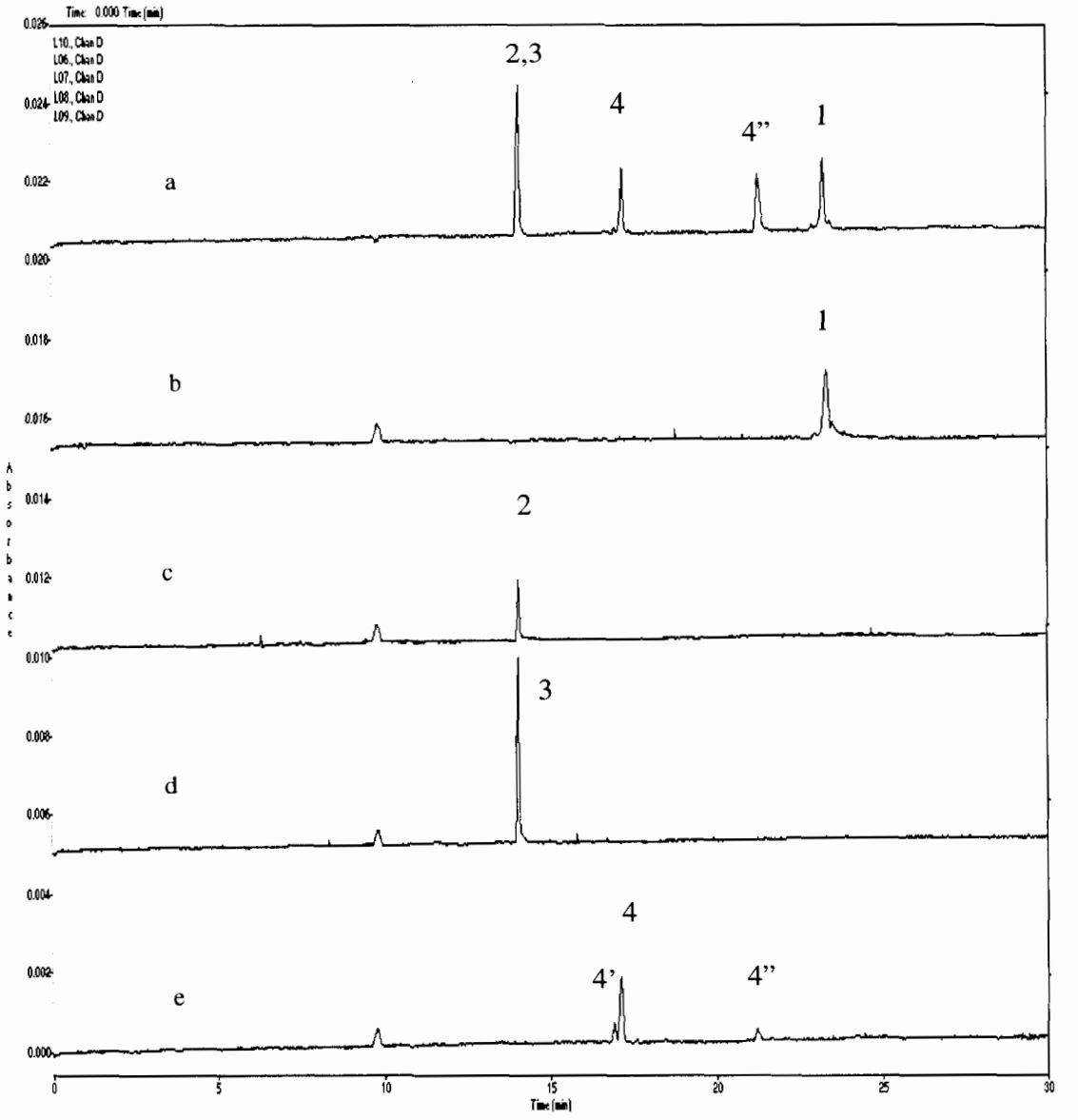

Fig.B-11 Electropherograms obtained for the effect of different percentage of MeOH in run buffer on the separation of GL, 18α-GA, 18β-GA and IQ by CD-MECC. Analytical conditions: 10 mM sodium tetraborate + 25 mM SC + 20 mM β-CD + 20% MeOH (buffer P); Voltage: 17kV; Capillary: 75 μm × 60.2 cm; distance to detector: 50 cm; Wavelength: 254nm.
(a) mixture; (b) GL (*1*); (c) 18α-GA (2); (d)18β-GA (3); (e) IQ (4, 4' and 4")

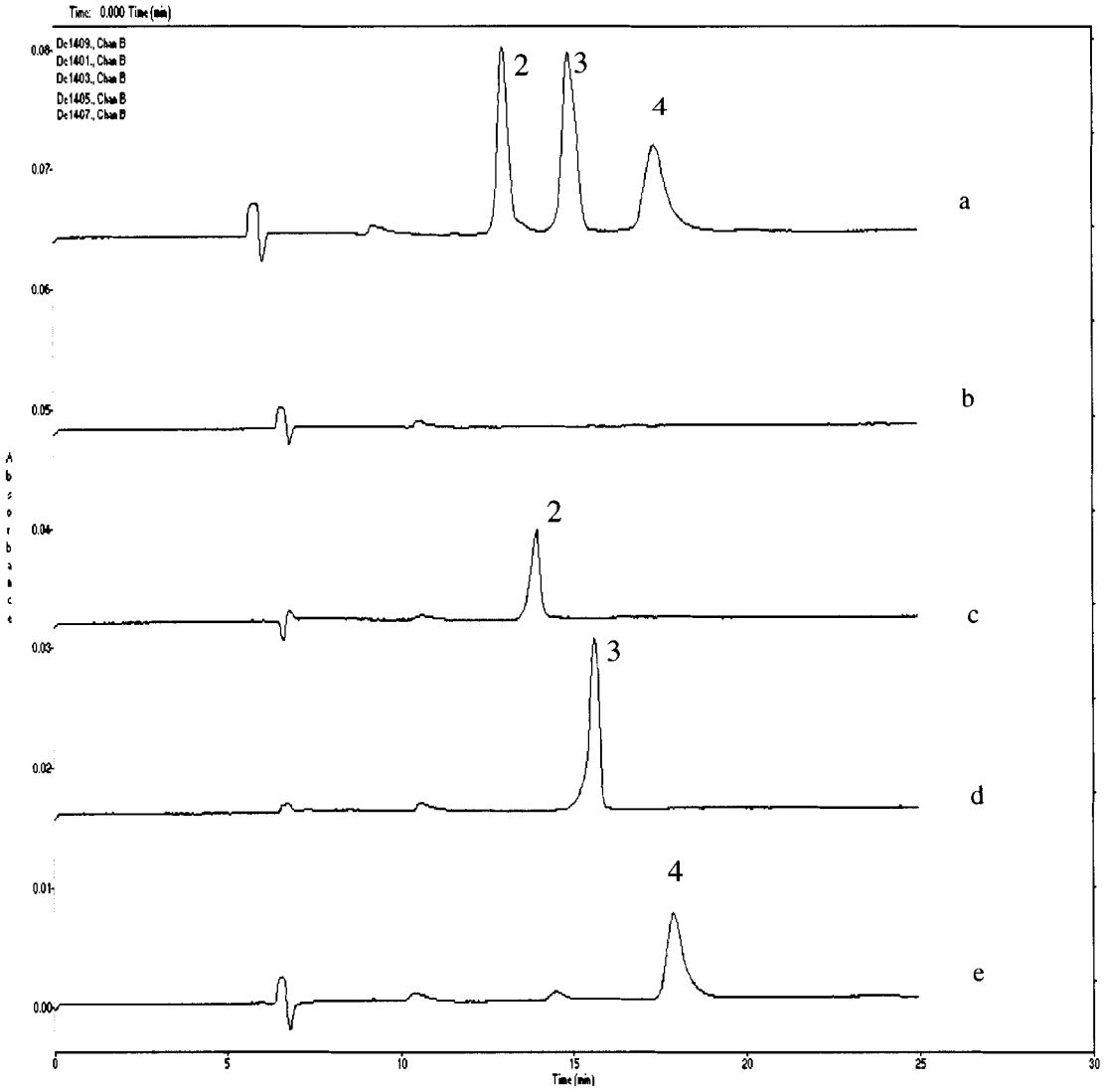

Fig.B-12 Electropherograms obtained for the separation of GL, 18α-GA, 18β-GA and IQ by CD-MECC. Analytical conditions: 50mM sodium tetraborate + 25 mM SDS + 20 mM β-CD (buffer C); Voltage: 10kV; Capillary: 75 μm × 60.2 cm; distance to detector: 10.2 cm; Wavelength: 254nm.

(a) mixture; (b) GL (peak 1); (c) 18α-GA (peak 2); (d)18β-GA (peak 3); (e) IQ (peak 4 and peak 4')

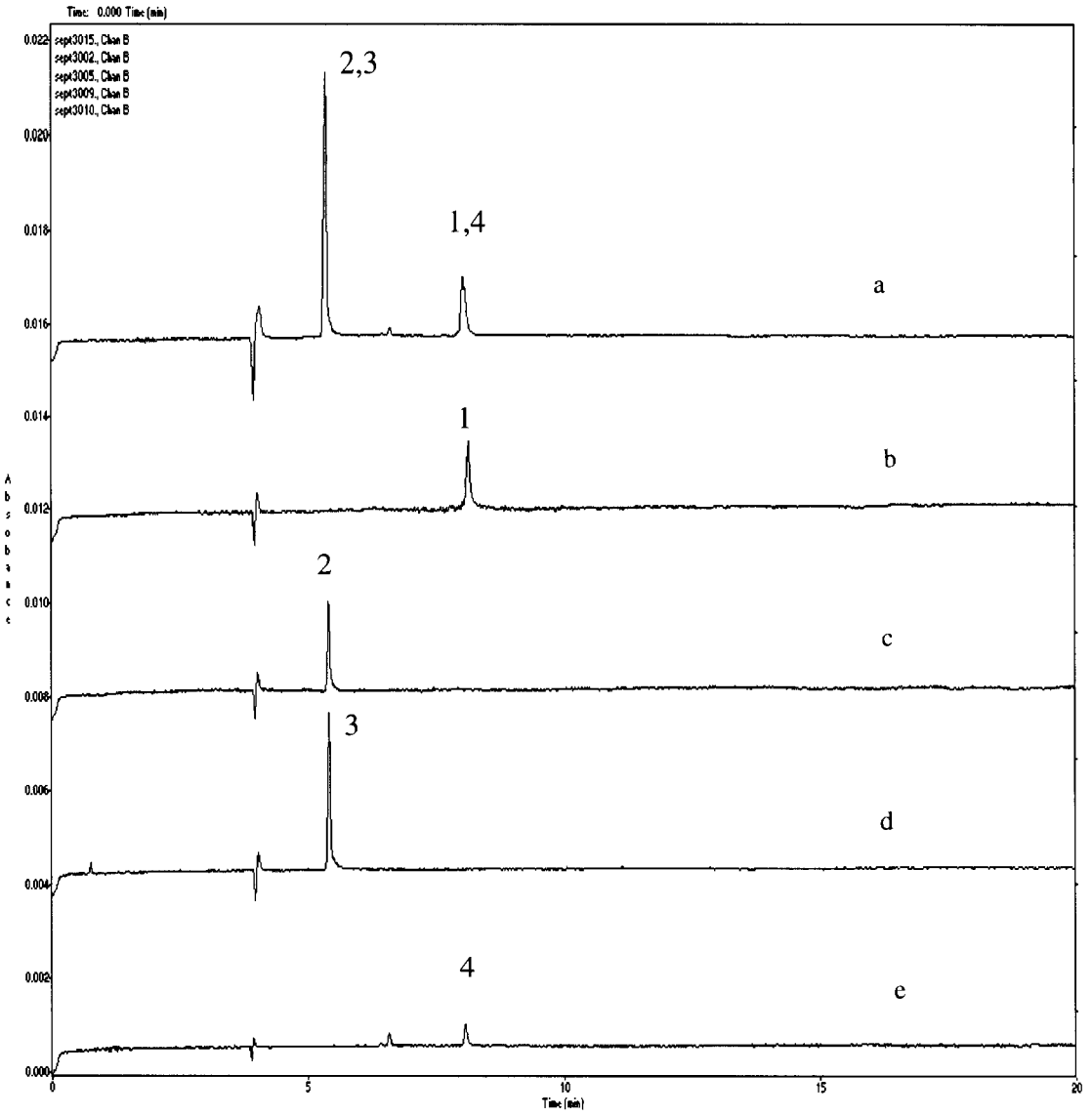

Fig.B-13 Electropherograms obtained for the separation of GL, 18α-GA, 18β-GA and IQ by CZE. Analytical conditions: 20mM sodium tetraborate; Voltage: 17kV; Capillary: 50 μm × 60.2 cm; distance to detector: 50 cm; Wavelength: 254nm.

(a) mixture; (b) GL (peak 1); (c) 18α-GA (peak 2); (d) 18β-GA (peak 3); (e) IQ (peak 4 and peak 4')

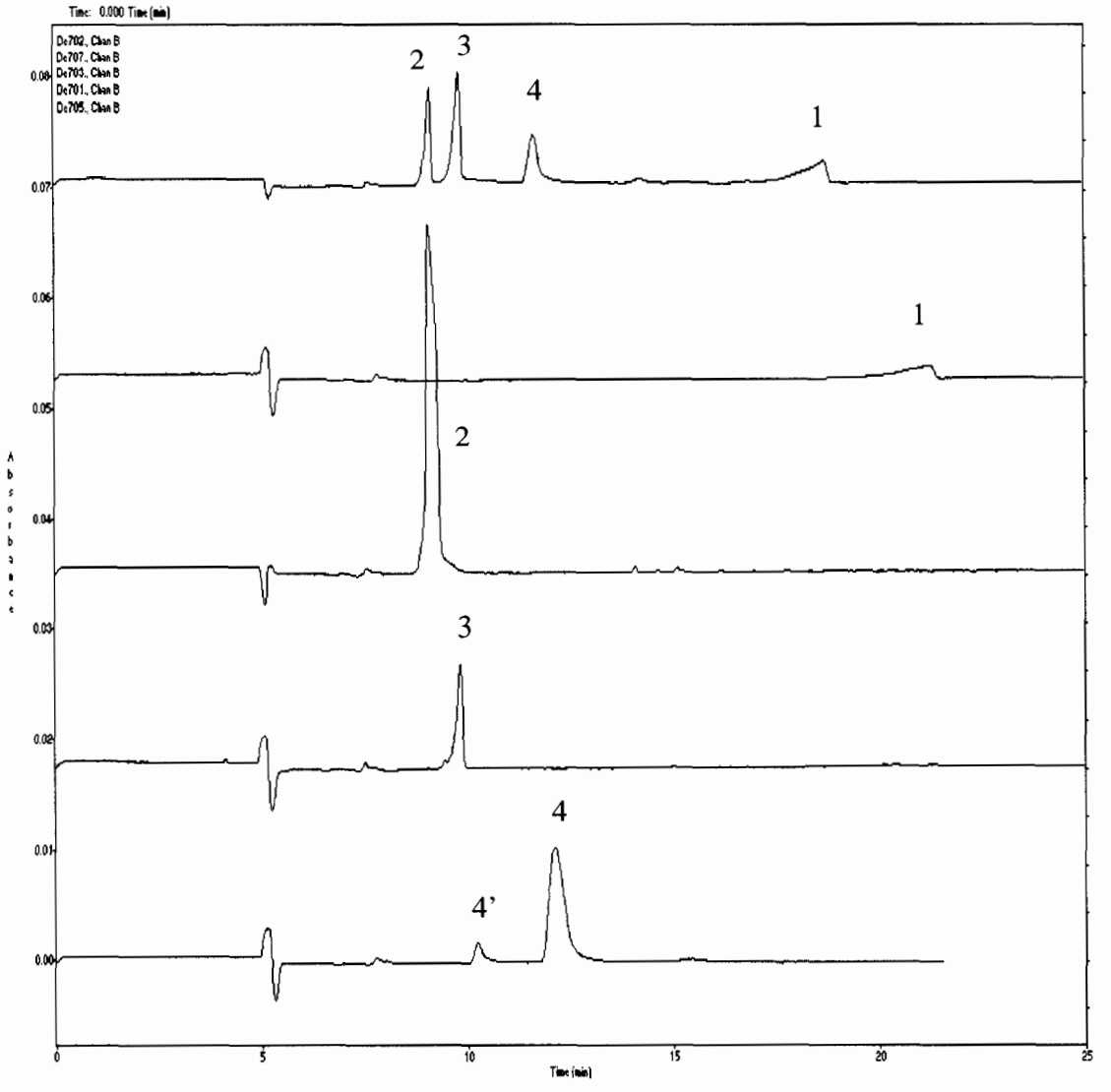

Fig.B-14 Electropherograms obtained for the separation of GL, 18α-GA, 18β-GA and IQ by CD-MECC. Analytical conditions: 50mM sodium tetraborate + 25 mM SDS + 20 β-CD + 15% MeOH; Voltage: 10kV; Capillary: 75 μm × 60.2 cm; distance to detector: 10.2 cm; Wavelength: 254nm.
(a) mixture; (b) GL (peak 1); (c) 18α-GA (peak 2); (d) 18β-GA (peak 3); (e) IQ (peak 4 and peak 4')

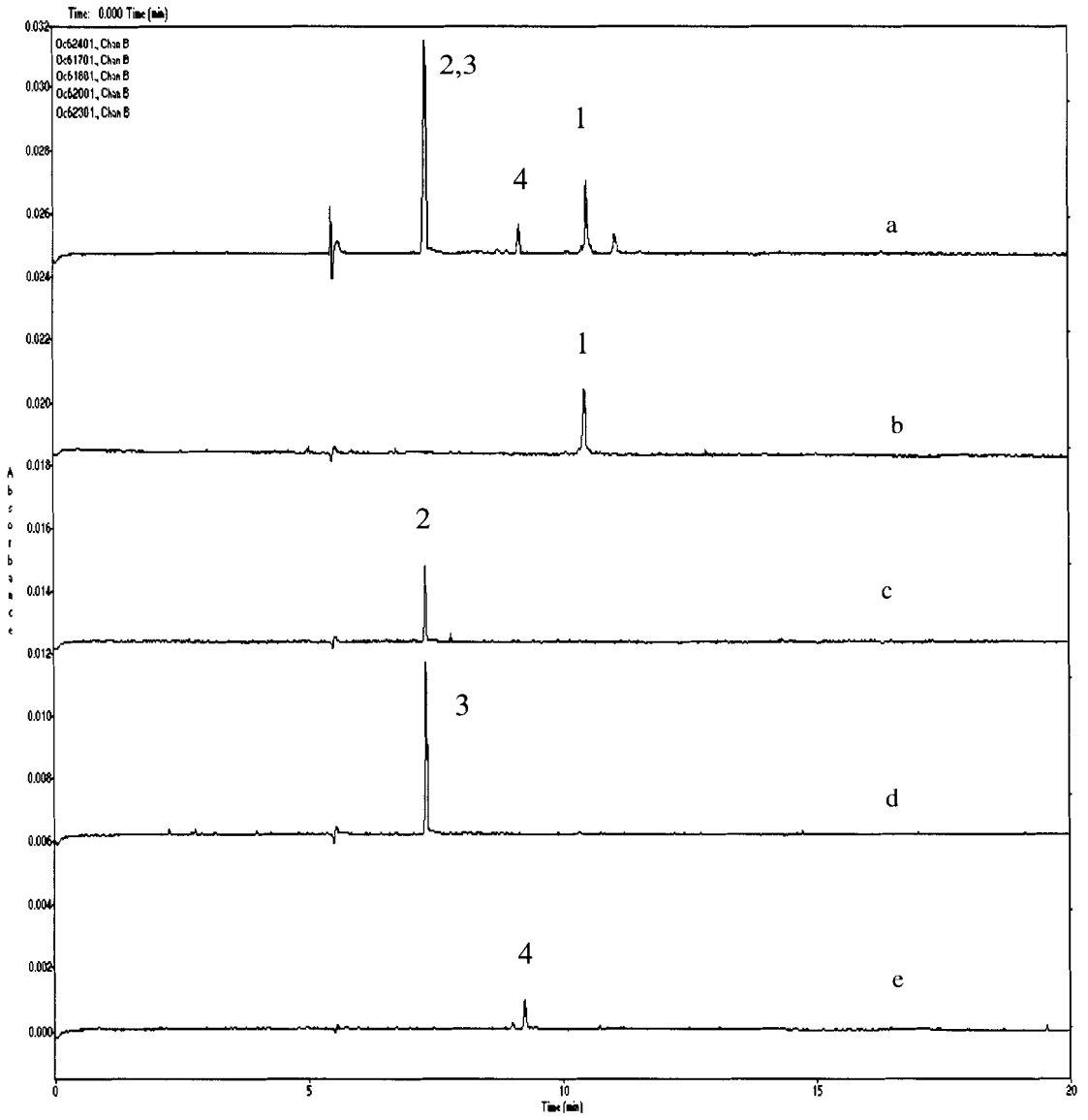

Fig.B-15 Electropherograms obtained for the separation of GL, 18α-GA, 18β-GA and IQ by MECC. Analytical conditions: 10mM sodium tetraborate + 25 mM SC (buffer H); Voltage: 17kV; Capillary: 75 μm × 60.2 cm; distance to detector: 50 cm; Wavelength: 254nm.
(a) mixture; (b) GL (peak 1); (c) 18α-GA (peak 2); (d) 18β-GA (peak 3); (e) IQ (peak 4 and peak 4')

Appendix 9 current profiles of selected runs

Fig.C-1 is the electric current profiles for Fig.A-1. Fig.A-1 shows that the effect of different concentrations of sodium tetraborate on the separation of four licorice components by CZE.

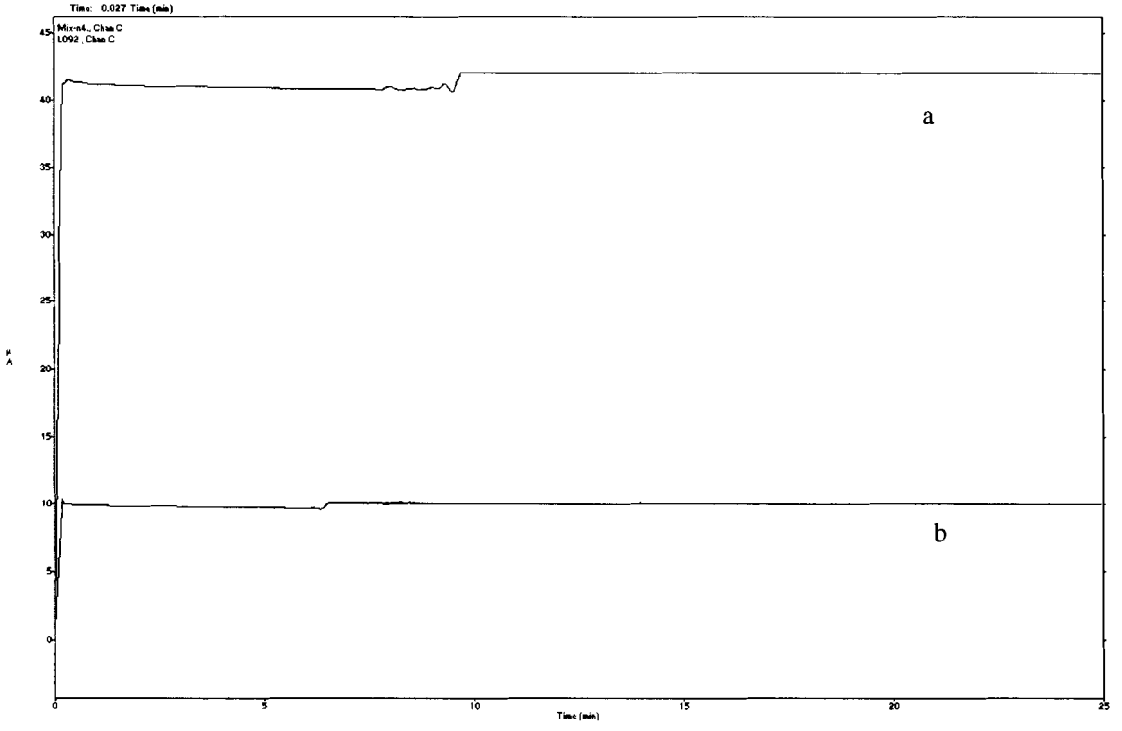

Fig.C-1 Electric current profiles for Fig.A-1. Analytical conditions: Voltage: 17 kV; Capillary: 50 μm × 60.2 cm; distance to detector: 50 cm; Wavelength: 254 nm. (a) 50 mM sodium tetraborate; (b) 10 mM sodium tetraborate. See Fig A-1 for electropherogram.

Fig.C-2 is the electric current profiles for Fig.A-2. Fig.A-2 shows that the effect of different concentrations of sodium tetraborate on the separation of four licorice components by MECC.

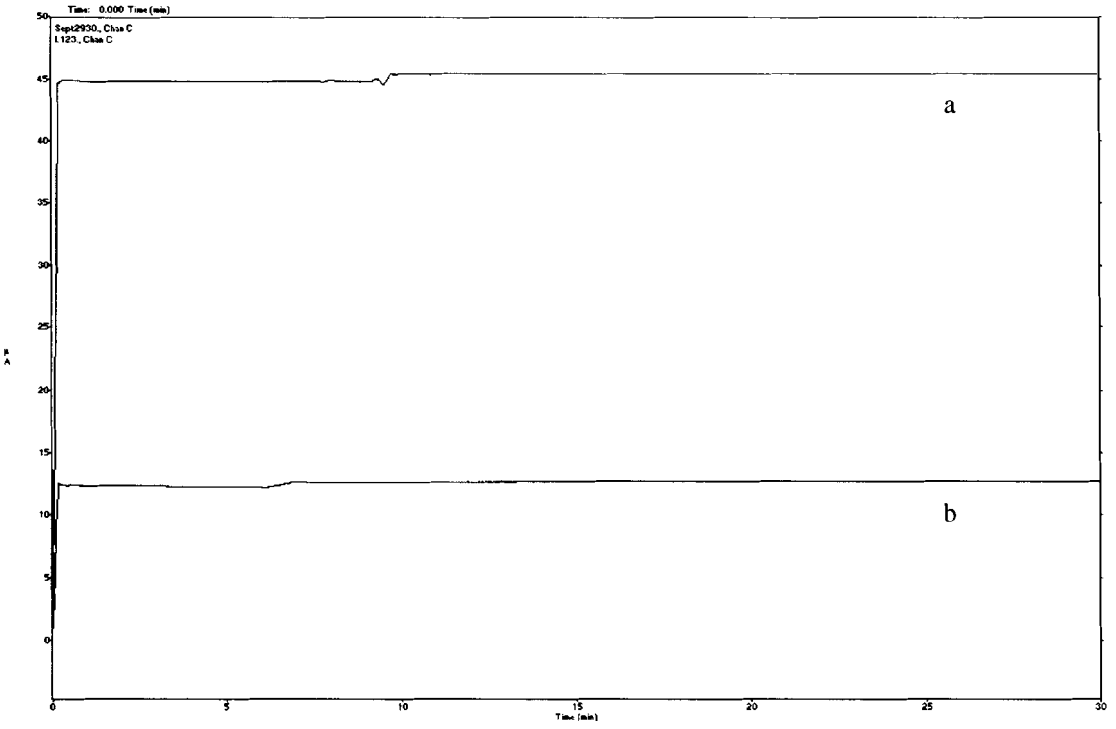

Fig.C-2 Electric current profiles for Fig.A-2. Analytical conditions: Voltage: 17 kV; Capillary: 50 μm × 60.2 cm; distance to detector: 50 cm; Wavelength: 254 nm. (a) 50 mM sodium tetraborate + 25 mM SDS (buffer B); (b) 10 mM sodium tetraborate + 25 mM SDS (buffer T). See Fig A-2 for electropherogram.

Fig.C-3 is the electric current profiles for Fig.A-4. We note that the current is lower when a capillary with a smaller i.d. (i.e.50 μm) is used.

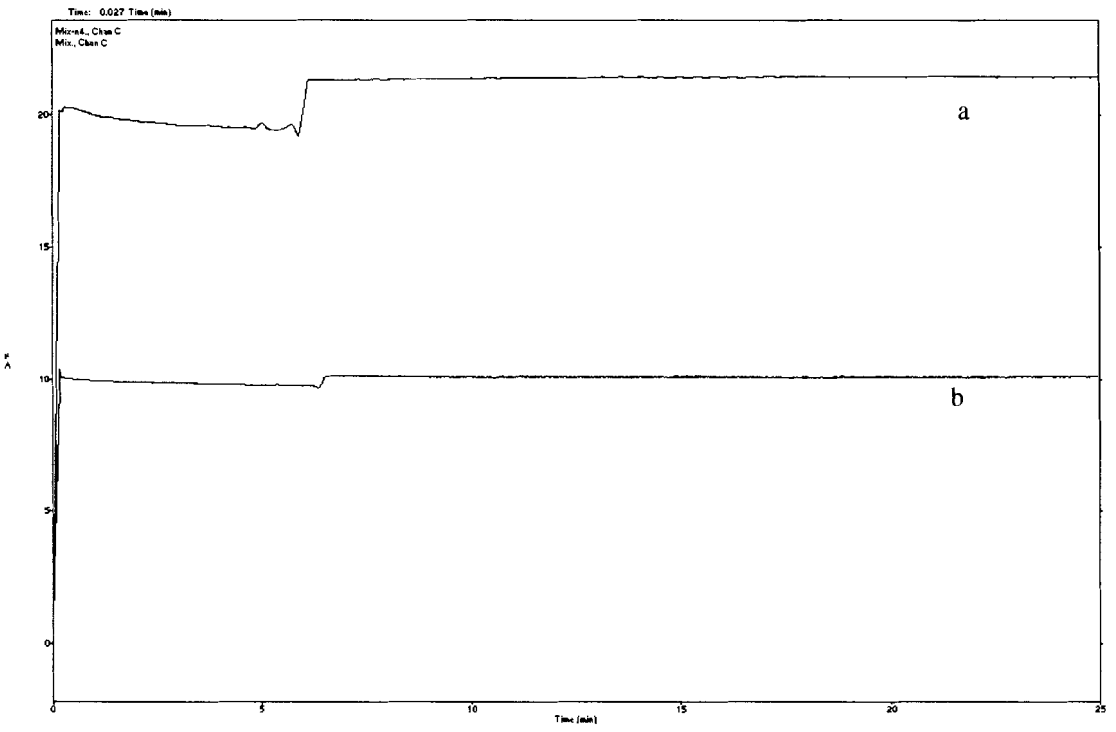

Fig.C-3 Electric current profiles for Fig.A-4. Analytical conditions: 10 mM sodium tetraborate; Voltage: 17 kV; Wavelength: 254 nm. (a) Capillary: 75 μm × 60.2 cm; distance to detector: 50 cm; (b) Capillary: 50 μm × 60.2 cm; distance to detector: 50 cm. See Fig A-4 for electropherogram.

Appendix 10 Analysis of raw and roasted licorice samples

(A) Analysis of raw licorice (S1) extract in methanol using 20 mM sodium tetraborate (buffer U)

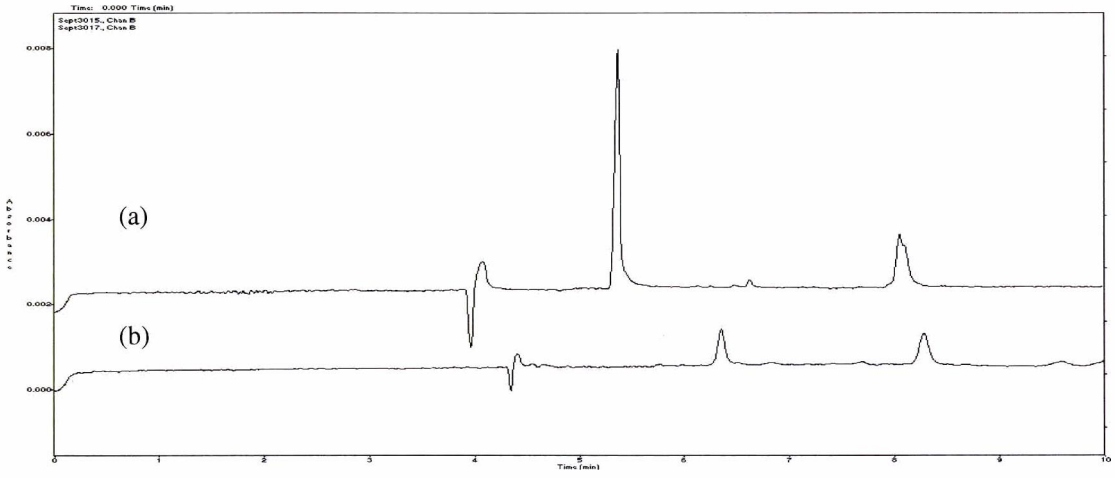

(c)

(d)

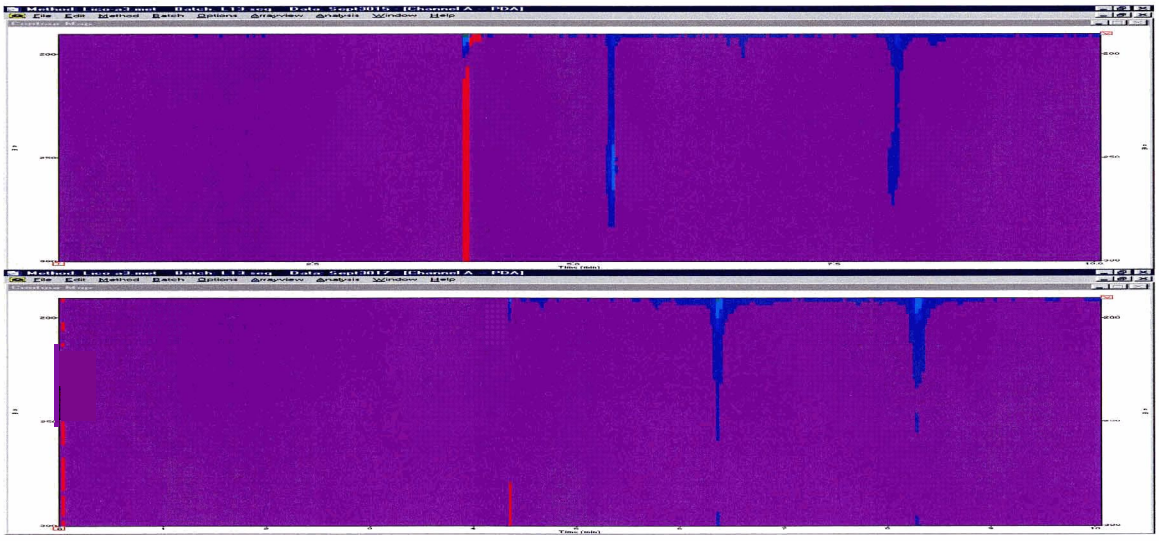

Fig.D-1 Electropherograms obtained for the separation of GL, 18α-GA, 18β-GA and IQ by CZE. Analytical conditions: 20mM sodium tetraborate (buffer U); Voltage: 17kV; Capillary: 50 μm × 60.2 cm; distance to detector: 50 cm; Wavelength: 254nm. (a) mixture; (b) raw licorice sample (S1), extracted by water; (c) UV contour for (a); (d) UV contour for (b) For component identification of (a), see Fig.B-13.

(B) Analysis of raw licorice (S1) extract in methanol using 10 mM sodium tetraborate + 25 mM SDS (buffer T)

As shown in Fig D-2, a-d show the electropherograms of standards. By comparing the electropherograms of the raw licorice extracts (e-g), there is a component which matches the migration time of peak 1 (GL). However, there are 2 unidentified components which migrate earlier than peak 1. There may also be a component which matches the migration time of peak 2 and 3. Fig.D-3 is the UV contour for Fig.D-2.

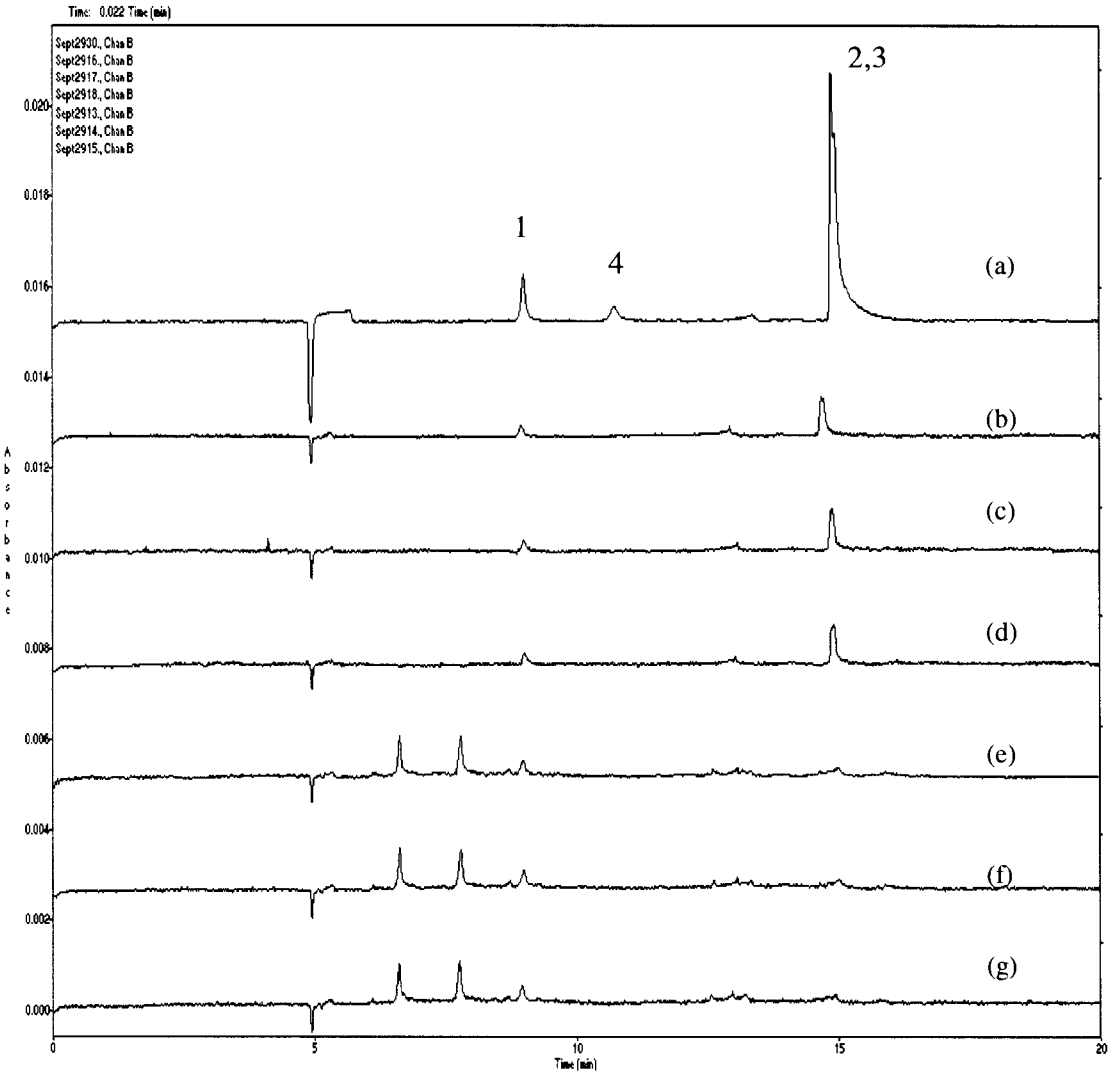

Fig.D-2 Electropherograms obtained for the separation of four compounds derived from licorice by MECC. Analytical conditions: 10 mM sodium tetraborate + 25 mM SDS (buffer T); Voltage: 17kV; Capillary: 75 μm × 60.2 cm; distance to detector: 50 cm; Temperature of capillary: 25 °C; Wavelength: 254nm.
(a)-(d) mixture; (e)-(g) raw licorice sample (S1), extracted by water . Component indentification for (a) are given in FigB-2.

(a)

(b)

(c)

(d)

(e)

(f)

(g)

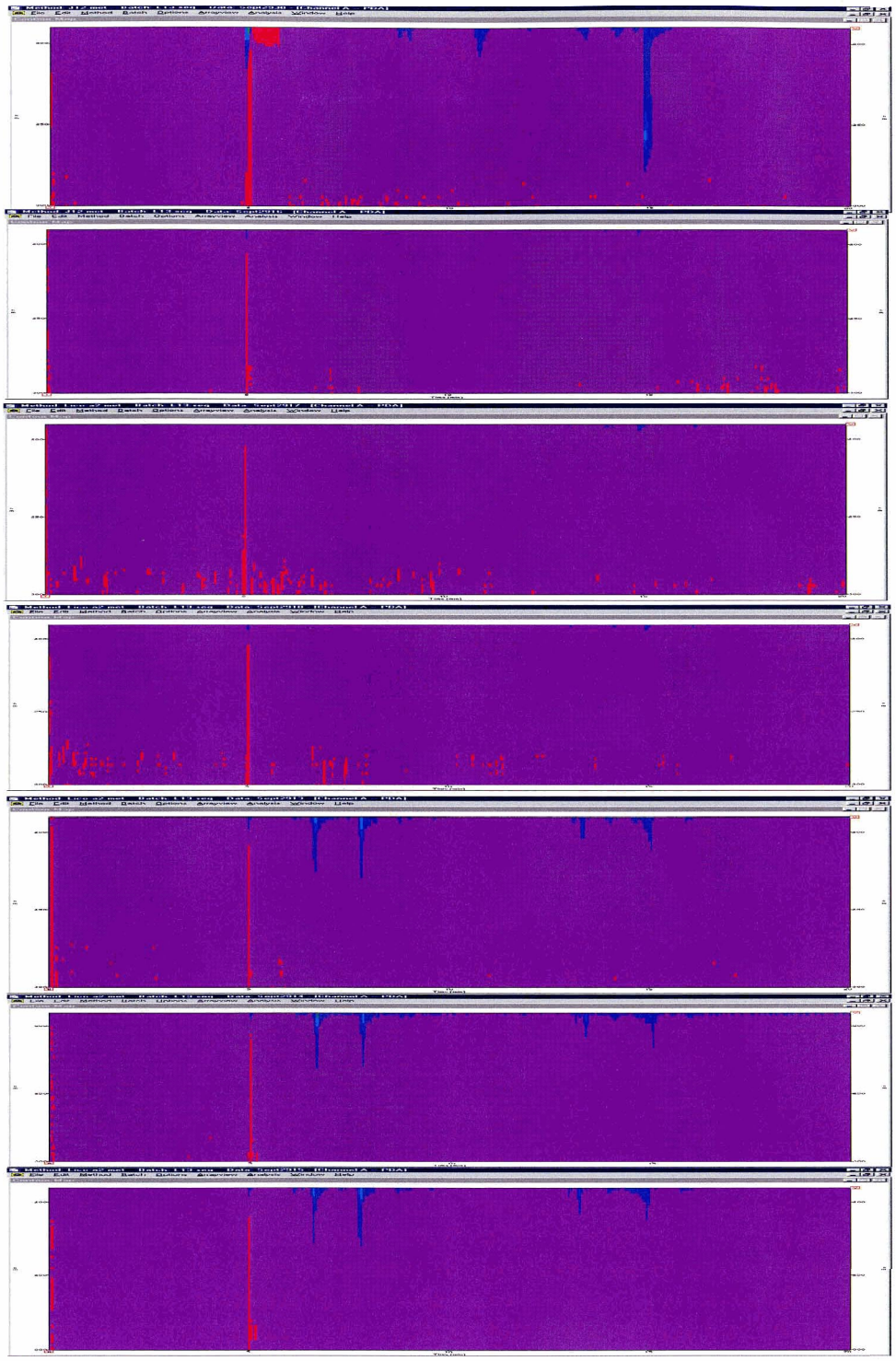

Fig.D-3 UV contour plots for Fig.D-2. For analytical conditions and legends, see Fig. D-2.
(a)-(d) mixture; (e)-(g) raw licorice sample (S1), extracted by water

(C) Analysis of raw licorice (S1) extract in methanol using 10 mM sodium tetraborate + 25 mM SC (buffer H)

As shown in Fig D-4, we observe matches in components in migration times corresponding to all components. UV contours are shown in Fig.D-5.

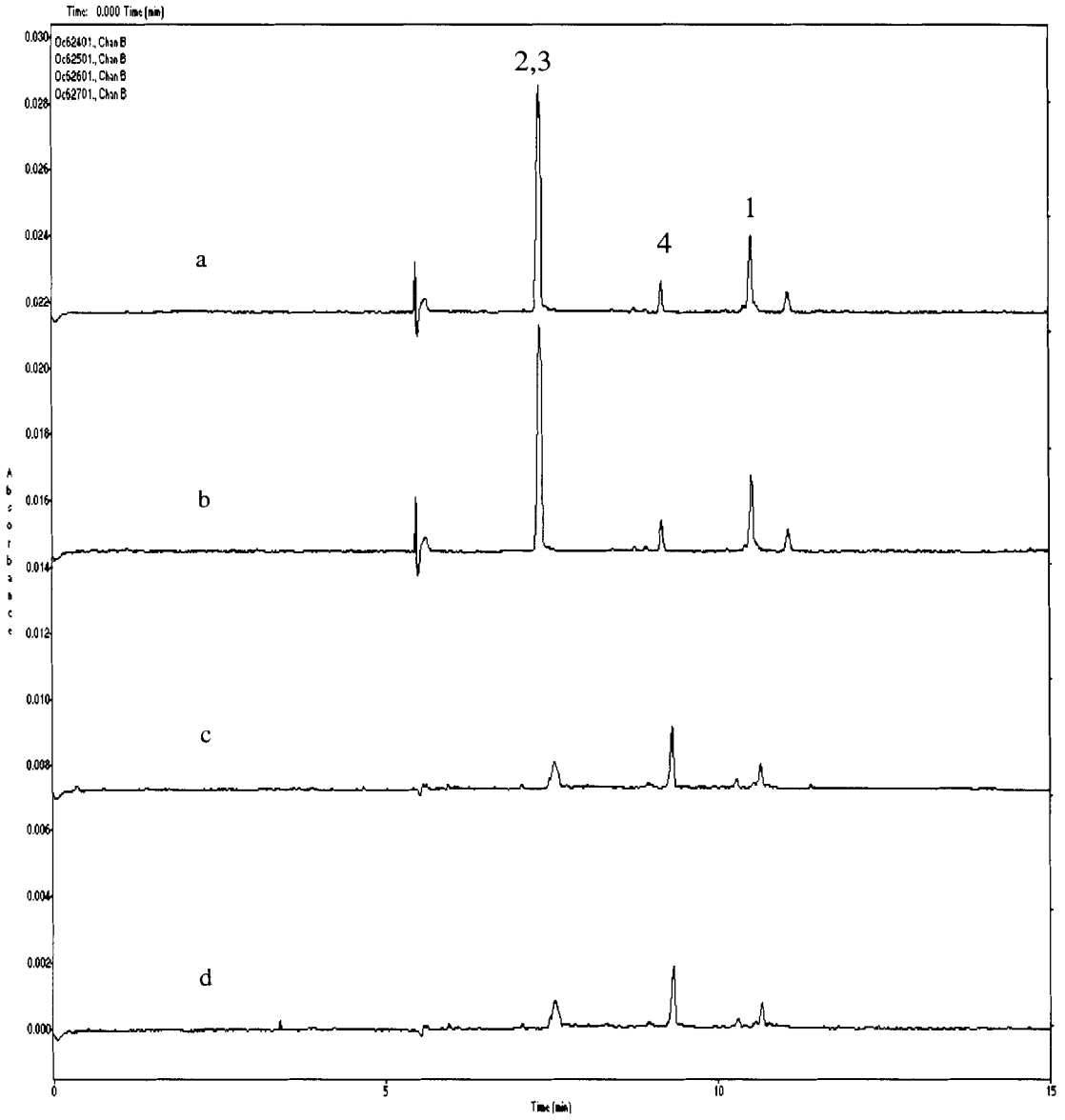

Fig.D-4 Electropherograms obtained for the separation of GL, 18α-GA, 18β-GA and IQ by MECC. Analytical conditions: 10mM sodium tetraborate + 25 mM SC (buffer H); Voltage: 17kV; Capillary: 75 μm × 60.2 cm; distance to detector: 50 cm; Wavelength: 254nm.
(a) and (b) mixture; (c) and (d) raw licorice sample (S1), extracted by water
Component identification for Fig.D-4a is given in Fig.B-15.

(a)

(b)

(c)

(d)

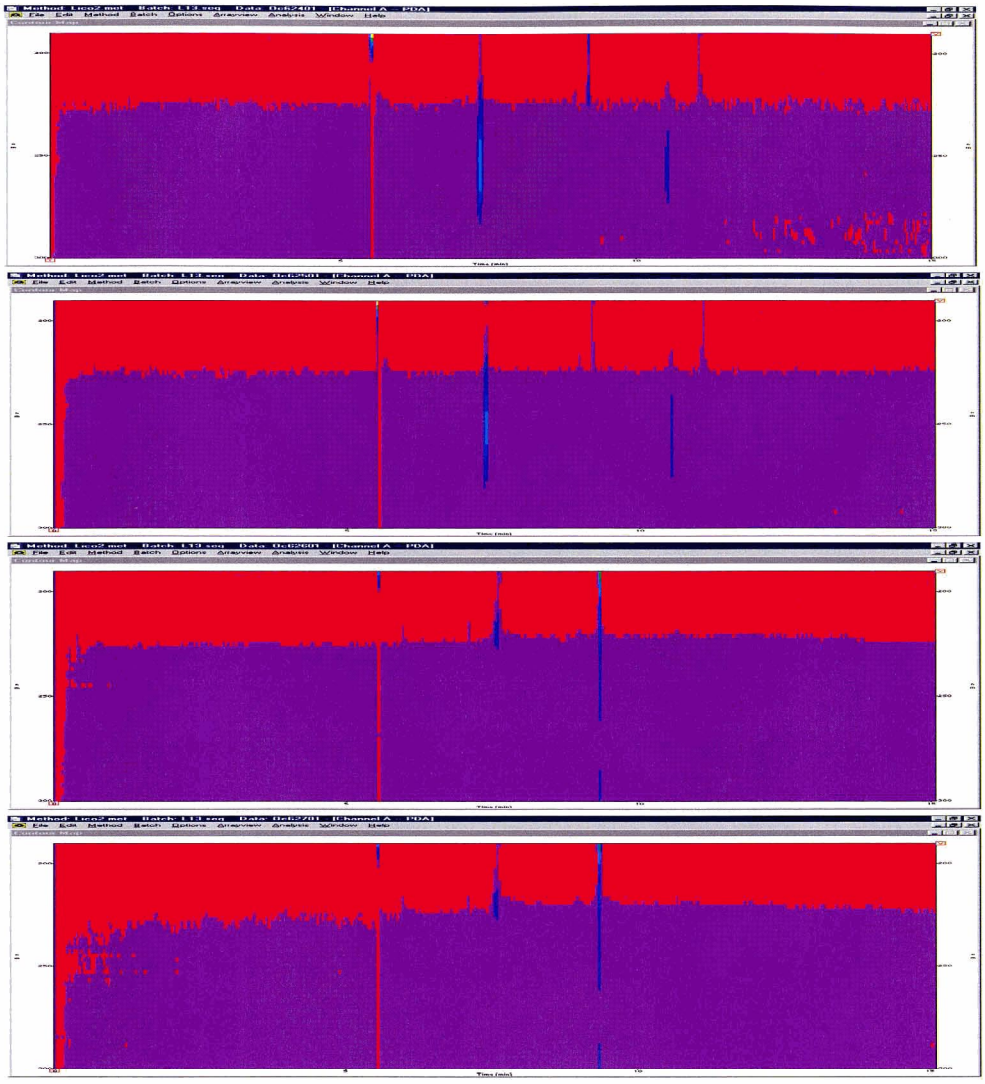

Fig.D-5 UV contour plots for Fig.D-4. For analytical conditions and legends, see Fig.D-4.
(a)-(b) mixture; (c)-(d) raw licorice sample (S1), extracted by water

(D) Analysis of raw and roasted licorice using 50 mM sodium tetraborate + 25 mM SDS + 15% MeOH (buffer E)

As shown in Fig D-6, although the match between all samples is satisfactory, there is a shift in migration time in the standards. We find that the 2 major components in the sample do not match any of the 4 standards. However, there are a lot of minor components which may match peaks 2, 3, and 4. UV contours are shown in Fig D-7.

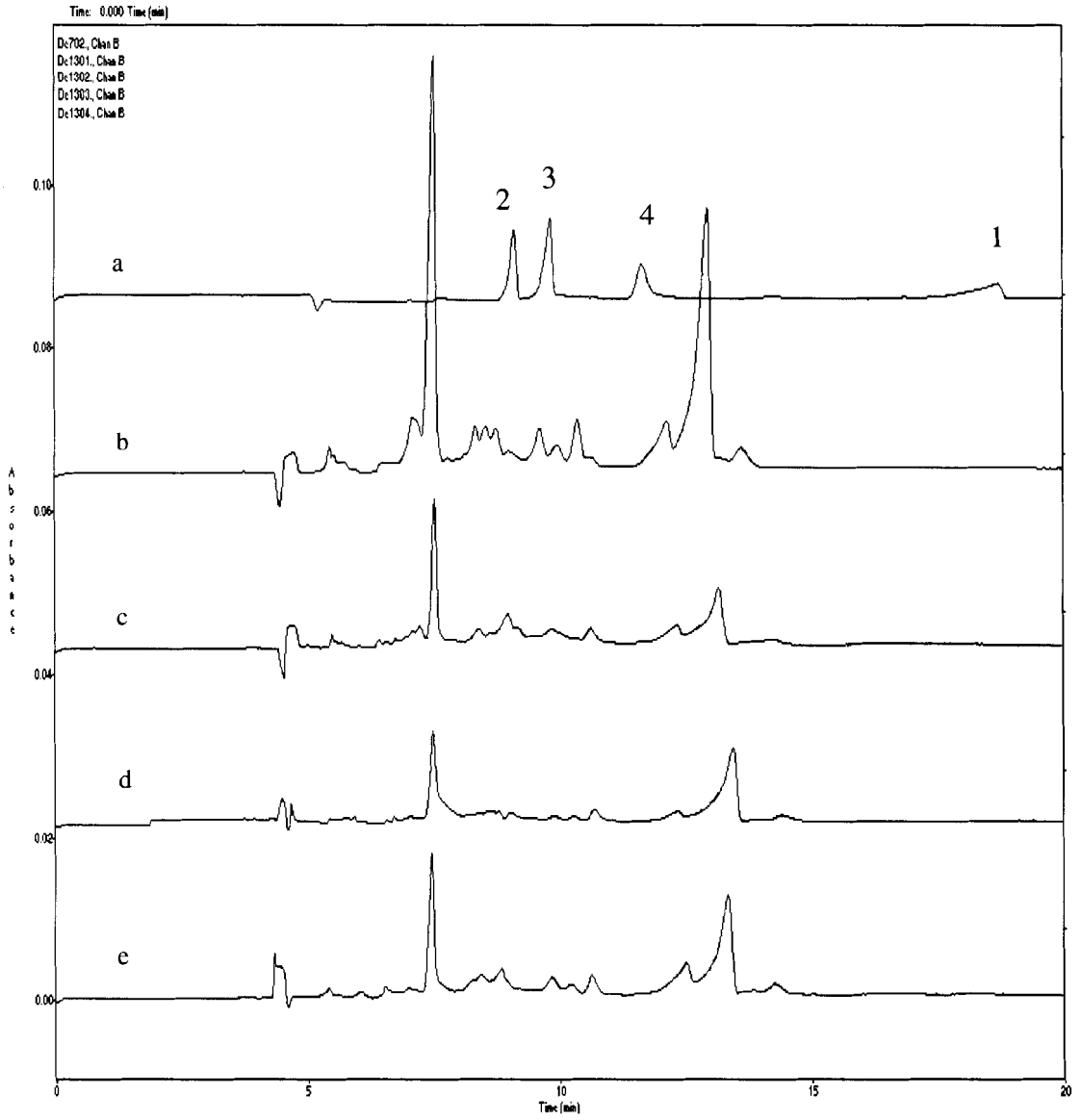

Fig.D-6 Electropherograms obtained for the separation of GL, 18α-GA, 18β-GA and IQ by CD-MECC. Analytical conditions: 50mM sodium tetraborate + 25 mM SDS + 20 β-CD + 15% MeOH; Voltage: 17kV; Capillary: 75 μm × 60.2 cm; distance to detector: 50 cm; Wavelength: 254nm.
(a) mixture; (b) raw licorice sample, extracted by methanol; (c) roast licorice sample, extracted by methanol; (d) raw licorice sample, extracted by water; (e) roast licorice sample, extracted by water

(a)

(b)

(c)

(d)

(e)

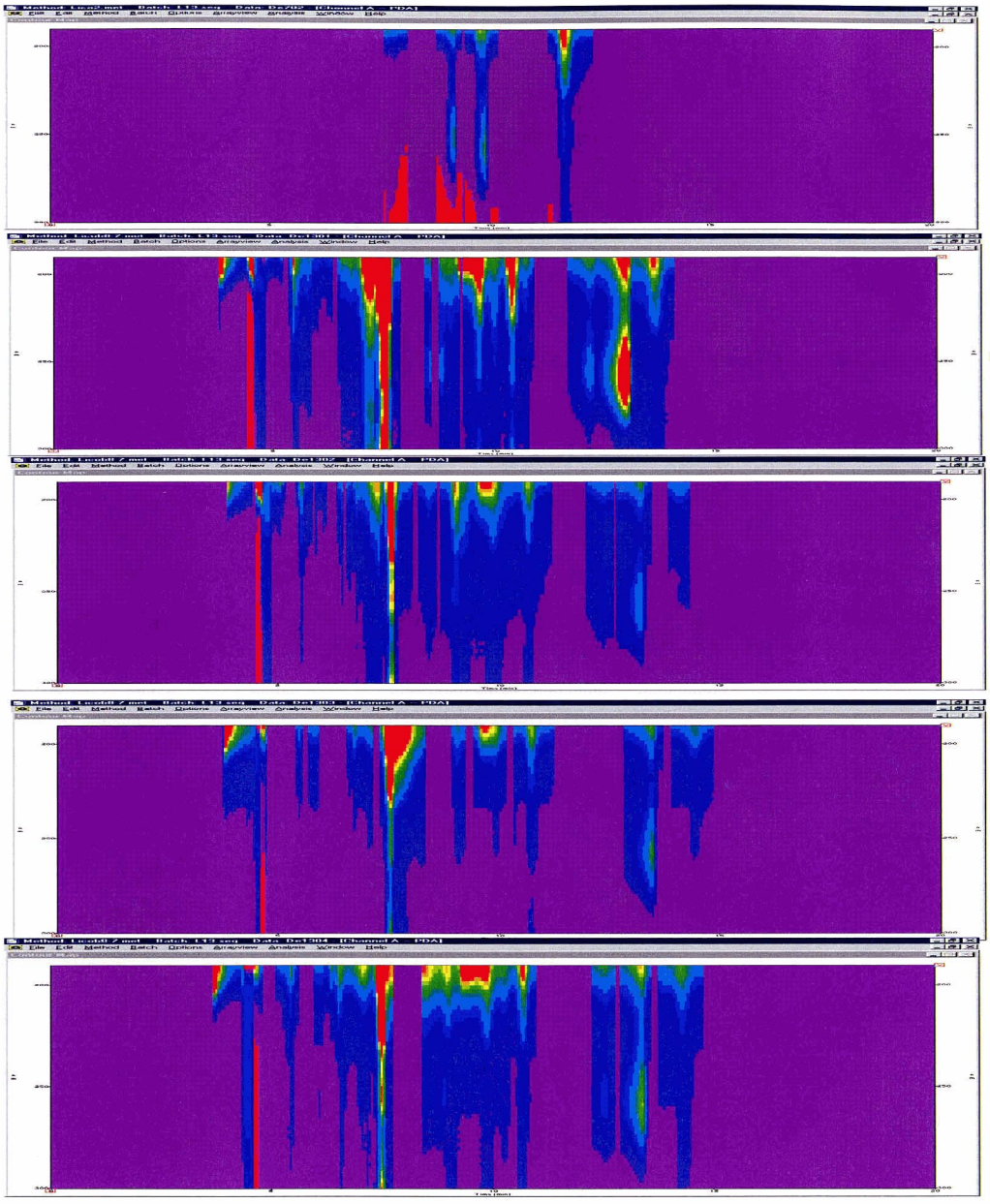

Fig.D-7 UV contour plots for Fig.D-6. For analytical conditions and legends, see Fig.D-6.
(a) mixture; (b) raw licorice sample (S4a), extracted by methanol; (c) roasted licorice sample (S4b), extracted by methanol; (d) raw licorice sample (S4a), extracted by water; (e) roasted licorice sample (S4b), extracted by water.

(E) Analysis of raw licorice using 50 mM sodium tetraborate + 50 SDS + 20 mM SC (buffer W)

As shown in Fig.D-8, we find good repeatability in the 3 electropherograms for the standards. Fig.D-9 is the UV contour for Fig.D-8.

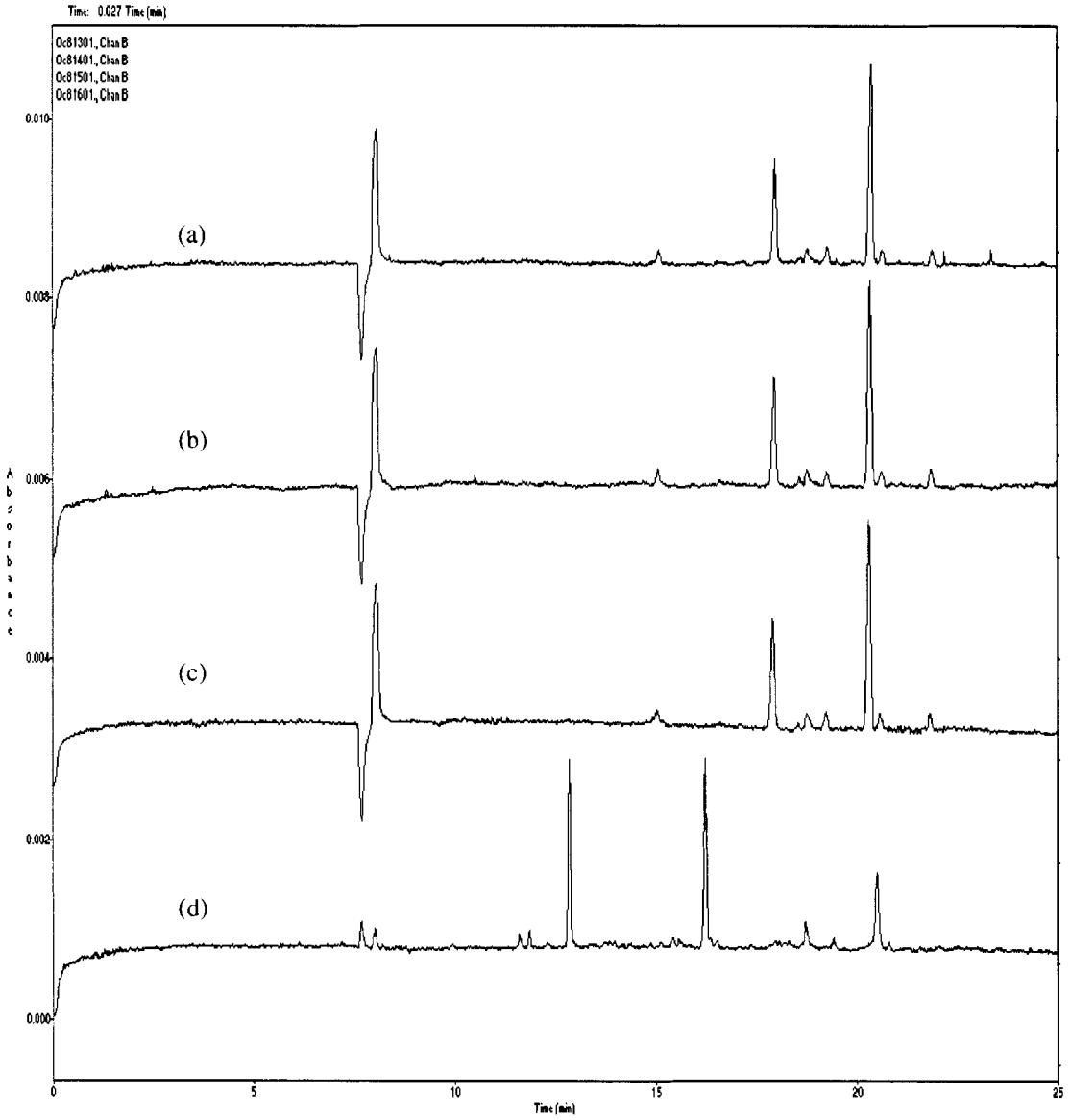

Fig.D-8 Electropherograms obtained for the separation of GL, 18α-GA, 18β-GA and IQ by MECC. Analytical conditions: 50mM sodium tetraborate + 50 mM SDS + 20 mM SC (buffer W); Voltage: 10 kV; Capillary: 50 μm × 60.2 cm; distance to detector: 10.2 cm; Wavelength: 254nm.
(a) –(c) mixture; (d) sample

(a)

(b)

(c)

(d)

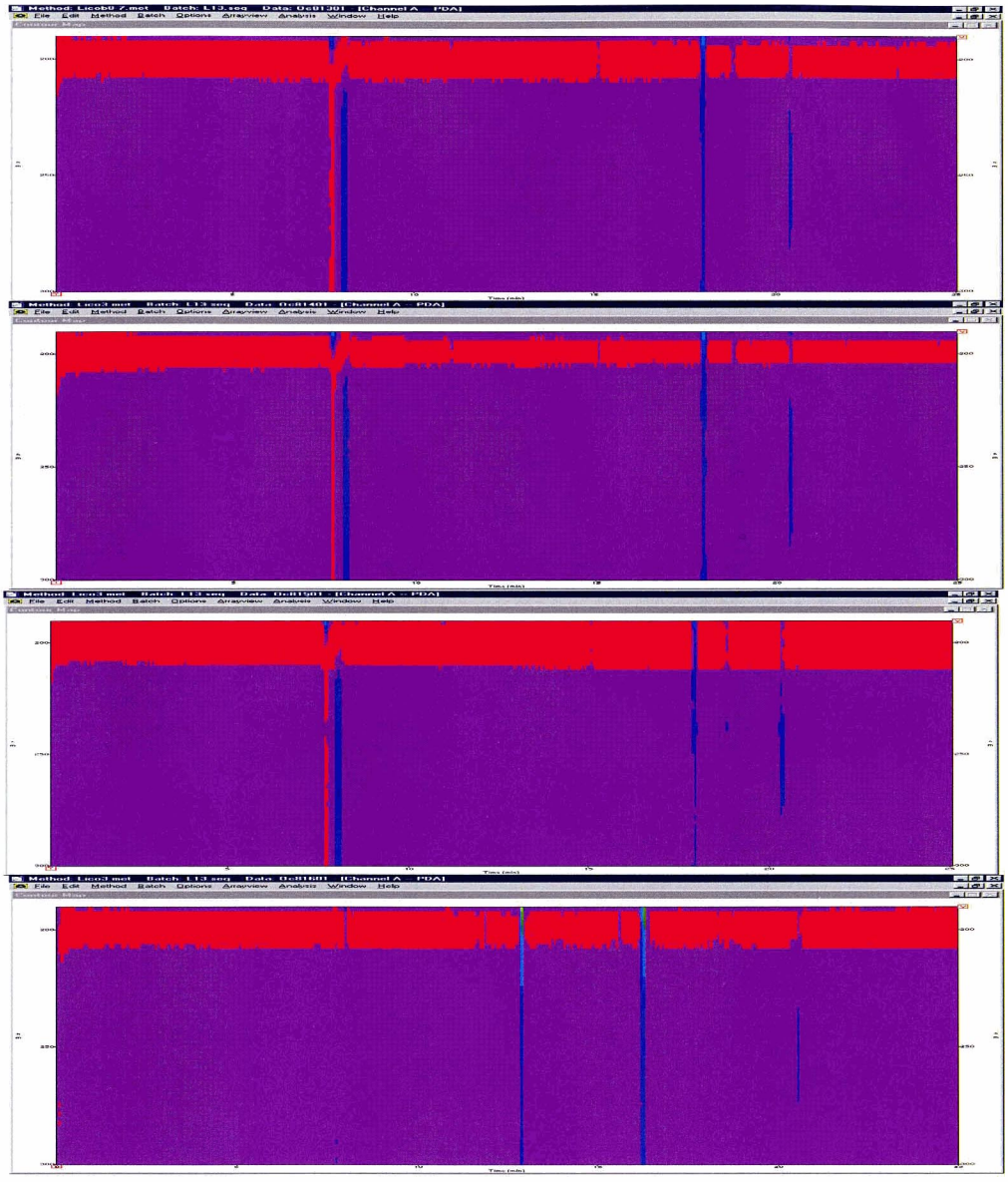

Fig.D-9 UV contour plots for Fig.D-8. For analytical conditions and legends, see Fig.D-8. (a)-(c) mixture; (d) sample

(F) Analysis of raw and roasted licorice using 50 mM sodium tetraborate + 25 mM SDS + 20 mM CD + 10 mM SC + 25 % MeOH (buffer V).

As shown in Fig.D-10 (c-d), we find that the component corresponding to peak 4 (IQ) is reduced in amount in roast licorice (b) or (d) as compared to the raw one (c). UV contour is shown in Fig.D-11.

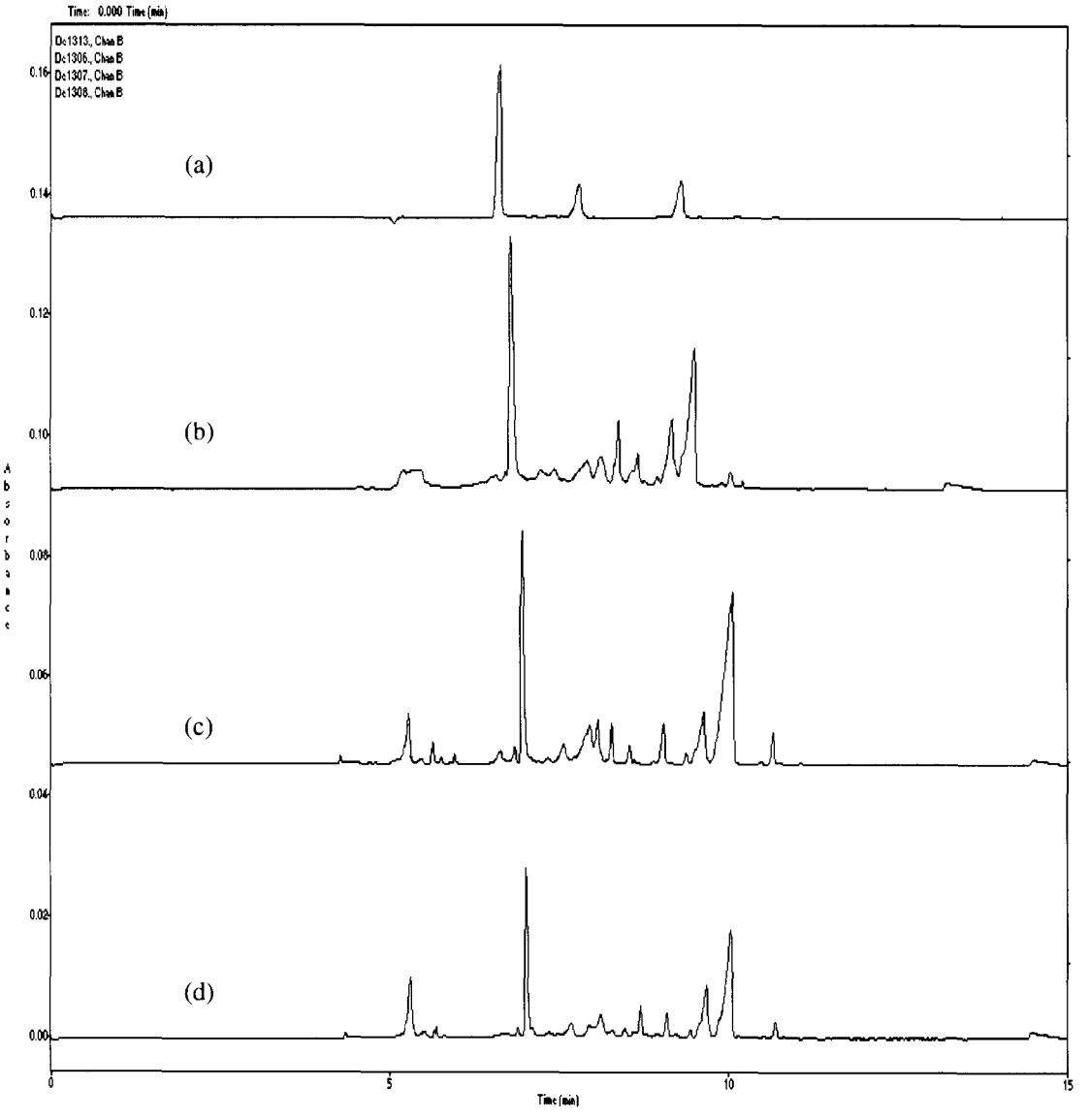

Fig.D-10 Electropherograms obtained for the separation of four compounds derived from licorice by CD-MECC. Analytical conditions: 50 mM sodium tetraborate + 25 mM SDS + 20 mM CD + 10 mM SC + 25% MeOH (buffer V); Voltage: 10kV; Capillary: 75 μm × 60.2 cm; distance to detector: 10.2 cm; Temperature of capillary: 25 °C; Wavelength: 254nm.
(a) mixture; (b) roast licorice sample, extracted by methanol; (c) raw licorice sample (S4a), extracted by water; (d) roasted licorice sample(S4b), extracted by water.
For component identification of (a), see FigB-16.

(a)

(b)

(c)

(d)

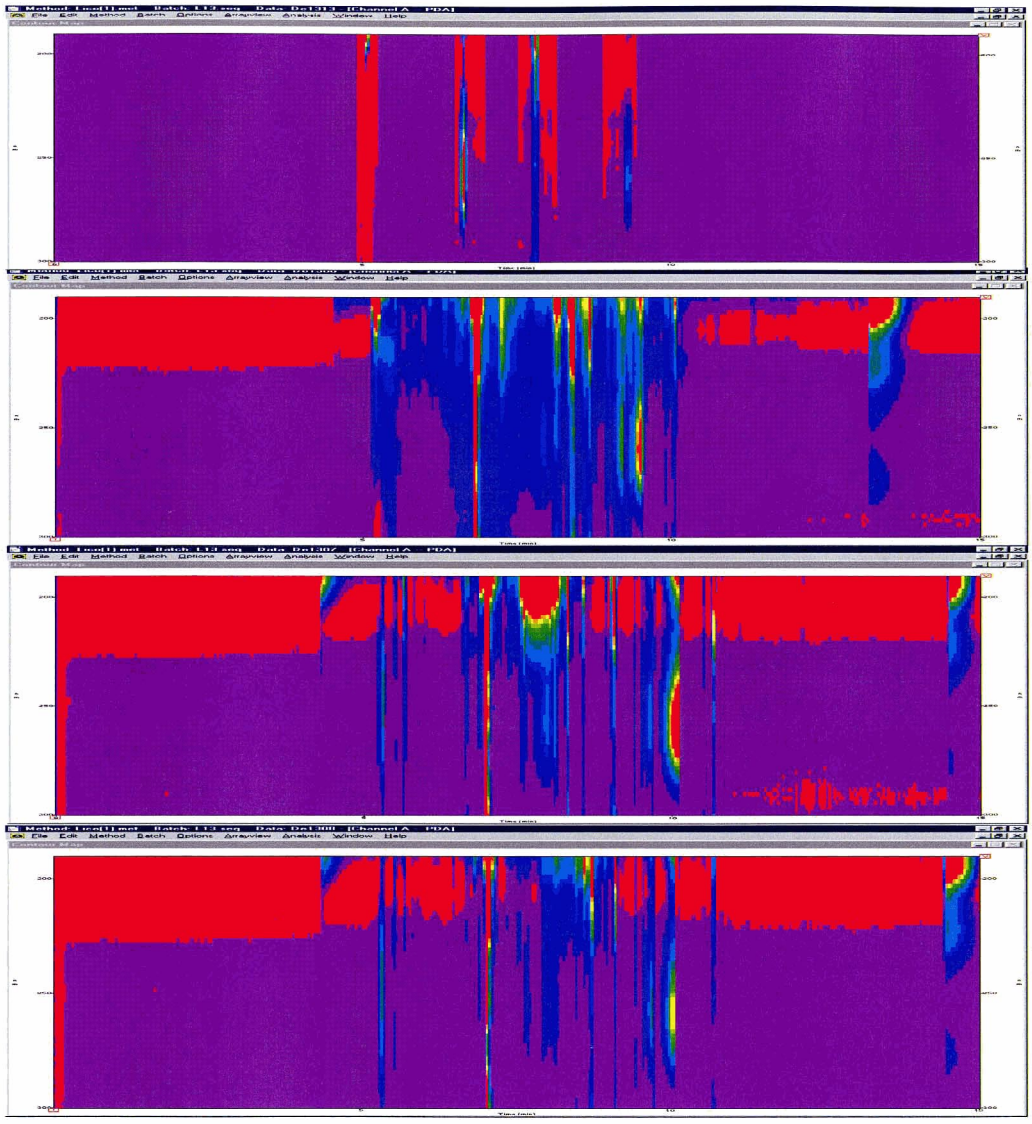

Fig.D-11 UV contour plots for Fig.D-10. For analytical conditions and legends, see Fig.D-10. (a) mixture; (b) roasted licorice sample, extracted by methanol; (c) raw licorice sample, extracted by water; (d) roasted licorice sample, extracted by water.

References

1. Fan, Y.G.; Shi, Z.Q.; He, B.L. Extraction separation and application for glycyrrhizic and glycyrrhetic acid. *Natural Product Research and Development.* 1996, *8*, 93-99

2. Shibata, S. Antitumor-promoting and anti-inflammatory activities of licorice principles and their modified compounds. *Food Phytochemicals II: Teas, Spices, and Herbs.* 1994: 308-321

3. Yang, L.; Liu, Y.L.; Lin, S.Q. The determination of flavonoid in 6 kinds of licorice root by HPLC. *Acta Pharmaceutica Sinica.* 1990, *25*, 840-848

4. Tsai, T.H.; Chen, C.F. High-performance liquid chromatographic determination of 18α-glycyrrhetinic acid and 18β-glycyrrhetinic acid in rat plasma: application to pharmacokinetic study. *Journal of Chromatography. Biomedical Applications.* 1991, *567*, 405-414

5. Shibata, S. A drug over the millennia: pharmacognosy, chemistry, and pharmacology of licorice. *Yakugaku Zasshi.* 2000, *120*, 849-862

6. Wang, Z.Y.; Agarwal, R.; Zhou, Z.C. Inhibition of mutagenicity in *Salmonella typhimurium* and skin tumor initiating and tumor promoting activities in SENCAR mice by glycyrrhetinic acid: comparison of 18α- and 18β-stereoisomers. *Carcinogenesis.* 1991, *12*, 187-192

7. Beasley, T.H.; Ziegler, H.W.; Bell, A.D. Separation of major components in licorice using HPLC. *Journal of Chromatography.* 1979, *175*, 350-355

8. Weinberg, D.S.; Manier, M.L.; Richardson, M.D. Identification and quantification of isoflavonoid and triterpenoid compliance markers in a licorice-root extract powder. *J. Agric. Food Chem.* 1993, *41*, 42-47

9. Andrisano, V.; Bonazzi, D; Cavrini, V. HPLC analysis of liquorice triterpenoids applications to the quality control of pharmaceuticals. *Journal of Pharmaceutical & Biomedical Analysis.* 1995, *13,* 597-605

10. Amagaya, S.; Sugishita, E.; Ogihara, Y. Separation and quantitative analysis of 18α-glycyrrhetinic acid and 18β-glycyrrhetinic acid in *Glycyrrhizae Radix* by gas-liquid chromatography. *Journal of Chromatography.* 1985, *320*, 430-434

11. Yvette, H.A.; Cheung, A.; Lim, P. Chiral separation of glycyrrhetinic acid by HPLC. *Journal of Pharmaceutical & Biomedical Analysis.* 1991, *9*, 805-809

12. Lu, Z.; Zhang, R.Y.; Tong, M. Determination of nine flavonoids and coumarins in licorice root by HPLC. *Journal of Chromatography* 1990, *513*, 247-254

13. Hiraga, Y.; Endo, H.; Takahashi, K. HPLC analysis of licorice extracts. *Journal of Chromatography.* 1984, *292*, 451-453

14. Zhang, Z.Y. Determination of glycyrrhizin and its metabolite glycyrrhetinic acid in rabbit plasma by HPLC after oral administration of licorizin. *Journal of Chromatography.* 1989, *495*, 343-348

15. Wang, J.Y.; Guo, J.S.; Li, H. Inhibitory effect of glycyrrhizin on NF-κB binding activity in CCl_4 -plus ethanol-induced liver cirrhosis in rats. *Liver.* 1998,*18*,180-185.

16. Wang, Z.Y. Anticarcinogenesis of licorice and its major triterpenoid constituents. *Food Phytochemicals II: Teas, Spices and Herbs.* 329-334.

17. Guillaume, C.F.; Molen, J.C.; Kerstens, M.N. Determination of urinary 18β-glycyrrhetinic acid by gas chromatography and its clinical application in man. *Journal of Chromatography B.* 1999, *731,* 323-334

18. Lu, Z.; Zhang, R.Y.; Lou, Z.Q. Separation and determination of three saponins in licorice by HPLC. *Acta Pharmaceutica Sinica.* 1990, *26*, 53-58

19. Aida, K.; Tawata, M.; Shindo, H. Isoliquiritigenin: a new aldose reductase inhibitor from *Glycyrrhizae Radix. Planta Med.* 1990, *56*, 254-258

20. Wegener, J.W.; Nawrath, H. Cardiac effects of isoliquiritigenin. *European Journal of Pharmacology.* 1997, *326*, 37-44

21. Yamamoto, S.; Aizu, E.; Jiang, H. The potent anti-tumor-promoting agent isoliquiritigenin. *Carcinogenesis.* 1991, *12*, 317-323

22. Wang, J.Z.; Chen, D.Y.; Zhao, X.H. Analytical study on drug-processing of the root of *Glycyrrhiza uralensis Fisch.* by HPLC. *Journal of Chinese Materia Medica.* 1995, *20*, 535-536

23. Kuwajima, H.; Taneda, Y.; Chen, W.Z. Variation of chemical constituents in processed licorice roots: quantitative determination of saponin and flavonoid constituents in bark removed and roasted licorice roots. *Yakugaku Zasshi.* 1999, *119*, 945-955

24. Tsubone, K.; Ohnishi, S.; Yoneya, T. Separation of glycyrrhizinic acid isomers by HPLC. *Journal of Chromatography.*1982, *248*, 469-471

25. Hurst, W.; McKim, J.; Martin, R. HPLC determination of glycyrrhizin in licorice products. *J. Agric. Food Chem.* 1983, *31*, 389-393

26. Rossum, T.J.; Vulto, A.G.; Hop, W.J. Pharmacokinetics of intravenous glycyrrhizin after single and multiple doses in patients with chronic hepatitis C infection. *Clinical Therapeutics.* 1999, *21*, 2080-2090

27. Hayashi, H.; Hiraoka, N.; Ikeshiro, Y. Seasonal variation of glycyrrhizin and isoliquiritigenin glycosides in the root of *Glycyrrhiza glabra L. Biol. Pharm. Bull.* 1998, *21*, 987-989

28. Liu, S.D.; Jiang, X.H.; Zheng, D. HPLC determination of glycyrrhizin in licorice root and preparations. *Journal of Huaxi Medicine.* 1994, *24*, 111-114

29. Kitagawa, I.; Chen, W.Z.; Taniyama, T. Quantitative determination of constituents in various licorice roots by means of HPLC. *Yakugaku Zasshi.* 1998, *118*,519-528

30. Akada, Y.; Sakiya, Y.; Kawano, S. Rapid estimation of glycyrrhizin in pharmaceutical preparations by HPLC. *Chem. Pharm. Bull.* 1978, *26*, 1240-1246

31. Sakiya, Y.; Akada, Y.; Kawano, S. Rapid estimation of glycyrrhizin and glycyrrhetinic acid in plasma by HPLC. *Chem. Pharm. Bull.* 1979, *27*, 1125-1129

32. Takino, Y.; Koshioka, M.; Shiokawa, M. Quantitative determination of glycyrrhizic acid in liquorice roots and extracts by TLC-densitometry. *Journal of Medicinal Plant Research.* 1979, *36*, 74-78

33. Kusano, A.; Nikaido, T.; Kuge, T. Inhibition of adenosine 3',5'-cyclic monophosphate phosphodiesterase by flavonoids from licorice roots and 4-arylcoumarins. *Chem.Pharm.Bull.* 1991, *39*, 930-933

34. Nozaki, M; Tsurumi, K.; Fujimura, H. Determination glycyrrhetinic acid by gas chromatography. *Yakugaku Zasshi.* 1970, *90*, 693-695

35. Kerstens, M.N.; Guillaume, C.F.; Wolthers, B.G. Gas chromatographic-mass spectrometric analysis of urinary glycyrrhetinic acid: an aid in diagnosing liquorice abuse. *Journal of Internal Medicine.* 1999, *246*, 539-547

36. Vampa, G.; Benvenuti, S.; Rossi, T. Determination of glycyrrhizin and 18α-, 18β-glycyrrhetinic acid in rat plasma by HPTLC. *IL Farmaco.* 1992, *47*, 825-830

37. Hu, S.; Li, P. Micellar electrokinetic capillary chromatographic separation and fluorescent detection of amino acids derivatized with 4-fluoro-7-nitro-2,1,3-benzoxadiazole. *Journal of Chromatography A.* 2000, *876*, 183-191

38. Rodriguez, R; Pico, Y; Font, G. Determination of urea-derived pesticides in fruits and vegetables by solid-phase preconcentration and capillary electrophoresis. *Electrophoresis.* 2001, *22*, 2010-2016

39. Li, G.B.; Zhang, H.Y.; Fan, Y.Q. Migration behavior and separation of active components in *Glycyrrhiza uralensis Fisch* and its commercial extract by micellar electrokinetic capillary chromatography. *Journal of Chromatography A.* 1999, *863*, 105-114

40. Song, J.Z.; Xu, H.X.; Tian, S.J. Determination of quinolizidine alkaloids in traditional Chinese herbal drugs by nonaqueous capillary electrophoresis. *Journal of Chromatography A.* 1999, *857*, 303-311

41. Iwagami, S.; Sawabe, Y.; Nakagawa, T. Micellar electrokinetic chromatography for the analysis of crude drugs (I) determination of glycyrrhizin in oriental pharmaceutical preparations. *Shoyakugaku Zasshi.* 1991, *45*, 232-239

42. Hansen, H.K.; Hansen, S.H.; Kraunsoe, M. Comparison of HPLC and CE methods for quantitative determination of glycyrrhizinic acid in pharmaceutical preparations. *European Journal of Pharmaceutical Sciences.* 1999, *9*, 41-46

43. Iwagami, S.; Sawabe, Y.; Nakagawa, T. Micellar electrokinetic chromatography for the analysis of crude drugs (II) simultaneous determination of glycyrrhizin and paeoniflorin in oriental pharmaceutical preparations. *Shoyakugaku Zasshi.* 1992, *46*, 49-54

44. Wang, P.; Li, S.Y.; Lee, H.K. Determination of glycyrrhizic acid and 18β-glycyrrhetinic acid in biological fluids by micellar electrokinetic chromatography. *Journal of Chromatography A.* 1998, *811*, 219-224

45. Zang, GQ; Ji, SG; Chai, YF. Determination of glycyrrhizin in *Radix glycyrrhzae* and its preparations by capillary zone electrophoresis. *Biomedical chromatography.* 1999, *13*, 407-409

46. Yin C; Wu Y. Determination of chlorogenic acid, glycyrrhizin and glycyrrhetinic acid in yinqiaojiedupian by high performance capillary electrophresis. *Se Pu.* 1999, *17*, 193-195

47. Khaledi, MG. *High-performance capillary electrophoresis: theory, techniques, and applications.* 1998:3-16

48. Li, S.F.Y. *Capillary Electrophoresis*: *Principles, practice and applications* 1992, *52*, 4

49. Foret, F.; Krivankova, L.; Bocek, P. *Capillary Zone Electrophoresis.* 1993. 8

50. Kuhn, R.; Kuhn, S.H. *Capillary Electrophoresis: principles and practice.* 1993, 17

51. Li, S.F.Y. *Capillary Electrophoresis*: *Principles, practice and applications* 1992, *52*, 15

52. Weinberger, R. *Practical Capillary Electrophoresis.* 2000, 32

53. Skanchy, D.J.; Xie, G.H.; Tait, R.J. Application of sulfobutylether-β-cyclodextrin with specific degrees of substitution for the enantioseparation of pharmaceutical mixtures by capillary electrophoresis. *Electrophoresis.* 1999, *20*, 2638-2649

54. Skoog, D; Leary, J. *Principles of instrumental analysis* 1992, 123

55. Camilleri, P. *Capillary Electrophoresis: theory and practice.* 1997, 139

56. Barnes, S.; Geckle, J.M. High resolution nuclear magnetic resonance spectroscopy of bile salts: individual proton assignments for sodium cholate in aqueous solution at 400 MHz. *J Lipid Res.* 1982, *23*, 161

57. Camilleri, P. *Capillary Electrophoresis: theory and practice.* 1997, 142

58. Terence, S.K.; Huie, C.W. Investigation of the effects of cyclodextrins and organic solvents on the separation of cationic surfactants in capillary electrophoresis. *Journal of Chromatography A.* 2000, *872*, 269-278

59. Boyce, M.C. Simultaneous determination of antioxidants, preservatives and sweeteners permitted as additives in food by mixed micellar electrokinetic chromatography. *Journal of Chromatography A.* 1999, *847*, 369-375

60. Miksik, I.; Eckhardt, A.; Forgacs, E. The effect of sodium dodecyl sulfate and pluronic F127 on the electrophoretic separation of protein and polypeptide test mixtures at acid pH. *Electrophoresis.* 2002,*23*,1882-1886

61. Camilleri, P. *Capillary Electrophoresis: theory and practice.* 1997, 34-35

62. Zhang, Y.P.; Li, X.J.; Yuan, Z.B. Analysis of carbaryl and other pesticides by capillary electrophoresis. *Se Pu.* 2002, *20,* 341-344

63. Roy, K.I.; Lucy, C.A. Influence of methanol as a buffer additive on the mobilities of organic cations in capillary electrophoresis. *Electrophoresis.* 2003, *24,* 370-379

64. Barron, D.; Lozano, E.J.; Barbosa, J. Prediction of electrophoretic behavior of a series of quinolones in aqueous methanol. *Journal of Chromatography A.* 2001, *919,* 395-406

65. Lin, C.E.; Chen, M.J. Separation and selectivity of benzophenones in micellar electrokinetic chromatography using sodium dodecyl sulfate micelles or sodium cholate modified mixed micelles. *Journal of Chromatography A.* 2001, *923*, 241-248

66. Khaledi, M.G.; Bumgarner, J.G.; Hadjmohammadi, M. Characterization of mixed micellar pseudostationary phases in electrokinetic chromatography using linear solvation energy relationships. *Journal of Chromatography A.* 1998, *802*, 35-47

67. Clothier, J.G.; Daley, L.M.; Tomellini, S.A. Effects of bile salt structure on chiral separations with mixed micelles of bile salts and polyoxyethylene ethers using micellar electrokinetic capillary chromatography. *Journal of Chromatography B.*1996, *683*, 37-45

68. Buskov, S.; Moller, P.; Sorensen, H. Determination of vitamins in food based on supercritical fluid extraction prior to micellar electrokinetic capillary chromatographic analyses of individual vitamins. *Journal of Chromatography A.* 1998, *802*, 233-241

69. Yang, S.; Bumarner, J.G.; Kruk, L.R. Quantitative structure-activity relationships studies with micellar electrokinetic chromatography influence of surfactant type and mixed micelles on estimation of hydrophobicity and bioavailability. *Journal of Chromatography A.* 1996, *721*, 323-335

70. Lin, C.E.; Chen, K.H. Enantioseparation of phenothiazines in capillary zone electrophoresis using cyclodextrins as chiral selectors. *Journal of Chromatography A.* 2001, *930*, 155-163

71. Lin, C.E.; Lin, W.C.; Chiou, W.C. Migration behavior and separation of sulfonamides in capillary zone electrophoresis. I. Influence of buffer pH and electrolyte modifier. *Journal of Chromatography A.* 1996, *755*, 261-269

72. Zhu, Y.; Chen, Y. Key factors in the control of electroosmosis with external radial electric field in CE. *Se Pu.* 1999, *17*, 525-528

73. Marchesini, A.F.; Williner, M.R.; Mantovani V.E. Simultaneous determination of naphazoline, diphenhydramine and phenylephrine in nasal solutions by capillary electrophoresis. *J Pharm Biomed Anal.* 2003, *31*, 39-46

74. Moroi, Y.; Sugioka, H. Temperature effect on solubilization of n-alkylbenzenes into sodium cholate micelles. *Journal of Colloid and Interface Science.* 2003, *259*, 148-155

75. Gailard, Y.; Pepin, G. Use of high-performance liquid chromatography with photodiode-array UV detection for the creation of a 600-compound library application to forensic toxicology. *Journal of Chromatography A.* 1997, *763*, 149-163